https://doi.org/10.1070/RCR4968

Ligands of G-quadruplex nucleic acids

Daria V. Andreeva,[a] Alexander S. Tikhomirov,[a, b] Andrey E. Shchekotikhin [a, b]

[a] *Gause Institute of New Antibiotics, Pirogovskaya ul. 11, 119021 Moscow, Russian Federation*
[b] *D. Mendeleev University of Chemical Technology of Russia, Miusskaya pl. 9, 125047 Moscow, Russian Federation*

The review summarizes advances in the development of low-molecular-weight ligands for G-quadruplex (G4) nucleic acid structures published in the past five years. Main chemical classes of these ligands (polyaromatic compounds, macrocyclic systems, metal complexes and heterocyclic derivatives) are considered. The chemical structures of the ligands and their influence on the stabilization of quadruplexes are analyzed. Future prospects of design of G4 ligands and their applications are discussed.
The bibliography includes 188 references.

Contents

1. Introduction 1
2. Polyaromatic G4 ligands 5
3. Macrocycic G4 ligands 17
4. G4 ligands based on metal complexes 19
5. G4 ligands based on (het)arenes 24
6. Conclusion 32

1. Introduction

Nucleic acids are essential biopolymers involved in the transfer and regulation of genetic information in living organisms. During 70 years of extensive research on nucleic acids after Watson and Crick discovery of the DNA double helix,† it was established that polynucleotides can form so-called non-canonical secondary structure elements, including triplexes, G-quadruplexes, i-motifs, *etc.*[1,2]

G-Quadruplexes (G4s) are widespread and biologically important secondary structure elements formed by guanine-rich sequences. Quadruplex-folded polynucleotides are non-canonical structures, in which four guanine bases of the same or different strands form a planar structure (G-quartet or G-tetrad, Fig. 1 *a*) stabilized by Hoogsteen hydrogen bonds.[3–5] The intermolecular and intramolecular G-quadruplexes are two different configurations of G-quadruplexes (Fig. 1 *b*). Adjacent G-tetrads are held together by π–π-stacking interactions and are additionally stabilized by metal cations. Guanine tetrads have the same folding pattern, but the sugar–phosphate backbone, forming loops that link the tetrads, has different orientations, resulting in topological differences. The quadruplexes are classified into parallel (4 + 0), hybrid (3 + 1) and antiparallel (2 + 2) according to the orientation of the 5′→3′ oligonucleotide sequence, in which 0, 1 or 2 G-forming strands run in the direction opposite to the other strands (see Fig. 1 *b*,*c*). The formation of G4s gives rise to lateral, diagonal or propeller-type loops (see Fig. 1 *b*). Hence, oligonucleotides fold in parallel quadruplexes adopting the single topology (propeller-type), whereas antiparallel and hybrid quadruplexes fold in several topologies.[6]

G-Quadruplex structures play an important role in the cellular homeostasis and the maintenance of genomic stability. In early studies, the formation of G4s by telomeric DNA regions containing repetitive TTAGGG sequences was related to the regulation of telomerase activity. Telomerase is responsible for the compensation for the shortening of telomeric regions of chromosomes owing to the incomplete replication of the ends of linear DNA. Therefore, this enzyme plays a key role in the control of the cell division and biological ageing and also in tumor cell immortalization.[7,8]

In the late 1990s, a series of chemical compounds (ligands), which are capable of stabilizing G4s and, as a consequence, inhibiting telomerase and blocking uncontrolled cancer cell division, were discovered, which has led

† See J.J.D.Watson, F.H.C.Crick. *Nature (London)*, **171**, 737 (1953); https://doi.org/10.1038/171737a0

D.V.Andreeva. PhD Student at the Laboratory of Chemical Transformation of Antibiotics at the GINA.
E-mail: andreeva.chemie@gmail.com
Current research interests: synthesis of bioactive compounds, heteroarene-fused anthraquinones, G-quadruplex ligands.
A.S.Tikhomirov. PhD in Chemistry, Senior Researcher at the Laboratory of Chemical Transformation of Antibiotics at the GINA, Senior Lecturer at the Department of Organic Chemistry of the MUCTR.
E-mail: tikhomirov.chem@gmail.com
Current research interests: synthesis of bioactive compounds, anticancer agents, heteroarene-fused anthraquinones, G-quadruplex ligands.
A.E.Shchekotikhin. Doctor of Chemical Sciences, Assistant Professor, Professor of the RAS, Director of the GINA, Head of the Laboratory of Chemical Transformation of Antibiotics at the GINA, Head of the Department of Organic Chemistry of the MUCTR.
E-mail: shchekotikhin@gause-inst.ru
Current research interests: methodology of organic synthesis, design of bioactive compounds, development of new chemotherapeutic agents.

Translation: T.N.Safonova

Received 11 June 2020

© 2021 Uspekhi Khimii, ZIOC RAS, Russian Academy of Sciences and IOP Publishing Limited

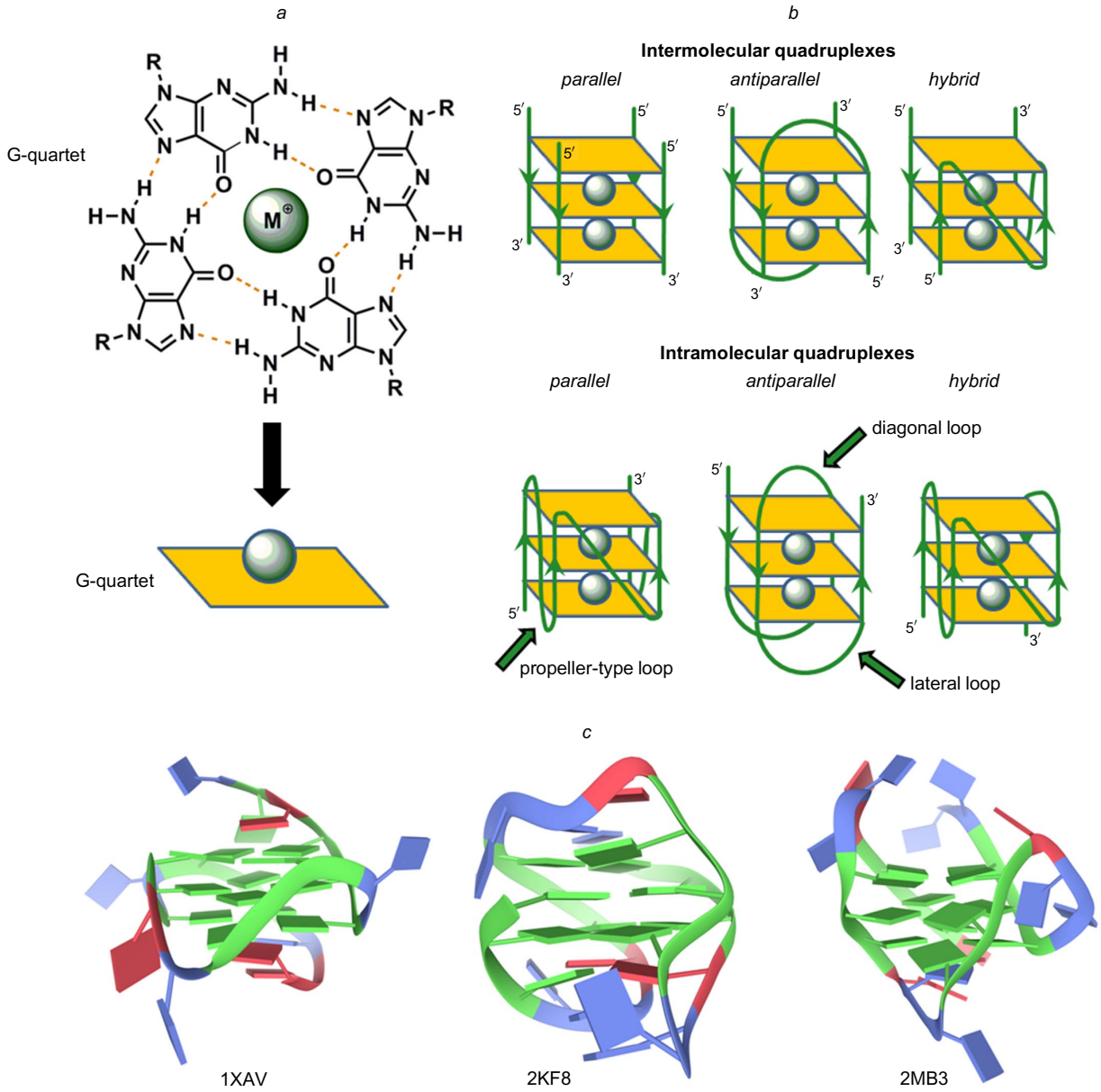


Figure 1. Formation of the G-tetrad (*a*), schematics of the topology of intermolecular and intramolecular quadruplexes (*b*)[6] and structures of quadruplexes: (4 + 0)-parallel c-Myc [based on the Protein Data Bank (pdb): 1XAV], (2 + 2)-antiparallel telomeric (pdb: 2KF8) and (3 + 1)-hybrid telomeric quadruplexes (pdb: 2MB3) (*c*). Guanosine is in green, thymidine is in blue and adenosine is in red.

to a growing interest in investigating the functions of quadruplexes and biological properties of G4 ligands. The bioinformatics analysis of the human genome revealed more that 350 000 potential G4-forming regions of DNA, and the formation of a number of these regions was experimentally confirmed.[9,10] Apart from telomeric DNA, quadruplexes were found in promoter sequences of a number of important genes, and dynamic duplex – quadruplex transitions were demonstrated to be involved in the regulation of gene expression, including a significant range of oncogenes, such as c-Myc, K-Ras, H-Ras, c-Kit, hTERT, VEGF, Sp1, Bcl-2, HIF1, *etc*. The stabilization of G4 elements from promoter regions can efficiently suppress or activate the transcription of the corresponding genes, thereby enabling the modulation of gene expression by low-molecular-weight G4 ligands. The relationship between the stabilization of G4s and biological effects induced by G4 ligands in cancer cells was demonstrated in numerous publications.[11 – 16]

Hence, G-quadruplexes can be considered as a promising target for anticancer therapy, and numerous research groups around the world have focused on the design of such ligands. Moreover, the quadruplex-forming ability was demonstrated for RNA polynucleotides,[17] and potential G4-forming regions were found in the genomes of other eukaryotes and viruses.[18] For example, some unique G4 sequences and the TTAGGG nucleotide repeat (human telomeric region) are present in the genomes of protozoan parasites, such as *Trypanosoma brucei*, *Leishmania major* and *Plasmodium falciparum*.[19,20] Stable G4s are described for the Epstein – Barr virus, immunodeficiency virus, SARS coronavirus and many other.[21 – 24] These data significantly expand the applied therapeutic potential of G4 ligands,

which attract interest as potential antiviral and antiparasitic agents.

An exponential growth in the number of publications on G4 elements and their ligands in the early 2000s resulted in the discovery of various classes of chemical compounds having high affinity for four-stranded nucleic acid structures. In recent years, considerable efforts have been made to optimize the structures of these classes of compounds with the aim of designing new ligands having higher binding selectivity for target sequences or improved therapeutic efficacy. Generally, G4 ligand molecules have characteristic structural features, such as the planar aromatic scaffold and side chains containing basic (amines, amidines, guanidines and so on) or cationic (*e.g.*, *N*-methylpyridinium) groups. The planar part of the molecule can interact with external G-quartets *via* π – π-stacking. Basic side groups of the ligand, being protonated under physiological conditions, form a network of electrostatic interactions and hydrogen bonds with the sugar – phosphate backbone or guanine nitrogen atoms, thereby enhancing the stabilization of the complex. It is evident that, despite the similarity of the architecture of different G-quadruplexes (see Fig. 1 *b*,*c*), they have significantly different topology, which allows the design of ligands specific for particular G4 structures formed by different sequences.

The chemical diversity of G4 ligands is rather large (Fig. 2); the key compounds are derived from acridine (BRACO19), perylenediimide (PIPER), fluoroquinolones (Quarfloxin), porphyrin (TMPyP4), polyheterocyclic macrocycles (Telomestatin), quinoline (Pyridostatin), phenanthroline (PhenDC3), *etc.*[25 – 27] Extensive studies in the field of synthetic and computational chemistry revealed other classes of chemical compounds, which outperform precursors in the affinity, selectivity, physicochemical and biological properties, the toxicological profile and other parameters.

Investigations of the topology and functions of G-quadruplex structures and studies aimed at designing and optimizing their ligands are ongoing. As with any rapidly evolving area of research, the published results require a systematic review and analysis, which can help the scientific community to use the available data for the more efficient work. Evidently, this review is not the only one. There are a number of reviews that cover different aspects of research on G-quadruplexes, including the design of their ligands. Many reviews concerned with G-quadruplex ligands have a narrow focus[28 – 30] and consider the most well-known classes of compounds (*e.g.*, naphthalene diimide derivatives,[31] alkaloids,[32,33] metal complexes,[34] *etc.*) or are focused on the biological,[35,36] photochemical (DNA probes),[37] *etc.* properties of molecules. Some reviews are devoted to several classes of chemical ligands, but they summarize the results of earlier studies.[38,39] Taking into account the gradual upgrading of the classes of ligands and advances in the optimization of the molecular structures of known compounds, it seems reasonable to analyze recent trends in the development of ligands regardless of their classes and properties. The present review of scientific literature published in the past five years includes numerous compounds based on various molecular scaffolds capable of binding to G-quadruplexes. The relationship between the structure and affinity of the compounds is analyzed and the biological action of some representatives is considered. Current trends in the development of G4 ligands are discussed and the most promising lines of the design and

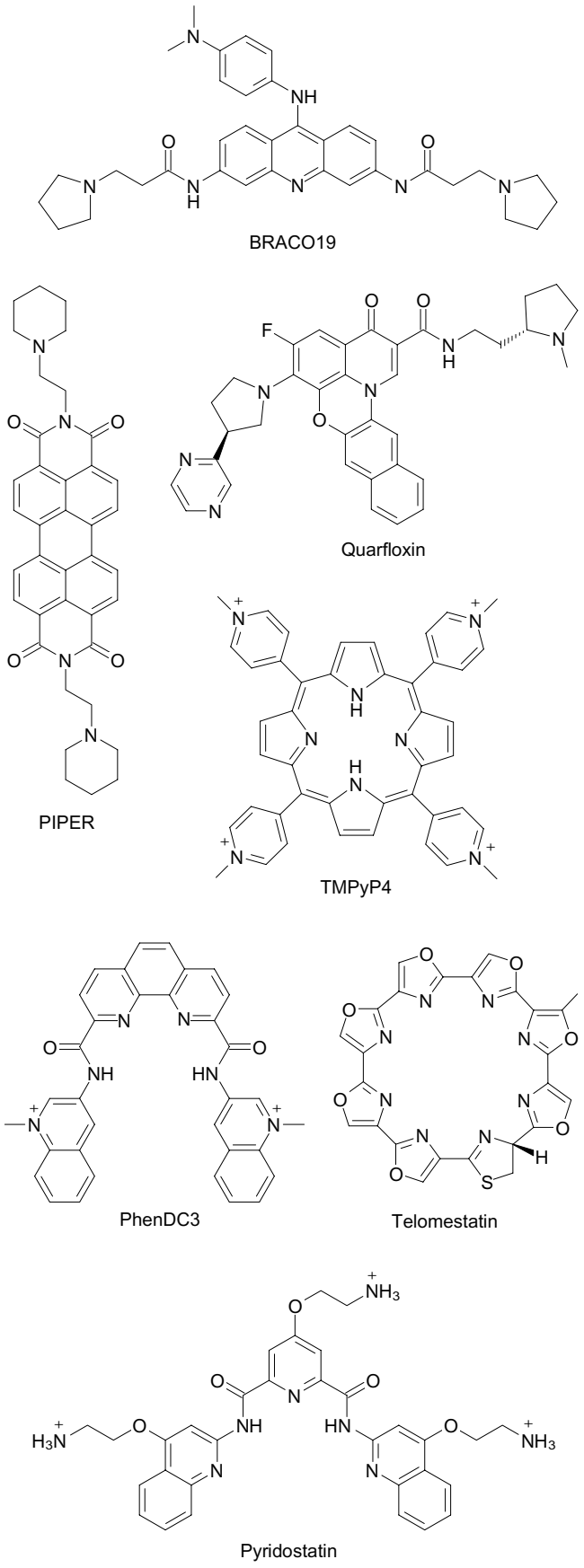


Figure 2. Structures of the most important G4 ligands.

evaluation of these biologically active products are highlighted.

In recent years, powerful experimental methods were developed for the determination of the nucleic acid secondary structures and for the qualitative and quantitative analysis of their interactions with various compounds. The physicochemical and biological methods most commonly used for the characterization of interactions between ligands and oligonucleotides are briefly summarized below.

1. Ultraviolet-visible (UV-Vis) optical and fluorescence (Fl) spectroscopy.[40] This basic spectral method is commonly used to investigate the ligand binding to different DNA structures, including real-time measurements. This method can be applied to determine the binding affinity constants or stability shifts, for example, ligand-induced changes in the melting temperature of the polynucleotide (ΔT_m) in titration experiments or melting assays. Advantages of optical spectroscopy are that it is fast, requires small amounts of compounds and does not affect the structure of oligonucleotides and their complexes with ligands. The main limitation for the analysis of the melting curves by optical methods is the low-intensity signal, resulting in low reliability of the data.

2. Förster resonance energy transfer (FRET) melting assay (relying on the mechanism of energy transfer between two chromophores from a donor to an acceptor). This is a sensitive screening method for the measurement of ΔT_m and preliminary evaluation of the selectivity of different derivatives upon the addition of a competitive oligonucleotide.[41] The assay is based on the quenching of the FRET effect of fluorescent dyes at the ends of the oligonucleotide (a pair of the fluorescent dyes FAM and TAMRA is most commonly used) due to thermal denaturation of G4 structures and their complexes with ligands. The drawbacks of the method are very small values of ΔT_m for stable structures, the effect of the dyes on the formation of G4s and the distortion of the FRET effect upon the binding of the ligands at the ends of the oligonucleotide. The advantage is the possibility to perform experiments in an automatic mode using real-time PCR amplification (PCR is the polymerase chain reaction).

3. Fluorescent intercalator displacement (FID) assay. It is one of the most rapid screening methods for the evaluation of the ligand affinity for nucleic acids, which is based on a decrease in the fluorescence of the dye [*e.g.*, thiazole orange (TO)] in the bound state upon its competitive displacement from the DNA by the ligand.[42] The FID assay is a rather widely used method because it allows the evaluation of the affinity, selectivity and stoichiometry of the binding and the assessment of the DNA binding mode. It should be noted that this method often cannot reveal the differences for the ligands with strong and very strong binding affinity, which have to be evaluated by other methods.

4. Circular dichroism (CD) spectroscopy. This method is focused on investigating changes in the quadruplex topology upon the ligand binding. The method is also often applied to determine ΔT_m from the effect of the ligand on thermal denaturation of G4s. Circular dichroism titration experiments can be used to obtain data on the ligand binding sites to the oligonucleotide.

5. Surface plasmon resonance (SPR) method. This method is used for the experimental determination of the binding and dissociation rates of the complex. Refractive index changes and, consequently, resonance frequency changes are indicative of the interaction of the ligand with immobilized oligonucleotides.[43] An important advantage of this method is the possibility of using low concentrations of oligonucleotides. The drawback is the influence of the surface to which the probe oligonucleotide is attached.

6. Microscale thermophoresis (MST). This method is applied to determine the binding constants of the ligand to the target. It is based on the thermophoretic motion dependent on the size, charge and hydration (solvation) shell of the molecule. Since the binding of the ligand to the probe molecule leads to a change in at least one of these parameters, it also changes the thermophoretic behaviour of the target.[44] Advantages of this method are low sample consumption, the possibility of performing experiments under close to *in vivo* conditions and the absence of immobilization of the molecule. The limitations are the necessity of using fluorescent probes for the G-quadruplex and potential errors in measurements when testing very small ligand molecules.

7. Nuclear magnetic resonance (NMR) spectroscopy. This is a direct method for probing the structures of nucleic acids and their complexes with ligands, which provides precise information about the mode and stoichiometry of the ligand binding to G4s.[45] The key drawbacks of this method are the requirement of high concentrations, which are much higher than physiologically relevant concentrations, the formation of a true solution for obtaining reliable data and problems with the interpretation of the results.[46]

8. High-resolution mass spectroscopy (HRMS), for example, in electrospray ionization mode (ESI). This method can also be employed to study interactions between nucleic acids and different molecules.[47] The quality of the HRMS analysis decreases with increasing concentration of K^+ and Na^+ ions, which are, however, necessary for the formation of G-quadruplexes of different topologies.

9. Isothermal titration calorimetry (ITC). This is an experimental method for the direct measurement of the enthalpy and Gibbs energy, the evaluation of enthalpy and entropy contributions to the complexation energy and the estimation of the dissociation constants (K_D) of complexes.[48] However, these investigations require large sample volumes and good solubility of the ligand in water, while the aggregation of the ligand can lead to serious errors in measurements.[49]

10. Polymerase stop assay (PCR stop assay). This commonly used biochemical assay of G4 ligands is based on the stabilization of the template strand by ligands, which blocks the polymerase activity and inhibits the target oligonucleotide synthesis at a particular site.[50]

11. Telomeric repeat amplification protocol (TRAP) assay. It is based on the measurement of telomerase activity, which is proportional to the number of TTAGGG repeats.[51]

The following abbreviations are used in the review:

DC_{50} — ligand concentration required to displace 50% of the dye,

dsDNA — double-stranded DNA,

EB — Epstein – Barr virus,

FID — fluorescent intercalator displacement,

FRET — Förster resonance energy transfer, a mechanism of energy transfer between two chromophores (from a donor to an acceptor),

G4 — G-quadruplex,

GI_{50} — concentration causing 50% inhibition of cell proliferation,

HIV — human immunodeficiency virus,

IC_{50} — concentration causing 50% inhibition (of a biological process),
K_D — dissociation constant,
MST — microscale thermophoresis,
NDI — naphthalene diimide,
PCR — polymer chain reaction,
RG4 — RNA G-quadruplex,
ROS — reactive oxygen species,
SAR — structure–activity relationship,
SI — selectivity index,
SPR — surface plasmon resonance,
ΔT_m — ligand-induced change in the melting temperature of polynucleotide,
T/C (treated to control) — the ratio of the mean tumour volume in treated animals to the mean tumour volume in the control group (%),
tel — telomerase,
TGI — tumour growth inhibition defined as the difference between the mean tumour volumes in the control and experimental groups divided by the mean tumour volume in the control group of animals (%),
TO — thiazole orange.

2. Polyaromatic G4 ligands

Compounds containing several fused aromatic rings are among the first classes of G4 ligands to be found to bind to DNA G-quadruplexes. Evidently, these compounds have attracted attention as promising candidates for searching for G4 ligands due to their ability to stabilize the DNA duplex through efficient π–π-stacking interactions with base pairs. The further optimization of the central polyaromatic core and the structures of the side chains resulted in the preparation of active ligands based on anthraquinone, perylene, acridine, carbazole, *etc*. Rather extensive research aimed at improving such ligands has been performed in the past 20–25 years. However, there are some limitations of this chemotypes associated with the practical applications of lead compounds (for the detailed discussion, see the last Section).

Naphthalene diimides (NDI) are a striking example of G4 ligands, which were studied since the late 2000s.[31, 52, 53] Important aspects of their biological activity, which are essential for their further use, were revealed. This chemical class is privileged for the development of G4 ligands due to the presence of the polyfused planar π-electron system, capable of efficiently stabilizing G-quartets of quadruplexes through stacking interactions, and owing to a considerable potential for diversification of the naphthalene diimide moiety.[54]

Islam *et al*.[55] reported the synthetic route to macrocyclic derivative **1** (Fig. 3) containing the naphthalene diimide moiety and characterized this compound in detail. Using a combination of advanced methods of physicochemical analysis, the authors demonstrated that naphthalene diimide **1** has high affinity for G4s, formed by the promoters of the c-Myc and c-Kit oncogenes, the thrombin-binding DNA aptamer (TBA) and the telomeric region of chromosome (α-core), whereas the binding constant with the duplex was found to be 2–3 orders of magnitude lower. It should be emphasized that the replacement of the terephthalamide-containing macrocyclic moiety by two 3-(*N*,*N*-dimethylamino)propyl groups leads to a radical change in the properties of the compound, making it specific to the DNA duplex. The affinity for the telomeric quadruplex is consistent with a high telomerase inhibitory activity (the concentration causing 50% inhibition (IC_{50}) is 0.9 μM).‡

Freccero's research group (University of Pavia) made a significant contribution to the development of G4 ligands based on naphthalene diimides. In 2015, Freccero and coworkers[56] synthesized a series of water-soluble dihydroquinoxaline-fused G4 ligands for human immunodeficiency virus (HIV) (*e.g*., derivatives **2**–**4** in Fig. 3). Based on the results of quantum chemical calculations, the authors suggested that the expansion of the surface of the planar π-system through the annulation of naphthalene diimides with dihydroquinoxaline will enhance the stacking interaction between the ligand and G-tetrads. The choice of the side chains in favour of 3-(*N*,*N*-dimethylamino)propyl groups was made based on the values of pK_a. Thus, the protonation of terminal amino groups under physiological conditions reduces self-aggregation of the ligands. Ligands **2**–**4** stabilize HIV-1 promoter quadruplexes with ΔT_m from 10 to 16 °C for the LTR-III and LTR-IV oligonucleotides. The quaternization of terminal amino groups (compound **3**) leads to the loss of binding specificity for G4s compared to the DNA duplex, and the introduction of the third chain (compound **4**) results in a considerable weakening of the binding to LTR-IV G4 ($\Delta T_m < 4$ °C). Besides, ligand **2** exhibits high antiviral activity against HIV-1, which, on the one hand, confirms that G4 can be considered as a promising target for antiviral therapy and, on the other hand, demonstrates that G4 ligands hold promise for the design of new antiviral agents.

Symmetrical 2,7-disubstituted naphthalene diimide derivatives containing benzimidazole moieties efficiently stabilize the human telomeric quadruplex (telG4).[57] The FRET, ITC and SPR assays demonstrated that compounds **5**–**7** (see Fig. 3) stabilize telG4, and their dissociation constants (K_D) are 10–100 times lower compared to those for duplex DNA. It is worth noting that the replacement of the benzimidazol-2-yl spacer by the trimethylene chain (ligand **5**) has no effect on the binding, whereas the introduction of the phenylene group (compound **7**) between the benzimidazole and naphthalene diimide moieties leads to an increase in the affinity of the ligand for G4s by two orders of magnitude. Naphthalene diimides **5**–**7** inhibit telomerase activity *in vitro*. The highest binding constant of derivative **7** correlates with the inhibitory activity against this enzyme. At a concentration of 1 μM, naphthalene diimide **7** induces apoptosis in HeLa cancer cells.

Arévalo-Ruiz *et al*.[58] synthesized carbohydrate conjugates of naphthalene diimide derivatives in order to increase the solubility, bioavailability and selectivity of the interaction between the resulting ligands and G4s. The authors suggested that an increase in the selectivity can be achieved through an interaction between the carbohydrate moiety of the conjugate and phosphate residues in the grooves of G4 DNA. Such compounds (*e.g*., β-mannopyranoside **8**, see Fig. 3) stabilize telG4 against thermal denaturation with high values of ΔT_m, being only slightly less efficient than analogous compounds, in which the glycosidic moiety is replaced by an aminoalkyl chain. Variations in the carbohydrate structure have no significant effect on the stabilization of the telomeric quadruplex. In the presence of a competitive duplex DNA (50 equiv.), ΔT_m decreases from

‡ Hereinafter, the concentration expressed in mol L^{-1} is denoted by the unit M.

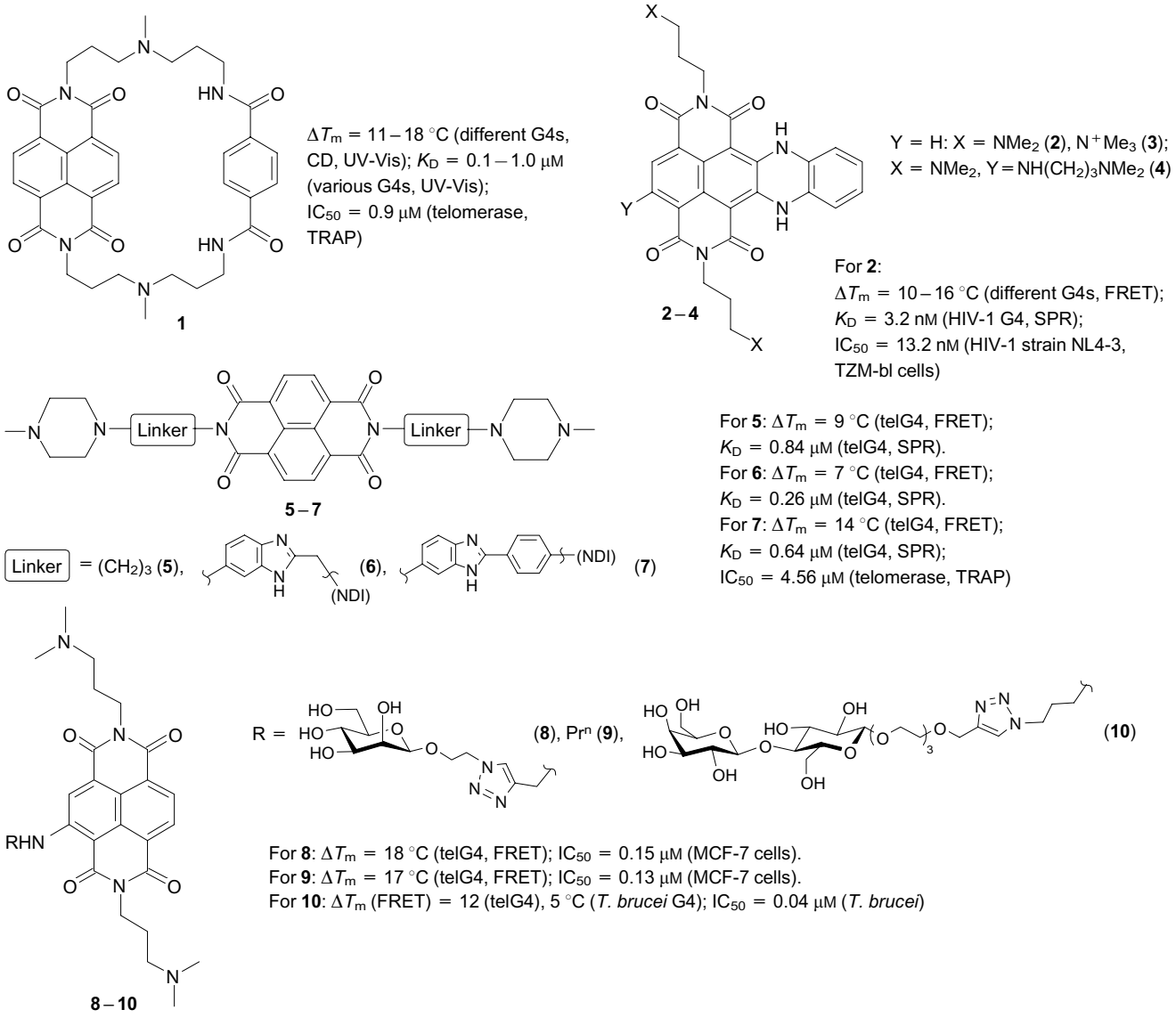


Figure 3. Structures of G4 ligands **1** – **10** based on naphthalene diimide.
Here and in other figures, the source of G4s and the method of evaluation are given in parentheses after the corresponding parameter; in some cases, the binding constants (K_a or K_b) published in the original works are converted to K_D (the dissociation constant, which is the reciprocal of K_a or K_b) in order to simplify the analysis of the efficiency of ligand binding.

18 to 5 °C, which is indicative of a satisfactory selectivity of the ligand binding to G4s; no selectivity for a particular quadruplex topology was revealed. The parameters of stabilization and specificity of ligand **8** are similar to those of naphthalene diimide **9** (see Fig. 3), in which the carbohydrate-containing side chain is replaced by the propyl substituent. Carbohydrate conjugates are accumulated in cancer cells somewhat less efficiently compared to reference compound **9**; however, their uptake occurs by the GLUT4-mediated active transport, which correlates with the cytotoxic properties of the ligands.

Apart from the above-described properties, glycosylated naphthalene diimides exhibit antiparasitic activity against human trypanosomiasis caused by *T. brucei*.[59] The genomes of these protozoan parasites contain G4-forming sequences.[60, 61] This fact gave impetus to investigate this potential target for a new approach to the treatment of parasitic diseases. β-Lactoside **10** (see Fig. 3) exhibited the highest activity against *T. brucei*. Physicochemical studies demonstrated that the synthesized conjugate stabilizes not only telomeric G4 but also the EBR1 quadruplex specific for *T. brucei*. Carbohydrate-conjugated naphthalene diimides are taken up in *T. brucei* cells by an active transport and are localized in nuclei, which is indirect evidence for the ability of G4s to serve as a target of action. The selectivity of this class of G4 ligands for the DNA duplex is also moderate and, consequently, a significant optimization of the structure of naphthalene diimide **10** is required. Nevertheless, this work is an interesting example of a new potential application of G4 ligands.

Shen *et al.*[62] synthesized a series of 2,7-diaminoxanthone derivatives containing amines at the terminal positions of the 2,7-side chains. Bis(*N*,*N*-dimethyl)glycine amide **11** (Fig. 4) is the most efficient compound in this series, which stabilizes the telomeric quadruplex through the binding to the terminal G-tetrad. The stabilization of G4 was con-

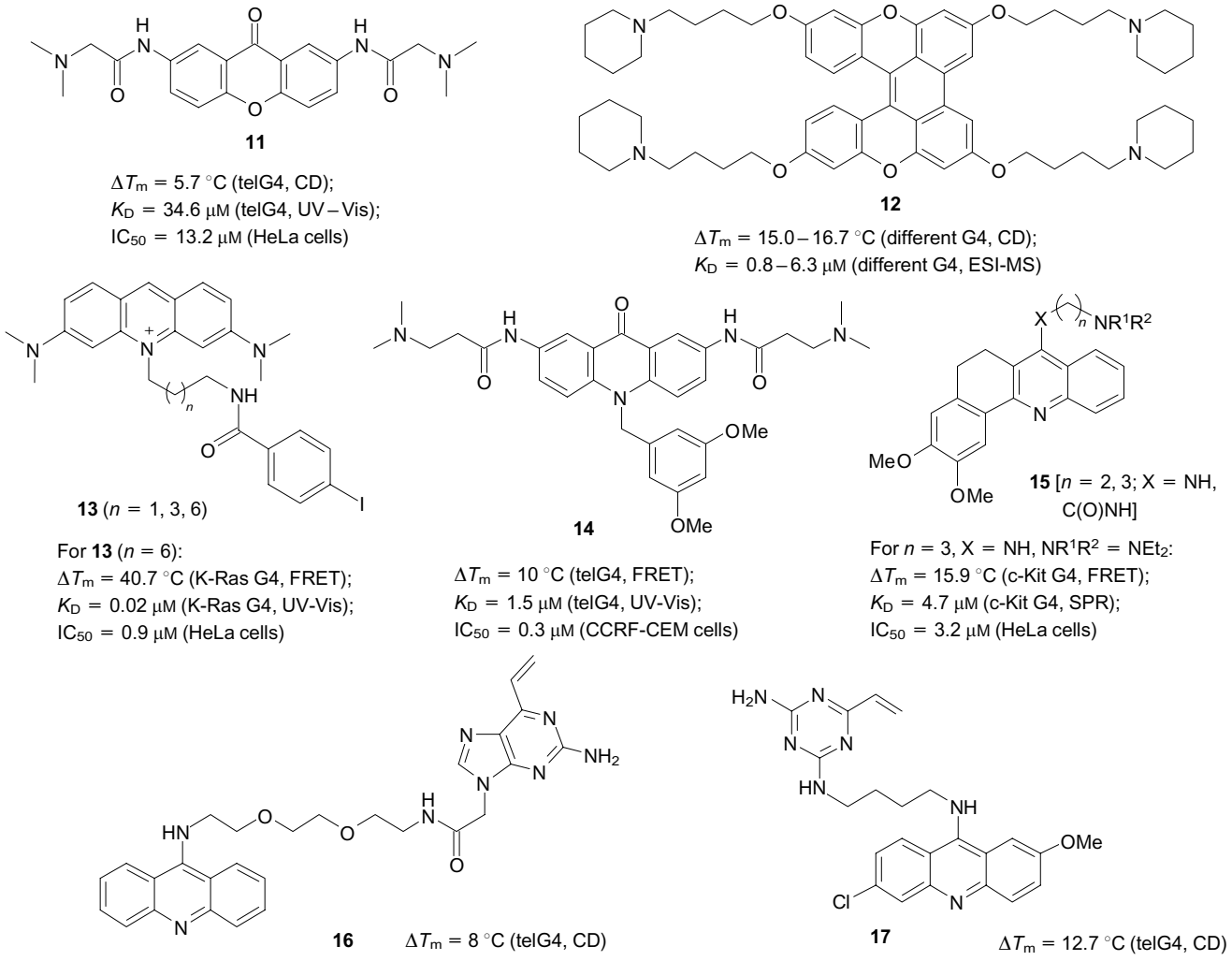


Figure 4. G4 ligands **11** – **17** based on xanthone and acridine.

firmed by the inhibition of PCR amplification of the G4-forming nucleotide, while the uptake of the mutant nucleotide is not retarded. The highest affinity of compound **11** was attributed to the fact that terminal dimethylamino groups protonated under physiological pH values form a network of electrostatic interactions with the loops of the quadruplex, with no steric hindrance, as in the case of pyrrolidine, piperidine and other moieties. Xanthone **11** exhibits a moderate antiproliferative effect, inducing apoptosis in HeLa cells.

Polyfused derivative **12** (see Fig. 4), which was synthesized by the dimerization of xanthone *via* the McMurry reaction, is also able to stabilize quadruplex structures of nucleic acids.[63] The affinity of ligand **12** for telG4 (K_D = 0.8 μM, ESI-MS) is much higher than that for the DNA duplex (K_D = 158.5 μM). It is important that the addition of competitive double-stranded DNA (dsDNA) to the mixture under study in a ratio of 1 : 1 leads only to a 10% decrease in the number of G4-nucleotides bound to the ligand. Dimer **12** forms strong interactions also with other quadruplex structures, such as Bcl-2 and c-Myc. This dimer exhibited high antiproliferative activity on the NCI-60 cancer cell line panel, inducing DNA damage (γH2AX and TIFF markers). The authors reported no more detailed evidence for the relationship between the biological effect and the action of the ligand on G4s.

Acridine derivatives were considered as promising scaffolds for the development of G4 ligands over more than two decades. This class includes one of the first telomerase inhibitors, the compound BRACO-19 (see Fig. 2), prepared by the rational design. This compound exhibits high *in vitro* and *in vivo* activity. In recent years, acridine derivatives have attracted less interest as compounds targeting G4s. Nevertheless, some research groups continue investigations aimed at optimizing their structure. In this review, the focus is on studies of original G4 ligands, while special modifications and(or) investigations of particular properties are not considered (*e.g.*, Ref. 64, in which the replacement of pyrrolidine in the side chains of the well-characterized ligand BRACO-19 by azetidine was reported to lead to a 1.5-fold increase in the G4-binding affinity).

Carvalho *et al.*[65] described derivatives of acridine orange (AO), the ω-(*p*-iodobenzamido)alkyl-containing fluorescent dye, as selective fluorescent probes for the K-Ras quadruplex. An elongation of the alkyl chain from n-propyl to n-octyl was shown to enhance the G4-binding properties. The most active ligand **13** (see Fig. 4) stabilizes the quadruplexes in the following order: K-Ras > c-Myc ≫ telG4. Studies by ^{1}H NMR spectro-

scopy and the Job plot analysis demonstrated that acridine **13** binds to K-Ras G4 in a ratio of 4 : 1, the complexation causing fluorescence enhancement. Ligand **13** and its analogues have strong cytotoxicity and, despite the presence of the quaternized core, are rapidly taken up by cells, being detected mainly in the nuclei (confocal microscopy data).

Gao *et al.*[66] synthesized 2,7-diaminoacridone derivatives containing different terminal amino groups as bioisosteres of xanthone **11**. Only *N*,*N*-dimethyl-β-alanine derivative **14** (see Fig. 4) displays significant antiproliferative activity against cancer cells. Compound **14** proved to be the least cytotoxic against normal 293T cells ($IC_{50} > 100$ μM), Hence, the author chose this compound for physicochemical studies. Acridone **14** can bind to human telomeric G4, which was confirmed by various methods (HRMS, CD, UV-Vis and FRET). The role of terminal groups at the 2 and 7 positions and the effect of the spacer length on the binding were not considered.

7-Substituted 5,6-dihydrobenzo[*c*]acridines (see Fig. 4) were used to synthesize G4-binding ligands targeting the c-Kit oncogene promoter.[67] Following the general trends in the design of G4 ligands, the authors synthesized a series of benzo[*c*]acridines with the side chain bearing the terminal amino group at the 7 position. The structure – activity relationship (SAR) analysis demonstrated that the quaternization of the acridine nitrogen atom or the replacement of the linker NH group by the C(O)NH moiety reduce the G4-stabilizing effect of the ligands, while an increase in the length of the side chain by one methylene group (to C_3) generally facilitates an increase in the affinity. The stabilizing effect of the new compounds on c-Kit1 and c-Kit2 G4 was in the range $\Delta T_m = 3.4 – 22.9$ °C. High affinity was confirmed by the SPR method ($K_D < 8.0$ μM). The most active ligand **15** (see Fig. 4) is selective for G4s compared to the DNA duplex and mainly inhibits *in vitro* the cancer cell growth (the selectivity index SI > 10). Assays showed that acridine **15** suppresses the c-Kit gene transcription and reduces the level of the c-Kit oncoprotein in cancer cells.

The conjugation of acridine with 2-amino-6-vinylpurine resulted in the development of a new class of efficient G4 ligands capable of forming covalent bonds with oligonucleotides.[68] 9-Aminoacridine derivative **16** (see Fig. 4) selectively stabilizes telG4 predominantly in the (3 + 1)-hybrid topology (in potassium buffer), having no effect on single- or double-stranded DNA. The difference in the electrophoretic mobility of the denatured complex [G4 – **16**] and the untreated polynucleotide attests to a significant amount of the covalently bound adduct (70% after 72 h incubation), the formation of which was confirmed by the HRMS method. The introduction of the active 4-amino-6-vinyltriazine moiety into the side chain of acridine derivatives also affords G4-selective covalently bound G4 ligands (*e.g.*, derivative **17** in Fig. 4).[69] The investigation of the mechanism of interaction of these ligands with the target demonstrated that the formation of the adduct occurs at the N atom in the 3 position of one of thymidine residues at the lateral loop of the (3 + 1)-hybrid quadruplex (Fig. 5).

Carbazole derivatives are widely used as quadruplex ligands due to their rigid V-shaped geometry, facilitating their overlap with the planes of the G-quartet through π – π-stacking interactions.[70] A new chemotype, 3,6-bis(benzimidazole) derivatives of carbazole, for this purpose was discovered as a result of systematic research on G4 ligands based on 1,3-phenylenebis(benzimidazole).[71] The replacement of the central phenyl moiety by polycyclic heteroaromatic scaffolds, in particular by carbazole moieties, leads to a significant enhancement of the ligand binding to G-quadruplexes.[72]

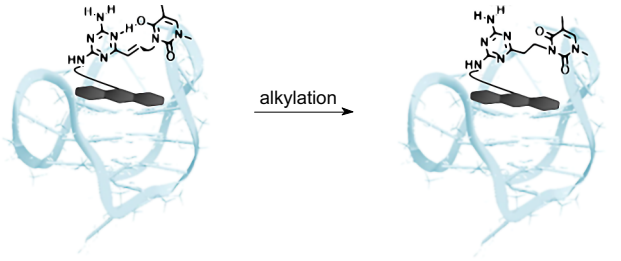


Figure 5. Molecular model of the interaction between ligand **17** and telG4 having the 3 + 1 hybrid topology and the covalent binding to thymidine at the lateral loop.[69] Reproduced with the permission of Elsevier.

New G4 ligands based on 3,6-bis(benzimidazole) derivatives of carbazole (see, for example, compounds **18** – **20** in Fig. 6) stabilizing DNA G-quadruplexes in the c-Myc, c-Kit, VEGF and Bcl-2 oncogene promoter regions have recently been described.[73] The structure – property relationship analysis showed that the introduction of the third carbazole-conjugated side chain into ligand **18** leads to a 2 – 4-fold increase in the G4-binding affinity of derivatives **19** and **20**. All ligands induce a significant thermal stability shift for the melting of quadruplexes. However, in this case ligands **19** and **20** also proved to be much more potent. Thus, the maximum values ($\Delta T_m = 21 – 25$ °C) were determined for the complexes with telG4 and with the c-Kit1 and c-Kit2 G-quadruplexes. Generally, the affinity for different G4s changes in the following series: c-Kit1 ≈ c-Kit2 > VEGF > c-Myc ≈ Bcl-2. In the presence of carbazole derivatives **18** and **19**, the oligonucleotides fold exclusively into parallel G4 structures, which is indicative of the selectivity of ligand binding to parallel G-quadruplexes.

Li *et al.*[74] described a series of conformationally flexible methylene-bridged carbazole oligomers and evaluated their effect on the cancer cell growth and the G4-binding ability. Only dimer **21** (see Fig. 6) exhibited satisfactory cytotoxic activity ($IC_{50} = 0.69 – 5.09$ μM) against four cancer cell lines. Hence, this compound was used to evaluate the G4-binding ability. Ligand **21** showed a moderate stability shift in the melting temperature of telG4 and had almost no effect on thermal denaturation of duplex DNA.

Ou *et al.*[75] synthesized selective G4 ligand **22** (see Fig. 6) containing the heteropolyaromatic scaffold based on 1,3,5-tris(carbazol-3-yl)benzene.[75] This compound has C_3 symmetry, which, on the one hand, creates steric hindrance to minimize ligand intercalation into the DNA duplex and, on the other hand, provides efficient π – π interaction with terminal G4 tetrads. In order to enhance the stabilization of quadruplexes, carbazole moieties were modified by aminoalkyl side chains. Most of such derivatives induce an increase in the stability shift for telG4. Thus, the highest value of ΔT_m (19.9 °C) was observed for compound **22** containing 3-(piperidin-1-yl)propyl moieties. The replacement of the C_3 spacer with C_2 and of the terminal cyclic amine (piperidine or pyrrolidine) by diethylamine or morpholine leads to a weakening of the interaction between the ligands and G4s. Ligand **22** shows significant selectivity. Thus, the addition of a 250-fold excess of competitive dsDNA decreases ΔT_m by only 7 °C. The screening of the

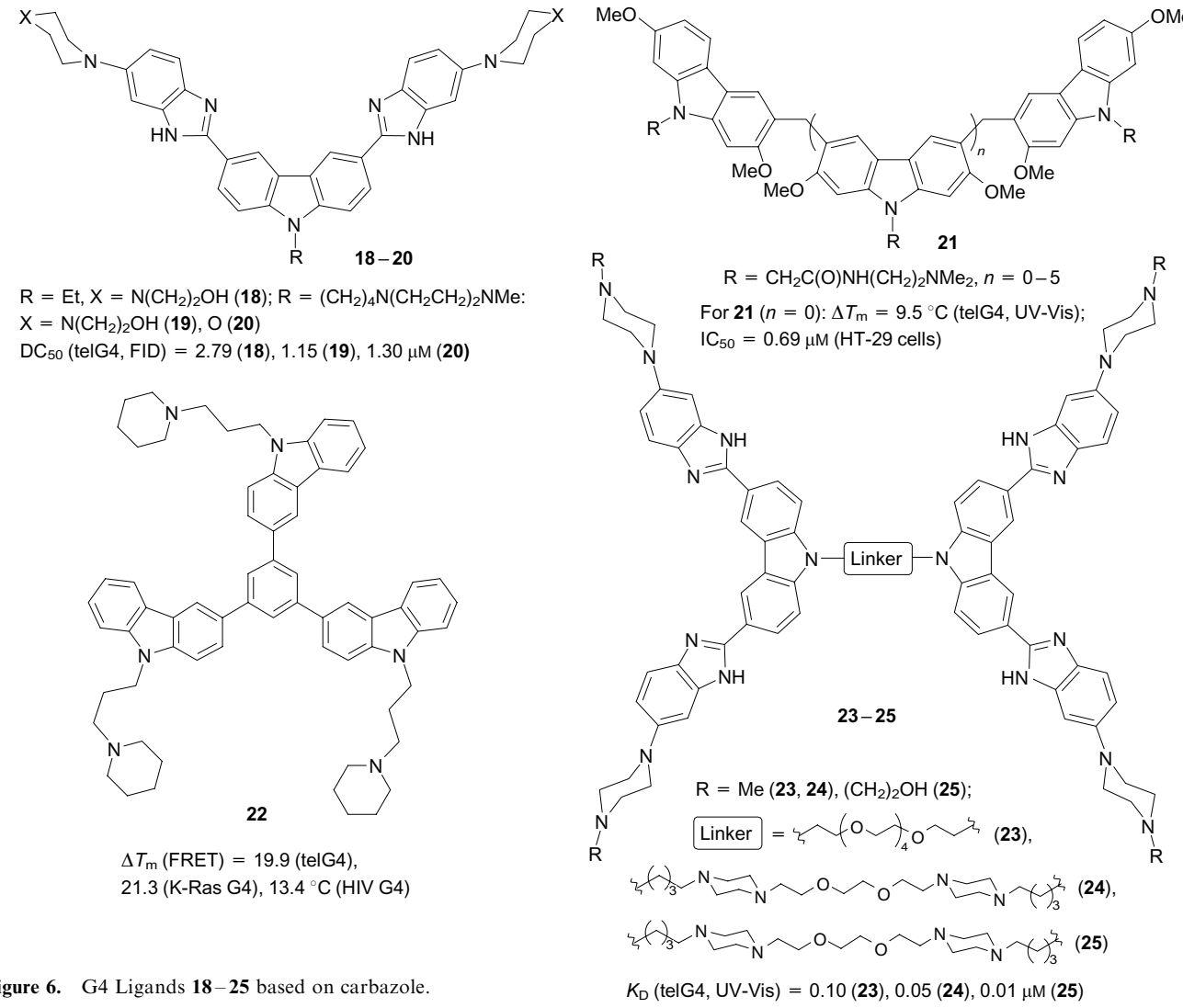


Figure 6. G4 Ligands **18** – **25** based on carbazole.

affinity demonstrated that 1,3,5-tris(carbazol-3-yl)benzene **22** also efficiently binds to G4 of the K-Ras oncogene promoter and the human immunodeficiency virus HIV PRO1.

Symmetrical dimers based on 3,6-bis(benzimidazole) derivatives of carbazole containing different linkers also interact with quadruplex nucleic acids.[76] The dissociation constants of dimeric ligands **23** – **25** (see Fig. 6) are 10 – 30 times lower compared to their monomeric analogue (K_D = 3.3 μM), which confirms the efficiency of this modification of G4 ligands. The presence of the piperazine ring in the linker improves the G4-binding affinity of compound **24** compared to ligand **23** containing the hexaethylene glycol moiety as the linker. The replacement of the methyl group by the hydroxyethyl group in the piperazine moiety also promotes an increase in the complexation constant. In the previous publication, Maji *et al.*[72] noted that the binding of monomeric ligands to G4s can lead to a change in its topology from hybrid to parallel; however, the data on the effect of the dimers on conformational changes in G4s were not reported.[76] Dimers **23** – **25** more efficiently suppress the elongation of the telomeric telomerase sequence compared to the monomeric analogue of ligand **25** (IC_{50} = 0.25 μM). It should be noted that the inhibition of the telomere synthesis by monomers and dimers correlates well with the G4-binding affinity of the ligands.

Phenanthroline is an angular heterocyclic compound which, like anthraquinone, carbazole, naphthalene diimide and other polyfused systems, can form stacking interactions with nucleic acid secondary structures. The presence of side chains bearing terminal amino groups is an important prerequisite for good G4-binding affinity of ligands. The nature of the spacer between the phenanthroline ring and the basic site apparently plays a key role in the binding selectivity of compounds with targets. Previous studies showed that alkyl, quinoline and triazole moieties can be successfully used for the construction of phenanthroline G4 ligands.[77 – 79]

In a recent series of studies,[80 – 82] structurally related G4 ligands were synthesized based on phenanthroline linked to cyclic amines (pyrrolidine, piperidine, piperazine) through the 4-aminophenol or 2,6-diaminopyridine bridge. A comparative evaluations of the compounds allowed the selection of ligands **26** and **27** (Fig. 7). These ligands are characterized by the best binding to telG4 and high selectivity compared to the duplex. Phenanthroline **26** stabilizes the c-Kit2 and c-Myc G-quadruplexes through the binding to the latter in a stoichiometric ratio of 2 : 1, which is indicative of stacking interactions with terminal G-tetrads. Com-

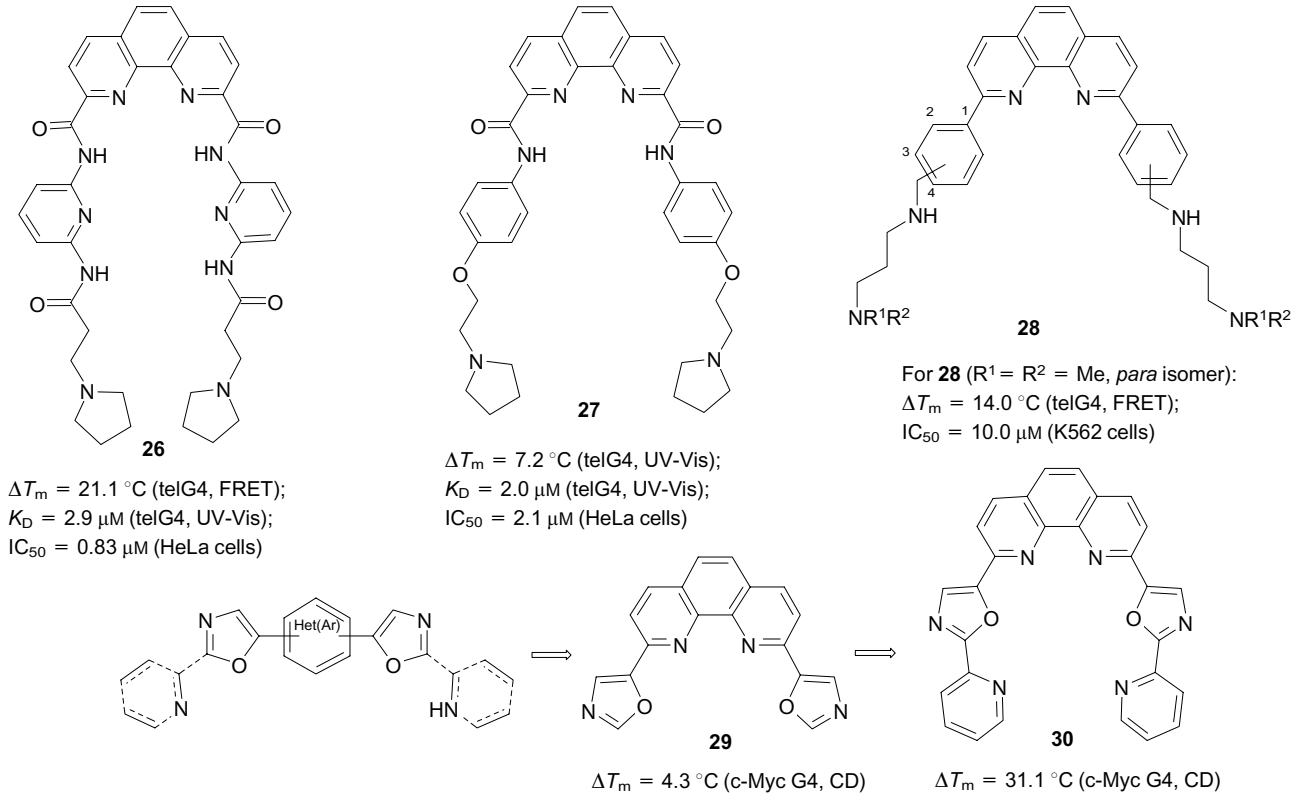


Figure 7. G4 ligands **26** – **30** based on phenanthroline.

pound **27**, in which the 2,6-diaminopyridine spacer is replaced by the 4-aminophenol group, forms complexes both with the quadruplex secondary structure and the i-motif (K_D = 2.0 and 6.3 μM, respectively). Both ligands inhibit the transcription of the c-Myc oncogene and act at the post-translational level, decreasing the expression of the c-Myc, Sp1 and hTERT proteins. Due to antiproliferative activity, phenanthroline derivatives **26** and **27** are rather promising ligands. Both these ligands suppress the division of several cancer cell lines at low micromolar or submicromolar concentrations.

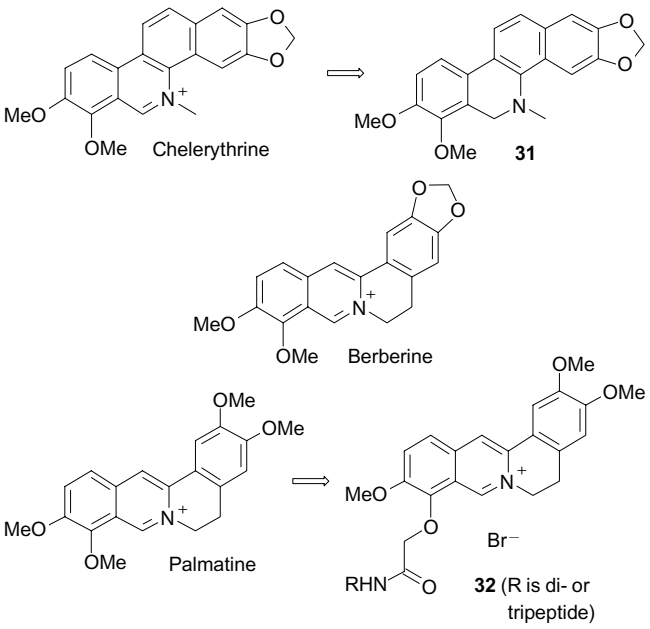
In other G4 ligands based on 2,9-diphenylphenanthroline, the *N*-(aminoalkyl)aminomethyl side groups are attached to benzene rings.[83] The screening of a series of these ligands using the FRET melting assay demonstrated that compound **28** (see Fig. 7) containing the *N*-[3-(dimethylamino)propyl]aminomethyl substituent at the 4 position of benzene rings is characterized by the largest stability shift for the telomeric quadruplex. The removal of one side chain bearing a basic group leads to a twofold decrease in the stabilization of G4s, which is evidence of their important role in the complexation. The evaluation of other G4-forming oligonucleotides demonstrated that ligand **28** has the highest affinity for telG4 and RG4. The addition of a 50-fold excess of the competitive self-complementary oligonucleotide ds26 causes a decrease in ΔT_m by only 3 °C, which is indicative of the binding specificity for G4s. Ligand **28** was demonstrated to have the stabilizing effect on G4s at the cell level through the inhibition of Pif1-helicase-mediated quadruplex unfolding. Compound **28** displayed moderate cytotoxic activity.

Medeiros-Silva *et al.*[84] performed the condensation of two key structural moieties of the G4 ligands of PhenDC3 and telomestatin (see Fig. 2), namely, 1,10-phenanthroline and oxazole, respectively (see Fig. 7). In order to extend the range of compounds for the SAR analysis, the following compounds were synthesized: 1) symmetrical and unsymmetrical ligands; 2) ligands in which 1,10-phenanthroline is replaced by other aromatic and heteroaromatic rings; 3) compounds containing an additional pyridine moiety linked to oxazole. It was found that only symmetrical phenanthroline-containing ligands **29** and **30** (see Fig. 7) can stabilize the telG4 and c-Myc G-quadruplexes, while having no effect on the DNA duplex. The introduction of two 2-pyridyl substituents at the oxazole rings of compound **29** leads to a significant increase in the G4-binding affinity (by a factor of ~4 – 8 for ligand **30**). An analysis of the NMR spectra shows that the top G-tetrad of the c-Myc quadruplex is the most probable G4-binding site of phenanthroline **30**. This investigation can be considered as an example of modification of G4 ligands based on polyheterocycles (for more details, see Section 3).

Therefore, the expansion of the aromatic structure of 1,10-phenanthroline-based ligands by introducing carbo- and heterocyclic moieties facilitates the interaction with G4s. Studies demonstrated that terminal basic groups are not necessary for 1,10-phenanthroline-based G4 ligands.

The structurally related alkaloids berberine and chelerythrine and other compounds having a planar scaffold can also be used as the molecular basis for the development of ligands for topologically different nucleic acid secondary structures.[2, 33] For example, the structures of complexes of a berberine derivative with telG4 in the crystalline state and in solution have recently been reported, which can be employed for the design of analogues.[85]

The total synthesis was developed for two chelerythrine derivatives, dihydrochelerythrine (**31**, Fig. 8) and 6-(2-oxopropyl)dihydrochelerythrine, and their selected biological



For chelerythrine: ΔT_m = 19.6 °C (c-Myc G4, CD);
K_D = 1.4 μM (c-Myc G4, UV-Vis).
For **31**: ΔT_m = 24.0 °C (c-Myc G4, CD);
K_D = 1.8 μM (c-Myc G4, UV-Vis);
For **32** (R is phenylalanyl-arginine):
ΔT_m = 21.7 °C (c-Kit G4, FRET)

Figure 8. G4 ligands **31** and **32** based on polyfused alkaloids.

properties were studied.[86] Dihydrochelerythrine (**31**) and chelerythrine can stabilize G4 DNA in the c-Myc and c-Kit1 oncogene promoters, demonstrating similar values of ΔT_m and K_D. Note that the 6-(2-oxopropyl) analogue does not bind to G4s. Computational modelling studies demonstrated that ligand **31** interacts with the c-Myc G-quadruplex (c-Myc G4) mainly through stacking interactions by exploiting both the top and bottom G-quartets in a stoichiometric ratio of 2 : 1 (Fig. 9). The new derivatives proved to have much lower cytotoxic activity. Thus, at a concentration of 20 μM, dihydroheleritrine (**31**) inhibits the cancer cell growth by 8% – 30%, whereas chelerythrine causes 100% inhibition of cell division in the HCT116, MDA-MB-231 and A431 cell lines. However, the possible loss of the relationship between the G4-stabilizing activity of ligand **31** and the cytotoxic activity was not discussed.

An international research group [87] developed G4 ligands based on peptide derivatives of palmatine (see Fig. 8). Previous studies [88, 89] showed that the introduction of amino acid residues into an alkaloid molecule results in a significant stabilization of G-quadruplex structures. Later, combinations of basic amino acids (lysine, arginine, histidine) and also phenylalanine and glycine were employed. The screening of the affinity for a series of ligands was performed using the G4-forming c-Kit1, c-Myc, telG4 oligonucleotides and the DNA duplex by means of the FRET melting assay. The stabilizing effect of most compounds towards the c-Kit1 and c-Myc G-quadruplexes was found to be higher than for the telomeric quadruplex and was virtually absent for the duplex. Phenylalanyl-arginine-containing dipeptide **32** (see Fig. 8) and its arginyl-arginine analogue had the highest G4-binding affinity, whereas the introduction of the third amino acid residue leds to a decrease in the G4-binding affinity of the ligands.

Apparently, due to the molecular complexity of the alkaloids chelerythrine and palmatine characteristic of many natural products, the high-throughput SAR analysis of such structures has not been performed as yet. Nevertheless, some modifications show that investigations of G4 ligands based on these compounds hold promise.

Diimidazo[1,2-*a*:1′,2′-*c*]pyrimidines comprise a relatively new class of polyaromatic heterocyclic G4 ligands. This molecular scaffold was studied by a research group at the University of Naples Federico II (Naples, Italy), which is best known for works on the search for G4-targeting anticancer agents. Bisguanidine **33** (Fig. 10), which stabilizes some quadruplexes, served as the basis for the structural optimization of the side groups.[90] A series of analogous diimidazopyrimidines with improved G4-binding affinity were synthesized. Ligand **34** (see Fig. 10), containing the 2-aminoimidazoline linked to the central scaffold through a hydrazone spacer, exhibited the highest affinity, specificity and cytotoxicity in this series. Compound **34** selectively binds to parallel c-Myc G4, without changing its topology, whereas its analogues and the starting bisguanidine **33** act as pan-quadruplex binding molecules. The

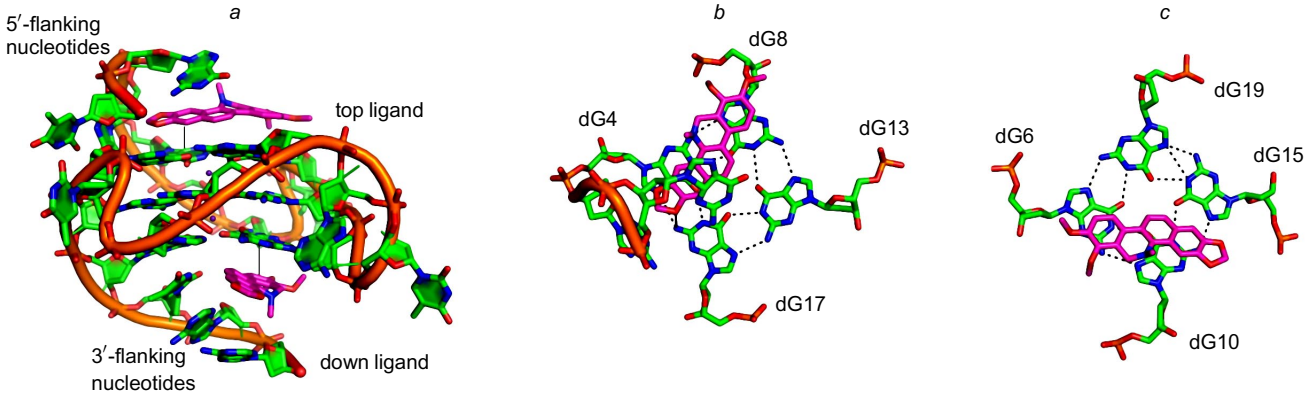


Figure 9. Structure of the complex of dihydrochelerythrine (**31**) with the c-Myc quadruplex determined by molecular modelling and molecular dynamics simulations (*a*), the top views of the complex stacking with the 5′-quartet (*b*) and the 3′-quartet (*c*).[86] Reproduced with the permission of Elsevier.

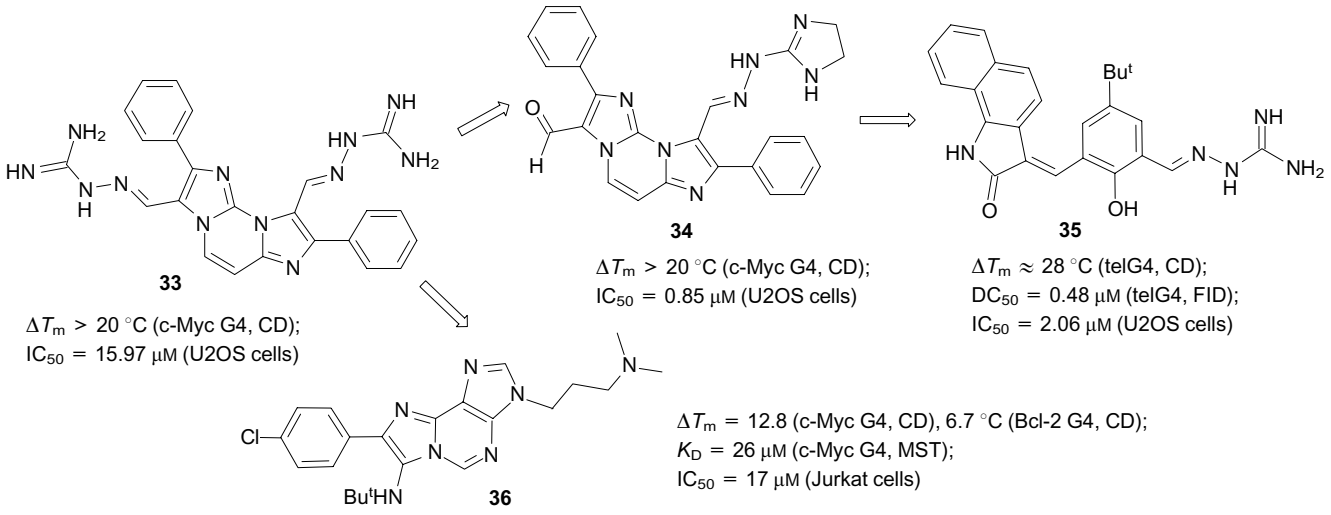


Figure 10. G4 Ligands **33** – **36** based on diimidazo[1,2-*a*:1′,2′-*c*]pyrimidines.

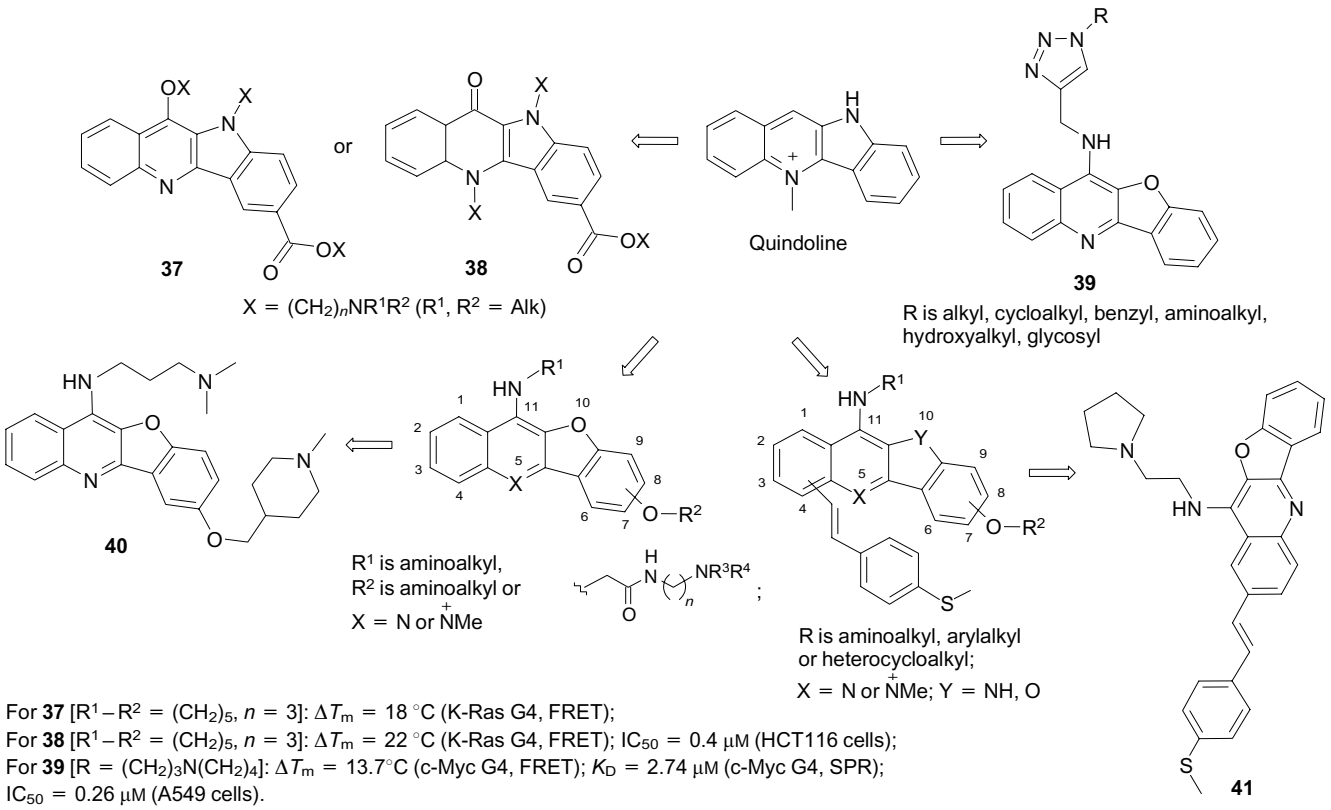
NMR study of ligand **34** demonstrated that it is stacked onto both 3′- and 5′-flanking G-tetrads of the parallel c-Myc and c-Kit2 quadruplexes; however, the differences in the NMR spectra suggest that additional hydrogen bonds are formed with c-Myc G4, resulting in a significant stabilization of the complex. It is worth noting that new G4 ligand **34** is an order of magnitude more efficient in inhibiting the cancer cell growth compared to its precursor **33**.

As part of continuing research, Amato *et al.*[91] applied another strategy for the modification of the molecular platform of the ligand (scaffold-hopping), by replacing the diimidazo[1,2-*a*:1′,2′-*c*]pyrimidine scaffold by pharmaceutically more relevant aromatic moieties. Based on the evaluation of the binding specificity, the authors selected derivative **35** (see Fig. 10). This compound better stabilizes parallel telG4 than other quadruplexes adopting the same topology (c-Kit1, c-Kit2, c-Myc) or hybrid telG4. A 50-fold excess of dsDNA did not change the values of ΔT_m for G4, which is indicative of high selectivity of derivative **35** as the G4 ligand. The visualization of G4 in U2OS human osteosarcoma cells confirms that pyrimidine **35** stimulates the formation of G4 foci at least at the level of the classical G4 ligand BRACO-19. The immunofluorescence microscopy study showed that compound **35** not only stabilizes G4 in U2OS cancer cells but also induces the formation of R-loops, composed of a hybrid (DNA/RNA) duplex and a displaced single-stranded DNA, simultaneously causing the cell death and micronucleus formation, which are characteristic of genome instability.

With the aim of designing a unique ligand and developing a new anticancer agent, Pelliccia *et al.*[92] continued the optimization of diimidazo[1,2-*a*:1′,2′-*c*]pyrimidines based on the structures of abundant naturally occurring (bioinspired approach) adenine, guanine and cytosine. The preliminary evaluation demonstrated that only imidazoadenine derivatives can stabilize the c-Myc and Bcl-2 quadruplexes. A compound library was synthesized by means of the three-component Groebke – Blackburn – Bienayme reaction and then screened for the ability to stabilize G4. Imidazo[2,1-*i*]purine derivative **36** (see Fig. 10) was found to have the highest stabilizing effect and high binding affinity only for c-Myc/Bcl-2 quadruplexes. The results of NMR spectroscopy and molecular docking provide evidence that imidazo[2,1-*i*]purine derivative **36** interacts with c-Myc G4 through π – π-stacking with the more accessible 5′-flanking G-tetrad and hydrogen bonding with the scaffold. It should be noted that ligand **36** binds to the Bcl-2 quadruplex in a totally different fashion. Thus, only hydrogen bonds but not π – π-stacking interactions are observed. Compound **36** exhibited selective cytotoxicity against Jurkat leukemia cells, in which the expression of the anti-apoptotic protein Bcl-2 plays a critical role in the regulation of cell viability. The treatment of Jurkat cells with ligand **36** caused a statistically significant decrease in the levels of both c-Myc and Bcl-2 mRNA and the proteins as such, resulting in the induction of apoptosis.

Quindoline derivatives (Fig. 11) is another promising chemotype for the design of ligands for four-stranded structures. The first structural modifications of this chemotype were reported about 15 years ago.[93,94] Brito *et al.*[95] synthesized a series of indolo[3,2-*b*]quinolines (see Fig. 11) bearing different aminoalkyl side chains. Compounds of this series can stabilize K-Ras G4, suppress the synthesis of the K-Ras protein through the inhibition of transcription and translation and induce colorectal cancer cell death through the activation of apoptosis. Derivatives **37** and **38** containing 3-piperidinopropyl groups (ΔT_m = 18 – 25 °C) have the highest affinity for K-Ras and HSP90A G4s. The SAR analysis led to contradictory conclusions. Thus, in some cases, the stability shift correlates with the basicity of the terminal amino groups of side chains, whereas in other cases this correlation is absent. The attachment of the third side chain at the oxygen (ligand **37**) or nitrogen (ligand **38**) atom of the pyridine moiety also does not provide an unambiguous answer to the question about the optimal structure of this class of ligands. The introduction of the morpholine moiety into the side chains leads to the loss of the ligand binding to G4, which is consistent with a decrease in the basicity of amino groups. The resulting compounds have low selectivity (SI = 2 – 6).

Zeng *et al.*[96] synthesized benzofuro[3,2-*b*]quinoline derivatives (see Fig. 11) as triazole-containing c-Myc quadruplex-binding ligands *via* click chemistry. The authors prepared a library of compounds containing alkyl, aryl, hydroxyalkyl, aminoalkyl groups and even carbohydrate



For **37** [$R^1-R^2 = (CH_2)_5$, $n = 3$]: $\Delta T_m = 18$ °C (K-Ras G4, FRET);
For **38** [$R^1-R^2 = (CH_2)_5$, $n = 3$]: $\Delta T_m = 22$ °C (K-Ras G4, FRET); $IC_{50} = 0.4$ μM (HCT116 cells);
For **39** [$R = (CH_2)_3N(CH_2)_4$]: $\Delta T_m = 13.7$°C (c-Myc G4, FRET); $K_D = 2.74$ μM (c-Myc G4, SPR);
$IC_{50} = 0.26$ μM (A549 cells).
For **40**: $\Delta T_m = 26.6$ °C (c-Myc G4, FRET); $K_D = 1.3$ μM (c-Myc G4, SPR); $IC_{50} = 4.7$ μM (RAJI cells).
For **41**: $\Delta T_m = 17.5$ °C (N-Ras RNA G4, CD); $K_D = 0.7$ μM (N-Ras RNA G4, SPR); $IC_{50} = 1.6$ μM (HCT116 cells)

Figure 11. G4 Ligands **37** – **41** based on quindoline derivatives and their analogues.

residues in the side chain of the triazole scaffold. The screening of the library using the FRET melting assay demonstrated that most of the compounds cause an increase in the melting temperature of the c-Myc quadruplex by more than 14 °C, whereas ΔT_m for the DNA duplex was at most 1.5 °C. A series of 27 compounds made it possible to perform the SAR analysis, which showed the following:

— amino, *N*,*N*-dimethyl(or diethyl)amino, pyrrolidine and piperidine derivatives, in which the amino group is linked to the scaffold through the C_2- or C_3-alkyl linker have the highest affinity;

— the presence of a primary amino group leads to a decrease in the selectivity for quadruplex structures;

— an alkyl or aryl group in the side chain causes a 2 – 3-fold decrease in ΔT_m compared with the highest observed values but slightly increases the selectivity, thereby providing evidence for an important role of stacking interactions with G-tetrads.

An important role of the triazole spacer (ligand **39**, see Fig. 11) was confirmed by experiments with a competitive duplex. The addition of a 62.5-fold excess of dsDNA does not virtually decrease ΔT_m of the quadruplex, whereas in the case of the analogue in which the (*N*,*N*-diethylamino)ethyl group is directly linked to benzofuro[3,2-*b*]quinoline, the addition of even 12.5 equiv. of competitive dsDNA decreases ΔT_m of the G-quadruplex down to zero. It should be noted that the SPR and MST assays revealed different lead compounds characterized by the highest ratio $K_D^{dsDNA}/K_D^{c\text{-Myc G4}}$. (In this case, candidates for the comprehensive evaluation of biological effects are generally selected upon complex analysis of the results of three or more methods.) Zeng *et al.*[96] clearly demonstrated the existence of the relationship between the stabilization of c-Myc G4 and the inhibition of the translation of c-Myc mRNA and the relationship between the apoptotic cancer cell death and the overexpression of the c-Myc gene. Lead compound **39** displayed relevant antitumour activity against the A549 human lung cancer xenograft model at a dose of 6.25 mg kg^{-1} comparable with the activity of doxorubicin used as the reference compound: the T/C ratio (treated to control, the ratio of the mean tumour volume of treated animals to the mean tumour volume in the control group) was 38%.

A treatment strategy for cancer using the expression of the c-Myc transcription factor is based on the blocking of the interaction between the NM23-H2 protein and the nuclease-hypersensitive element (NHE III1) of the c-Myc promoter,[97,98] the nucleotide sequence of which is rich in guanine and can form G4 DNA. A research group[99] at the Sun Yat-sen University (Guangzhou, People's Republic of China) described four series of c-Myc G4 ligands based on disubstituted furan analogues of quindoline — benzofuro[3,2-*b*]quinoline derivatives (see Fig. 11). Key differences between these series are variations in the position of the substituent R^2 and the nature of the spacer (alkyl or carboxamide) in R^2 and also the quaternization of the nitrogen atom of quinoline or the terminal amino group of the side chain at the 11 position. The addition of a second arm bearing a basic group (particularly at the 7 position) enhances the binding of the compounds to c-Myc G4, and

the quaternization of the N(5) atom leads to an increase in ΔT_m to a record value of 36.7 °C. However, the binding specificity ($K_D^{dsDNA}/K_D^{c\text{-}Myc\,G4}$) of these compounds was low and varied from 2.9 to 9.7. Ligand **40** (see Fig. 11) showed the highest inhibition of the NM23-H2/c-Myc interaction compared to the other derivatives (>80% at a concentration of 10 μM), resulting in a decrease in the expression of the c-Myc gene in RAJI Burkitt's lymphoma cells and the induction of cell death. Compound **40** also exhibited a significant antitumour effect on the RAJI Burkitt's lymphoma xenograft model (at a dose of 15 mg kg^{-1}, the T/C ratio was ~33%).

It is worth noting that the above-considered structures proved to be able to stabilize only polydeoxyribonucleotide quadruplexes but not RNA. In attempting to design RNA G4 ligands (RG4), the quindoline scaffold was hybridized with the styryl moiety (see Fig. 11), which was commonly used in molecules linked to RNA G4s.[100] It was shown that the introduction of the *p*-(methylthio)styryl side substituent enhances the specific binding to N-Ras RG4. Benzofuro[3,2-*b*]quinoline derivatives (Y = O) exhibit higher activity than indoloquinolines (Y = NH); the replacement of the terminal amino group by the hydroxy group, aryl or heteroaryl moiety leads to the loss of the G4-binding ability, and the methylation of the quinoline nitrogen atom causes a decrease in the selectivity for RG4. The affinity of lead compound **41** (see Fig. 11) for the RNA oligonucleotide is characterized by $K_D = 0.7$ μM and correlates with the inhibition of the cancer cell growth. Ligand **41** suppresses the translation of N-Ras *via* the binding to N-Ras RG4, inducing the G_0/G_1 phase arrest of the cell cycle and subsequent cell death. Therefore, these studies of the Chinese researchers demonstrated that RG4 ligands can be successfully employed to develop new anticancer agents targeting non-canonical nucleic acid structures.

Amato *et al.*[101] from the University of Naples Federico II described a focused library of compounds based on naphthoquinone-fused furobenzoxazines. This chemotype was found by the virtual screening of 6000 compounds. The subsequent experimental evaluation demonstrated that the hit compound (R = cyclo-C_6H_{11}, Fig. 12) stabilizes G4s both under extracellular conditions and in living cells.[102] The screening was performed using the original the G4-CPG assay (controlled pore glass support — a solid support based on controlled porosity glass), which employs affinity chromatography and allows the evaluation of the number of bound ligand molecules. Most of the new derivatives were bound to the telG4, c-Myc, c-Kit1, c-Kit2 and hTERT1 quadruplexes, but only ligand **42** did not interact with the duplex at all. The CD melting assay demonstrated that compound **42** stabilizes c-Myc G4, but has no effect on the duplex and telG4. According to the results of the experimental assay and computational calculations, ligand **42** binds to the c-Myc quadruplex groove, which may account for its high selectivity (Fig. 13). Almost all ligands in this series produced DNA damage (γH2AX and TRF1 markers), and ligand **42**, taken at a concentration of 2 μM, reduces HeLa cell viability to ~65%.

Zoidis *et al.*[103] described indeno[1,2-*c*]cinnoline derivatives containing a side chain bearing terminal amino groups with different structures, characterized their multiple effects on nucleic acids and enzymes of their synthesis. The compounds of this series (*e.g.*, ligand **43**, see Fig. 12) can stabilize telG4 and c-Kit G4, increasing the melting temperature as efficiently as berberine ($\Delta T_m = 9-12$ °C). The

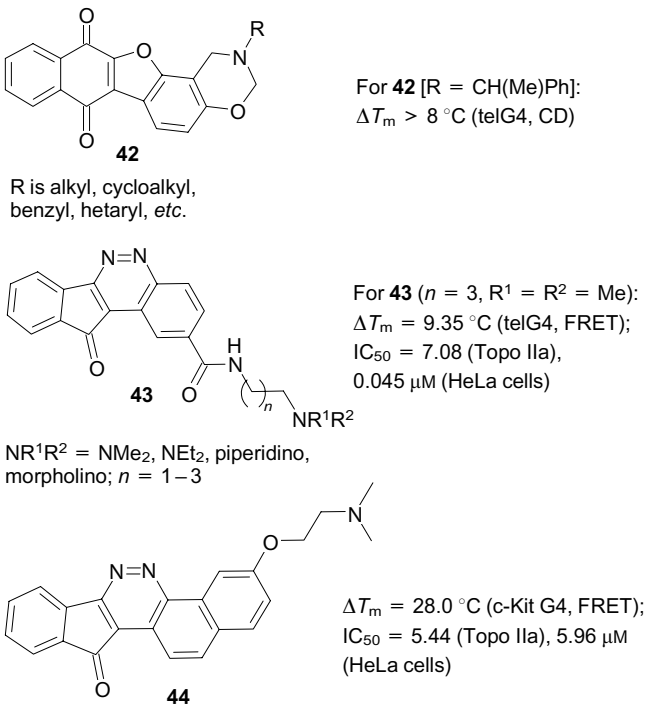


Figure 12. G4 Ligands **42**–**44** based on indeno[1,2-*c*]cinnoline derivatives.

increase in ΔT_m is proportional to the elongation of the side chain from the C_2- to C_4-linker; the replacement of the terminal *N*,*N*-dimethylamino group by other amine moieties (*N*,*N*-diethylamine, piperidine, morpholine) leads to a 2–4-fold decrease in the binding. The annulation of an additional benzene ring to the cinnoline moiety (compound **44** in Fig. 12) leads to a significant increase in the stability shift, which also confirms the importance of the size of the

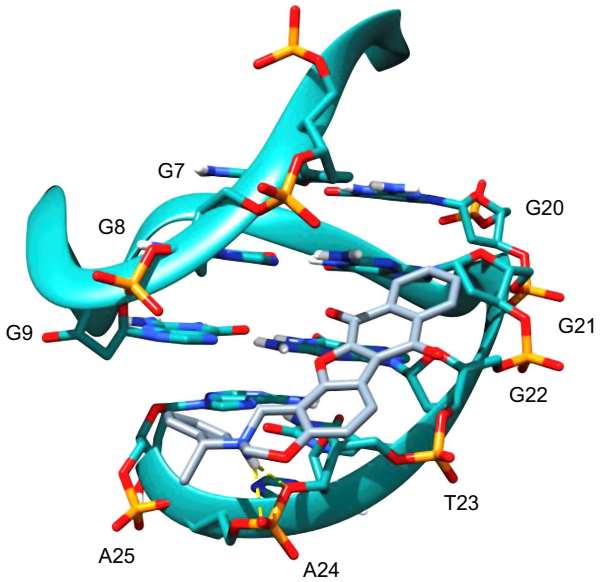


Figure 13. Molecular model (docking) of the binding of benzofuronaphthoquinone derivative **42** to c-Myc G4.[101] Reproduced with the permission of Elsevier.

planar surface of the ligands. The selectivity (SI) of ligands **43** and **44** evaluated from the values of ΔT_m varies from 3 to 6. However, it should be noted that the authors used a considerable (40-fold) excess of the ligand with respect to G4 in FRET melting experiments, which is, on the average, 4 – 8 times larger than that employed in other studies. The topoisomerase II (Topo IIα) inhibitory activity of ligands **43** and **44** is comparable with that of doxorubicin and, consequently, these derivatives exhibit multi-target action against cancer cells. However, the antiproliferative activity of cinnoline derivatives better correlates with the TopoIIα inhibiton than with the G4-stabilizing effect. Hence, the mechanism of the induction of cell death remains an open question.

Anthraquinone derivatives are the first chemical class that served as the platform for the development of G4 ligands as telomerase inhibitors described in the pioneering study of Hurley and co-workers.[104] Despite a rather comprehensive investigation of this class of compounds, new successful lines of research have emerged for the development of G4 ligands in recent years. Thus, Roy *et al.*[105] recently described a new type of G4 ligands based on anthraquinone containing oligopyrrole moieties of varying lengths in the side chains. Ligand **45** (Fig. 14) showed the highest affinity (K_D = 0.3 μM) for the c-Myc quadruplex. This ligand contains three terminal pyrrole-2-carboxamide moieties in the side chains at the 2 and 6 positions of the anthraquinone scaffold. Ligand **45** rather selectively binds to G4s. Thus, the constant K_D for c-Kit G4 is 380 times smaller than that for dsDNA. The molecular docking showed that the anthraquinone moiety stacks on the G-tetrad, and the pyrrolecarboxamide groups of the side chain interact with G4 grooves and phosphate groups. The authors used cyclic voltammetric titration to analyze the character of binding of G4 ligands. The observed positive shift of the half-wave potential ($E_{1/2}$) was considered as a consequence of intercalation or another stacking interaction. It is worth noting that ligand **45** exhibits specific biological activity. It blocks the replication of the G4-forming c-Myc polynucleotide and shows selective cytotoxic activity against cancer cells (see Fig. 14) compared to normal cells (IC_{50} > 100 μM).

Anthraquinones fused to the heterocyclic core, hetareneanthraquinones, have attracted great attention in the past few years. The multi-target action of these compounds, high activity against cancer cells with activated mechanisms of multidrug resistance and great synthetic potential for modification open up broad prospects for the potentiation and(or) combination of different mechanisms of antitumour

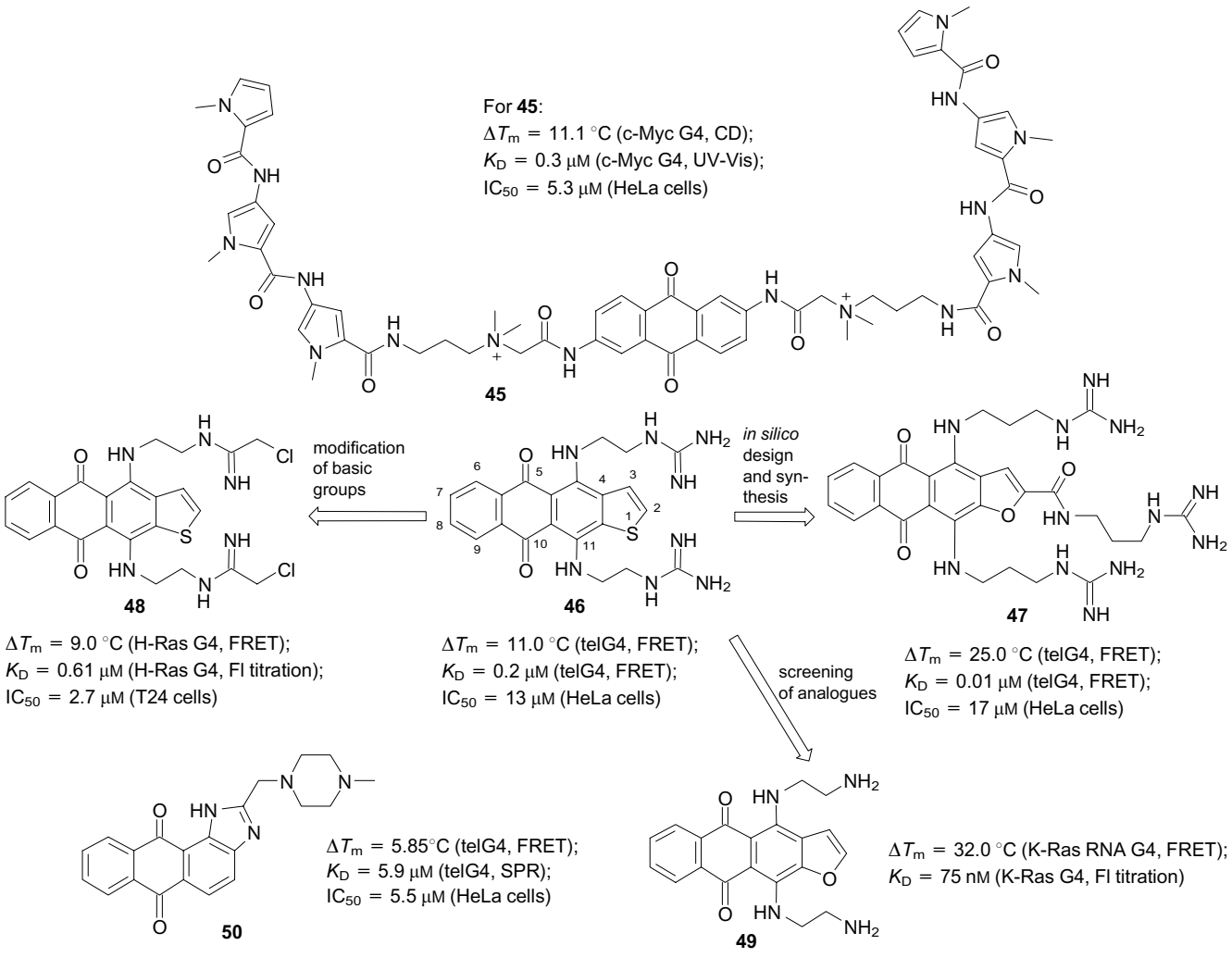


Figure 14. G4 Ligands **45** – **50** based on anthraquinones and their hetarene-fused derivatives.

activity of hetareneanthraquinones, in particular, for the design of specific G4 ligands.[106]

Bis(guanidino)anthrathiophene **46** (see Fig. 14) was the first G4 ligand described in the series of hetareneanthracenedinones. This compound has high affinity for telG4 and exhibits telomerase inhibitory activity at submicromolar concentrations.[107] Besides, bisguanidine **46** has high affinity for G4s in the c-Myc or H-Ras oncogene promoters (ΔT_m = 12–22 °C, K_D = 0.15–0.37 μM, FRET).[108] Dynamic duplex–quadruplex transitions play a key role in the regulation of transcription. Thus, the formation of two G4s (hras-1 and hras-2) in the H-Ras promoter region blocks the transcription of this oncogene. The binding of the MAZ transcription factor causes the unfolding of G4-elements in the promoter, resulting in the H-Ras transcription initiation.[109] It was shown that bisguanidine **46**, taken at micromolar concentrations, stabilizes the regulatory hras-1 and hras-2 G-quadruplexes and prevents their unfolding by the MAZ factor, thereby facilitating the blocking of H-Ras transcription and the selective suppression of its expression in cancer cells.

The structure–activity relationship analysis of G4 ligands based on anthrathiophenediones and anthrafurandiones revealed important relationships between the effect of side chains on the constants and the ligand binding selectivity for G4.[110,111] It was found that, although terminal basic groups with delocalized charges (such as guanidino and acetamidino groups) in side chains provide high affinity of ligands for a broad G4 panel, their introduction and an increase in the size of spacers lead to the uptake of the ligands in cancer cells.

The model of the complex of bisguanidine **46** with telG4 (Fig. 15) obtained by the docking and molecular dynamics simulations was successfully used for the rational design of a new generation of G4 ligands.[112] According to the results of molecular modelling, an increase in the spacer length and the introduction of an additional guanidine-containing side chain into the heterocyclic scaffold lead to a 2–2.5-fold increase in the stability shift of the complex of trisguanidine **47** (see Fig. 15) with telG4 and a 10–15-fold increase in the binding constant due to the ionic interaction energy and hydrogen bonding of the ligand to the target. Besides, three-armed ligands have much higher specificity for G4 compared to duplex DNA (up to 75 times for ligand **47**). However, compounds of this type exhibit moderate antiproliferative activity (IC_{50} = 9–21 μM) due to a decrease in their transport across cell membranes as a results of the introduction of an additional guanidine group.

The structural optimization of the terminal groups of bisguanidine **46** afforded ligands for the H-Ras oncogene promoter with high *in vitro* and *in vivo* antitumour activity.[113] It was demonstrated that the replacement of guanidine groups by chloroacetamidine moieties results in the improvement of the cellular uptake due to an increase in the lipophilicity of the ligand with the retention of high basicity and the bidentate binding ability of amidines towards phosphate groups of the G4 scaffold. The binding constants of bis(chloroacetamidine) **48** (see Fig. 14) to different G4 structures are similar to those of bisguanidine **46**, whereas the intracellular concentrations of compound **48** in cancer cells are an order of magnitude higher. Besides, bis(chloroacetamidine) **48** down-regulates transcription of the H-Ras oncogene through the stabilization of regulatory hras-1 and hras-2 G-quadruplexes and, at micromolar concentrations, causes a statistically significant decrease (up to 95%–99%) in the amount of the H-Ras translation product ($p21^{HRAS}$ protein) in cancer cells. Anthrathiophene **48** exhibits high antitumour activity in the T24 bladder cancer xenograft model. Thus, the use of this agent four times at a dose of 1.7 mg kg^{-1} causes the tumour growth inhibition (TGI) by 50%–55% and a 70% increase in the life span of animals.

As mentioned above, RG4 structures, which were found recently in 5′-untranslated regions of mRNA of some oncogenes, serve as a relatively new target for the development of anticancer agents. Dynamic transitions from RNA hairpins to RG4 structures play an important role in the regulation of translation. The screening of a series of analogues of bisguanidine **46** revealed anthra[2,3-*b*]furan-5,10-dione **49** (see Fig. 14)[114] exhibiting high affinity for RG4s. Ligand **49** stabilizes all three RG4 elements (*utr*-1, *utr*-4 and *utr*-z) located in the 5′-untranslated region of K-Ras mRNA (K_D = 75–251 nM, ΔT_m > 30 °C), whereas other ligands, including bis- and trisguanidines have lower affinity for RG4s.[115] Besides, the uptake of ligand **49** in

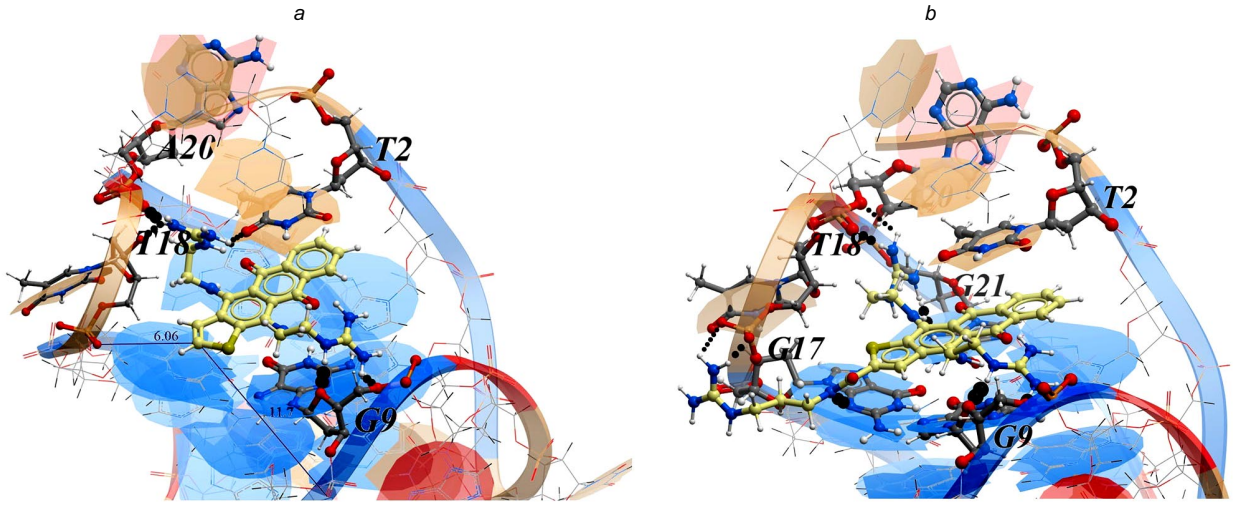


Figure 15. Molecular models (docking + molecular dynamics) of the binding of ligands **46** (*a*) and **47** (*b*) to telG4, which demonstrate the possibilities of the rational design of new-generation G4 ligands.[112] Reproduced with the permission of Elsevier.

cancer cells is 1 – 2 orders of magnitude more efficient compared to related anthrathiophenediones. The stabilization of the *utr*-1, *utr*-4 and *utr*-z RG4 elements by ligand **49** hinders the binding of the K-Ras transcript to ribosome and leads to the selective blocking of translation of this oncogene and a dose-dependent decrease in the $p21^{K\text{-}Ras}$ protein levels in Panc-1 pancreatic cancer cells at micromolar concentrations. Anthrafuran **49**, taken at submicromolar concentrations, causes the activation of caspase 3, mediating the cleavage of the PARP enzyme and inducing apoptosis in Panc-1 pancreatic adenocarcinoma cells with high expression of the K-Ras oncogene.

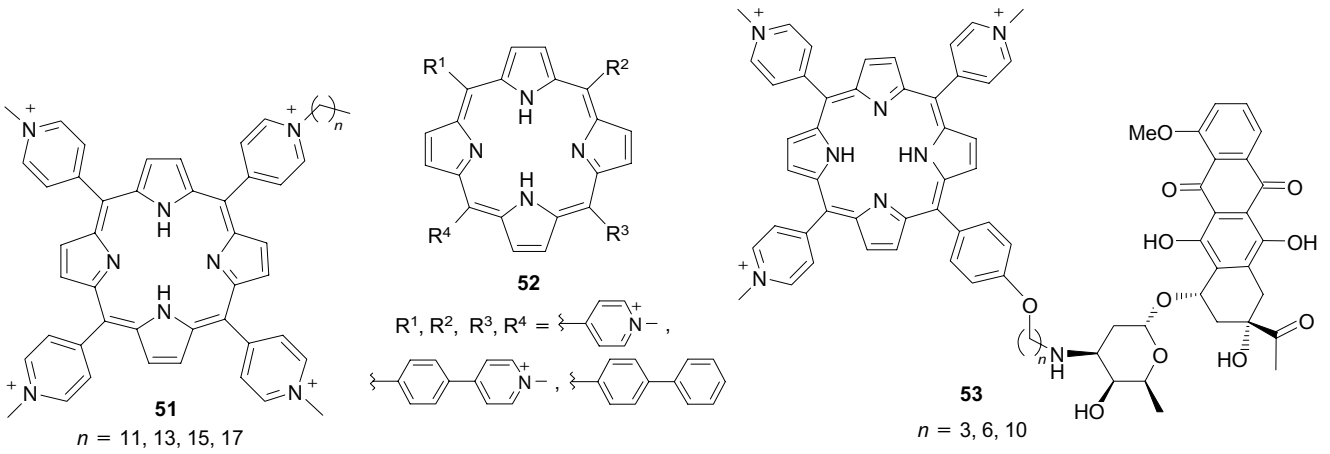
Angular hetareneanthraquinones also have G4-binding ability. 2-(*N*-Methylpiperazino)methylanthraimidazole **50** (see Fig. 14) shows selectivity for the telG4 (3 + 1)-hybrid, stabilizing neither the antiparallel form nor the duplex DNA.[116] The quaternization of the *N*-methyl group of the piperazine moiety in ligand **50** leads to an increase in ΔT_m by 1 – 2 °C but causes the complete loss of antiproliferative activity.

3. Macrocycic G4 ligands

The chemical diversity of G4 ligands based on macrocyclic organic compounds is much lower compared to polycyclic quadruplex ligands. However, their biological properties are of no less importance. The first and most important representatives of macrocyclic G4 ligands are synthetic *meso*-tetrakis(*N*-methyl-4-pyridyl)porphyrin (TMPyP4) and telomestatin (see Fig. 2), the secondary metabolite isolated from *Streptomyces anulatus*. The ability of these compounds to bind to nucleic acid quadruplexes with various topologies was discovered more than twenty years ago.[117, 118] Nevertheless, researchers working in this field still find new approaches to modify these unique molecules.

As shown above, the TMPyP4 porphyrin displays photosensitizing activity and has high affinity for different G4 elements.[119] However, quaternized pyridine moieties in the TMPyP4 molecule impair the penetration of this compound across cell membranes, which significantly interferes with the evaluation of its biological properties and limits its practical application. The replacement of one methyl group in TMPyP4 by an aliphatic n-C_{12} – C_{18} chain allowed the synthesis of efficient photoactive RG4 ligands (Fig. 16), which, unlike the starting compound, can penetrate into cancer cells.[120] The introduction of the tetradecyl substituent not only leads to a 2 – 3-fold increase in the binding constant of ligand **51** to RG4 in the 5′-untranslated region of K-Ras mRNA (*utr*-1, *utr*-4 and *utr*-z) but also causes an increase in the accumulation of porphyrin in the cancer cell cytoplasm by two orders of magnitude. The synthesis of biotinylated analogue **51** and the subsequent biotin-streptavidin assay (pull-down assay) demonstrated that the designed G4 ligands have high *in cellulo* binding specificity for K-Ras mRNA. The treatment of cancer cells with nanomolar concentrations of ligand **51** and the subsequent irradiation with light of a wavelength of 660 nm cause the reactive oxygen species (ROS)-induced degradation of the K-Ras transcript, resulting in a decrease in metabolic activity of cancer cells followed by the induction of tumour cell apoptosis and death. The antitumour activity of compound **51** as a representative of a new class of RG4-selective photosensitizers was confirmed in the Panc-1 pancreatic mouse subcutaneous tumour xenograft model. The single injection of this compound at a dose of 3 mg kg^{-1} followed by the irradiation of the tumour with a diode laser induces a statistically significant tumour growth retardation (by 72% – 53%) two weeks after the treatment, while the starting G4 ligand TMPyP4 was found to be inactive even at a dose of 30 mg kg^{-1}.

Jin *et al.*[121] synthesized a series of cationic porphyrins by expanding the conjugated system of substituents at the *meso* positions of the porphyrin core to enhance interactions with G-tetrads. The physicochemical study of the interactions between the new derivatives and telG4 demonstrated that the replacement of the *N*-methylpyridinium moiety by the 4-(*N*-methylpyridinio-4-yl)phenyl group has almost no effect on the G4-binding affinity of the ligands, whereas the introduction of uncharged biphenyl groups into the porphyrin impairs the binding ability proportional to the number of these substituents. The best binding characteristics were observed for porphyrin **52** (see Fig. 16) contain-



For **51** (n = 13): K_D = 107 nM (K-Ras RNA G4, FI titration); EC_{50} = 13.7 nM (Panc-1 cells)

For **52** (R^1 — 4-(1-methylpyridinio-4-yl)phenyl; R^2 = R^3 = R^4 — 1-methylpyridinio-4-yl): ΔT_m = 12.4 °C (telG4, FRET); K_D = 0.12 μM (telG4, UV-Vis); IC_{50} = 6.33 μM (Ag8.653 cells)

For **53** (n = 6): ΔT_m (FRET) = 14.2 (telG4), 6.7 °C (i-motif); K_D (FID) = 0.1 (telG4), 0.2 μM (i-motif)

Figure 16. G4 Ligands **51** – **53** based on *meso*-tetra(pyridin-4-yl)porphyrin.

ing one 4-(*N*-methylpyridinio-4-yl)phenyl group and three *N*-methylpyridinium groups. The interactions of these groups with telG4 were demonstrated by surface-enhanced Raman spectroscopy (SERS), which is rarely used to investigate the properties of G4 ligands. The antiproliferative activity of the new ligands was about 10 – 20 times lower than that of the starting TMPyP4 and was observed only upon visible light irradiation.

This research group [122] also described hybrid compounds containing TMPyP4 porphyrin and rubomycin moieties and evaluated their binding to the DNA G-quadruplex and i-motif. Despite the valuable properties of these moieties of such heterodimers, the factors responsible for the conjugation between the duplex ligand (rubomycin) and the G-quadruplex ligand (TMPyP4) are unclear and were not discussed in the publication. It was found that the ligands provide somewhat better stabilization of DNA G4s over the i-motif, as evidenced by an increase in the stabilization temperature and the binding constant. The C_6-linker (compound **53**, see Fig. 16) imparts flexibility to the heterodimers and enhances their binding to both G4s and the i-motif. This is apparently attributed to the fact that the second binding site becomes accessible.

Over twenty years of investigation of telomestatin as the G4 ligand, the chemical modification of its structure was developed along the following main lines of research:

— evaluation of the effect of the number of side chains, their structures and mutual arrangement;

— variations in the macrocycle size and the replacement of particular heterocyclic units;

— replacement of the macrocyclic scaffold by an acyclic moiety.

Despite of extensive available data, seemingly well-described structure – activity relationships and the known potential and limitations of the practical application of this class of derivatives, several groups continued research on optimization of the structures of telomestatin and its analogues.[123, 124]

Nagasawa and co-workers [125, 126] published a series of studies aimed to design DNA G4 ligands based on hexaoxazole macrocycle **54**. In recent studies, two unsymmetrical macrocycles **55** and **56** [125] and two derivatives **57** and **58** (Fig. 17) containing four ω-amino(or guanidino)alkyl side chains [126] were synthesized and characterized. Unsymmetrical analogues **55** and **56** show lower thermal stabilization towards telG4s compared to symmetrical ligand **54** but the selectivity over duplex DNA is retained. The introduction of two additional side chains (compounds **57** and **58**) leads to an increase in ΔT_m to 25 °C. The most interesting result of modification of the hexaoxazole macrocycle is that ligands with different G4 topologies can be employed for the modulation. Thus, the starting symmetrical macrocycle **54** induces the folding of the oligonucleotide into (2 + 2)-antiparallel G4s; isomeric ligands **55** and **56** change the topology towards the (3 + 1) hybrid, and compounds **57** and **58** induce the formation of the G4 (4 + 0)-parallel topology. The calculation of the molecular geometry demonstrated that the isomerization of ligand **54** leads to distortion of the planarity of the polycyclic moiety in ligands **55** and **56** ($\Delta \approx 30°$). Molecular modelling calculations demonstrate that additional side chains in derivatives **57** and **58** interact with lateral loops of G4 adopting (4 + 0)-parallel topology and enhance the complexation, whereas (2 + 2)-antiparallel G4s, on the contrary, cause steric hindrance.

Based on the structure of the complex of **54** with telG4, the rational design of a new series of its analogues was performed relying on the assumption that the additional flexible side chain bearing terminal amine should be located

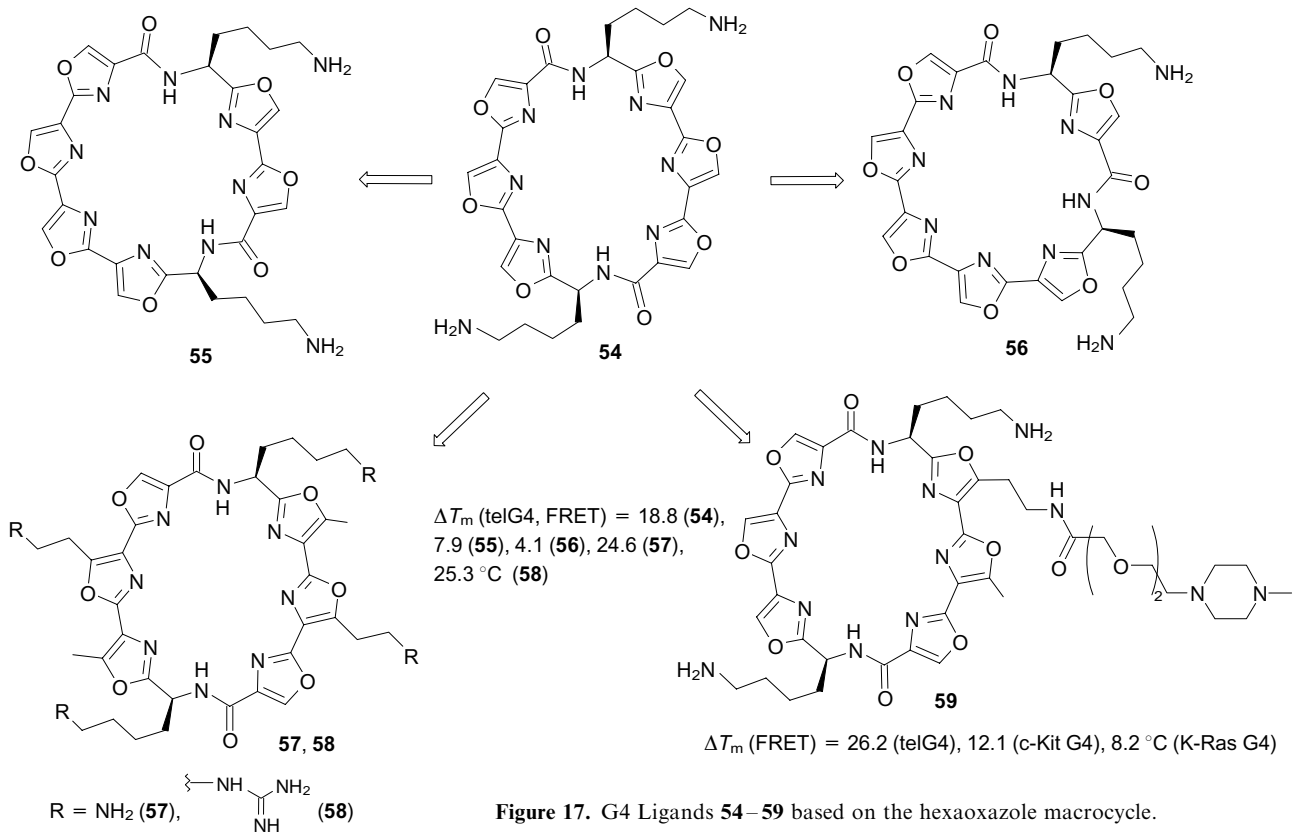


Figure 17. G4 Ligands **54** – **59** based on the hexaoxazole macrocycle.

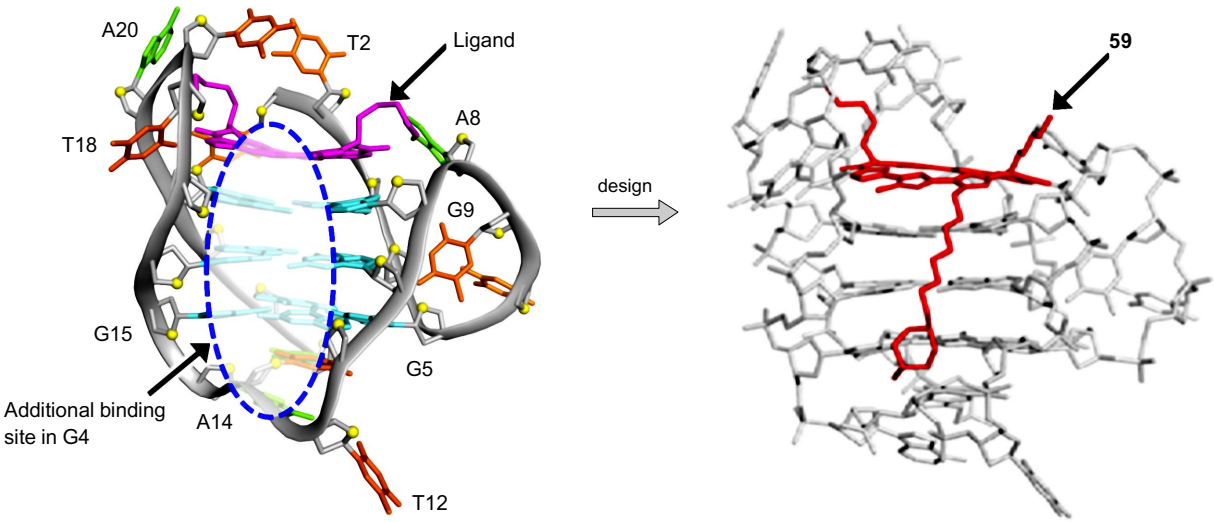


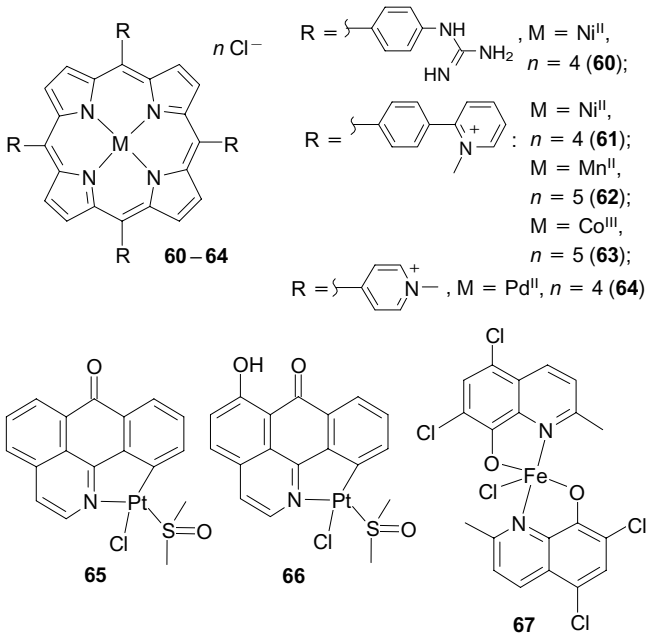
Figure 18. Design of ligand **59** based on the NMR molecular model of the binding of telomeric G4 to the precursor of compound **59** in which the amide-containing side chain is replaced by the methyl group.[127] Reproduced with the permission of MDPI (Multidisciplinary Digital Publishing).

in the groove of antiparallel G4 and additionally contribute to the binding energy due to an ionic component (Fig. 18).[127] The evaluation showed that in this series, derivative **59** (see Fig. 17) containing the *N*-methylpiperazine moiety linked to the macrocycle by the diethylene glycol spacer has the highest affinity for telG4 with antiparallel topology rather for parallel G4s in the c-Kit and K-Ras oncogene promoters.

4. G4 ligands based on metal complexes

Apart from organic molecules, metal complexes have recently attracted great attention as low-molecular-weight G4 ligands due to their specific chemical and biological properties and high binding selectivity to oligonucleotides. Advantages of the construction of G4 ligands based on metal complexes are the synthetic accessibility and the controlled change of the geometry and charge of the central metal ion. The structural diversity of metal complexes provides a large number of binding modes. For instance, the π-stacking with terminal G-quartets is preferable for planar molecules, whereas nonplanar molecules can be involved in alternative interactions, such as the binding in G4 grooves or loops. As shown below, many metal complexes have unique optical, magnetic or catalytic properties and exhibit antitumour activity.

Sabater *et al.*[128] synthesized Ni^{II} and Co^{III} *meso*-tetra(guanidinophenyl)porphyrin complexes and evaluated their ability to stabilize telG4s. The introduction of metal ions leads to a significant change in the properties of this type of ligands. First, the presence of metal decreases the electron density in the porphyrin core of the ligand, thereby increasing the contribution of cation – π-stacking interactions. Second, the location of the G4 ligand in such a way that the metal ion is positioned above the cenre of the G-tetrad results in an increase in the contribution of its electrostatic interaction with G4s. Nickel complex **60** (Fig. 19) exhibits higher stabilization towards telomeric G-quadruplex compared to its analogue based on Co^{III} and free porphyrin and displays a good selectivity over dsDNA (ΔT_m < 5 °C). Ligand **60** exhibits cytotoxic activity



For **60**: ΔT_m = 13 °C (telG4, FRET); K_D = 20 nM (telG4, SPR); IC_{50} = 7 – 8 μM (A549 cells).
For **61** – **63**: ΔT_m (telG4, FRET) = 12 (**61**), 25 (**62**), 16 °C (**63**).
For **63**: K_D = 17 nM (telG4, SPR).
For **64**: ΔT_m = 30.9 °C (telG4, FRET); K_D = 0.1 μM (telG4, UV-Vis).
For **65**: ΔT_m (FRET) = 6.83 (telG4), 12.83 °C (c-Myc G4); DC_{50} (FID) = 2.50 (telG4), 1.35 μM (c-Myc G4); IC_{50} = 4.8 μM (SKOV3/DDP cells).
For **66**: ΔT_m (FRET) = 8.54 (telG4), 14.54 °C (c-Myc G4); DC_{50} (FID) = 1.31 (telG4), 0.55 μM (c-Myc G4); IC_{50} = 4.5 μM (SKOV3/DDP cells).
For **67**: IC_{50} = 5.04 μM (Hep-G2 cells)

Figure 19. G4 Ligands **60** – **67** based on metal complexes of porphyrin, azabenzanthrone and 8-hydroxyquinoline.

against human cancer cells and induces the displacement of the hPOT1 protein from telomeres, which is indirect evidence of G4 stabilization at the cellular level.

In continuation of this line of research, Ni^{II}, Mn^{III} and Co^{III} phenylpyridinium-containing porphyrin complexes were synthesized and characterized.[129] Metalloporphyrins **61** – **63** (see Fig. 19) induce an increase in thermal stabilization of the telomeric quadruplex in the ΔT_m range from 12 to 25 °C. In this series, complex **63** with Co^{III} exhibited the highest quadruplex-binding affinity and a three orders of magnitude weaker affinity for the duplex. The ^1H NMR study showed that the ligand binds to the extremal G-quartet by stacking, which is characteristic of this class of G4 ligands.

Sabharwal *et al.*[130] demonstrated that the complexation of the well-characterized G4 ligand TMPyP4 with the transition metal ions Pt^{II} and Pd^{II} increases the stabilizing activity towards telG4s up to $\Delta T_m \approx 30$ °C (see compound **64** in Fig. 19). The difference in the activity of the platinum and palladium porphyrin complexes was insignificant. The fluorescence of both complexes is enhanced upon the binding to DNA secondary structures; however, they showed no preference for a particular architecture of oligonucleotides.

Chen *et al.*[131] synthesized organic complexes based on Pt^{II} and 1-azabenzanthrone.[131] Compounds **65** and **66** (see Fig. 19) selectively displace the competitive fluorescent dye from the telG4 and c-Myc G4 sequences [the ligand concentration required to displace half of the dye (DC_{50}) is 0.5 – 2.5 μM, FID], resulting in considerable increase in the thermal stabilization temperature. Both parameters (DC_{50} and ΔT_m) indicate that nonmetallated azabenzanthrone derivatives display a weaker binding affinity for G4s and, consequently, this chemical modification is promising for the development of G4 ligands. The antiproliferative activity of azabenzanthrone complexes **65** and **66** is higher than that of the reference compound (cisplatin) against cisplatin-resistant ovarian cancer cells (SKOV3/DDP), and the effect of these compounds on non-tumour cells is minor ($IC_{50} > 100$ μM). The mechanism of anticancer action of Pt azabenzanthrone **66** is through the inhibition of telomerase activity and interactions with telG4, c-Myc G4 and Bcl-2 G4. Both complexes show a statistically significant anticancer activity *in vivo*. Thus, these compounds, injected as a single dose of 6 mg kg^{-1}, more efficiently retard tumour growth in colon (HCT-8) and lung (NCI-H460) cancer xenograft models than cisplatin at a dose of 2 mg kg^{-1}.

It was shown that iron(III) complex **67** based on 8-hydroxyquinolinol (see Fig. 19)[132] exhibits a cytotoxic effect comparable to that of cisplatin against five cancer cell lines. The investigation of the mechanism of action demonstrated that, unlike cisplatin, compound **67** inhibits telomerase activity by suppressing the c-Myc and hTERT gene expression. Experiments using c-Myc gene transfection into Hep-G2 cells demonstrated that the addition of 5 μM complex **67** leads to a twofold decrease in luceferase luminescence. The authors attributed this effect to the blocking of c-Myc gene transcription through the stabilization of regulatory quadruplexes in the promoter region. However, the physicochemical parameters of the interaction of complex **67** with G4s were not reported.

Complexes of 1,10-phenanthroline derivatives are widely used as metal catalysts in organic chemistry.[133] Due to photo- and physicochemical properties, such compounds are a promising platform for the development of G4 ligands. Two new G4 and RG4 ligand based on the Pt^{II} complex with the azabis(phenanthroline) scaffold were described.[134] Ligands **68** and **69** (Fig. 20) stabilize thermal denaturation of the telomeric DNA sequence with the maximum values of ΔT_m equal to 40 and 38 °C, respectively. The replacement of the methyl group (ligand **68**) by the piperidinoethyl group (ligand **69**) leads to a decrease in the binding ability. It is worth noting that complexes **68** and **69** show good binding affinity for RG4s, although this effect towards the G4-forming polyribonucleotide is much weaker. These compounds have higher affinity for G4s with antiparallel basket-type topology than for the parallel topology, the ligand being stacked on top of the external G-quartet. Azabisphenanthroline complexes **68** and **69** inhibit tumour cell growth at micromolar concentrations (MTT assay). Hence, compounds of this series can be considered as promising anticancer agents.

It should be noted that most of the above-described ligands interact with G4s through π – π-stacking. Data on the compounds specifically recognizing G4 groove and(or) loops are rather scarce. Apparently, this is due to the polymorphism of G4 structures, which largely depends on the nucleotide sequence, the concentration and composition of the ionic medium and is related to the lack of data on the 3D structures of G4s under physiological conditions. Meanwhile, studies aimed at the synthesis of compounds capable of selectively recognizing G4 grooves or loops have been published in recent years.

Thus, Duskova *et al.*[135] suggested that the introduction of a carbohydrate residue can enhance the binding to DNA grooves and that the planar heteroaromatic system can interact with G4s by stacking. The authors synthesized a series of Cu^{II} complexes with 1,10-phenanthroline and different carbohydrate derivatives (see Fig. 20). All the synthesized glycosides moderately stabilize telomeric oligonucleotides, having no effect on the DNA hairpin ($\Delta T_m < 1$ °C). In this series, L-rhamnoside (ligand **70**) displayed the highest affinity. All ligands have higher binding affinity for G4 hybrid topology over the antiparallel basket-type quadruplex. Derivatives of this series do not show high affinity or selectivity, but they are of interest as compounds for which both stacking and recognition of G4 grooves and(or) loops play a key role.

By continuing research in this area, Jäger *et al.*[136] synthesized glycosylated Cu^{II} complexes with diazafluorene (see Fig. 20). In general, the replacement of 1,10-phenanthroline in the ligands leads to a weakening of the stabilizing effect towards telG4s, and the largest values of ΔT_m were observed for β-D-glucopyranoside and its 2-deoxy analogue (ligand **71**). It is worth noting that compound **71** inhibits the tumour cell growth at micromolar concentrations, whereas IC_{50} for its β-D-glucopyranoside analogue is higher than 100 μM.

Chen *et al.*[137] synthesized and characterized several Ru^{II} complexes with 1*H*-imidazo[4,5-*f*]-1,10-phenanthrolines. Derivative **72** (see Fig. 20) containing the 4-guanidinophenyl substituent in the imidazole ring proved to be more selective for telG4s compared to promoter G4s and the duplex. Changing the position of the guanidino group from the 4 to 3 position of the benzene ring have no effect on the thermal stability temperature but decreases the binding constant to telG4s by an order of magnitude. The Job plot analysis of the stoichiometry of the complex of phenanthroline **72** with telG4 showed that three ligand molecules interact with one G4 molecule. Based on the analysis of

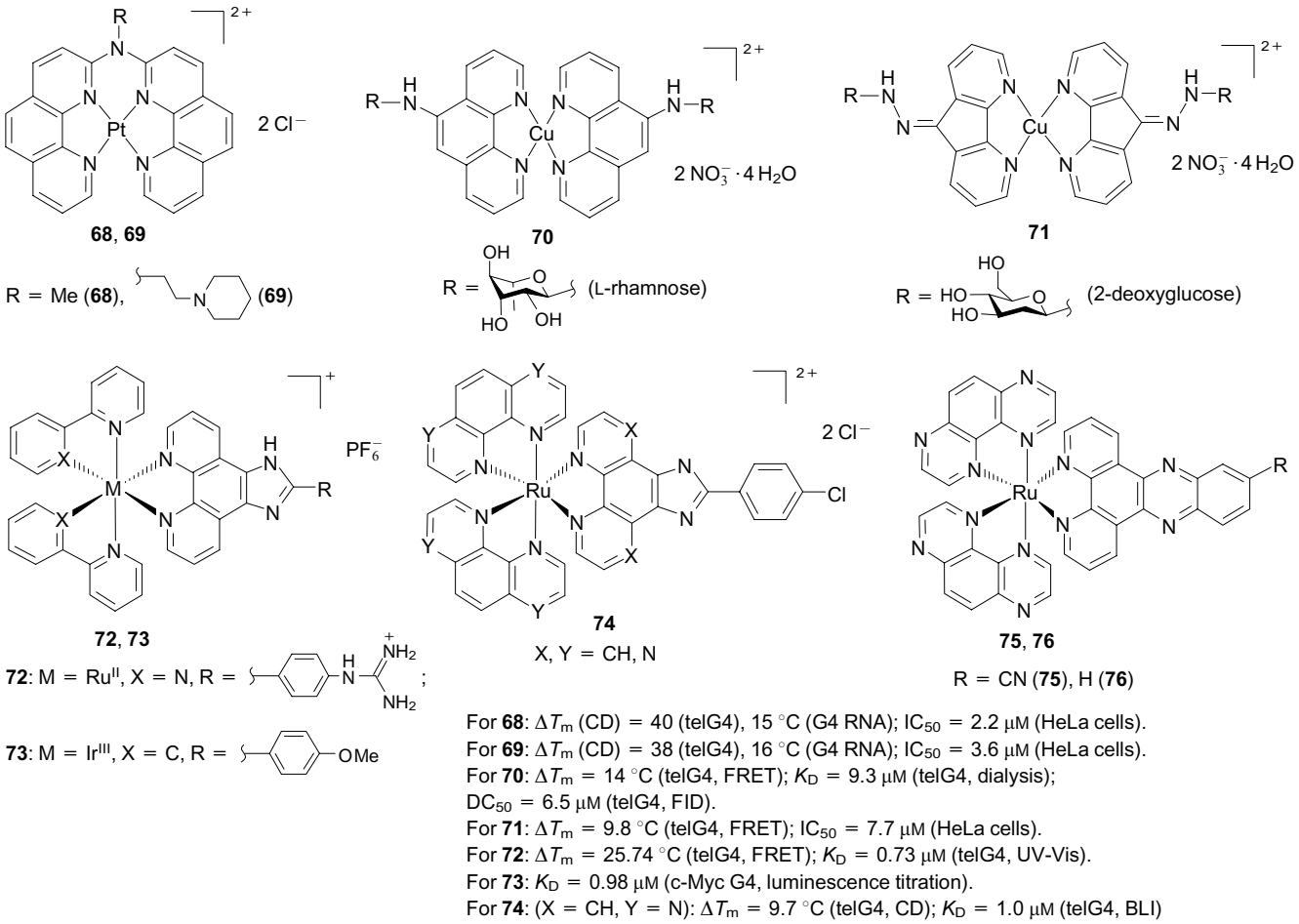


Figure 20. G4 Ligands **68** – **76** based on metal complexes of 1,10-phenanthroline, 1,10-phenanthroimidazole and 1,4,5,8-tetraazaphenanthroimidazole.

the changes in the circular dichroism spectrum, the authors suggested that ligand **72** intercalates into telG4.

In recent years, iridium complexes have attracted increasing interest as labels for the binding and detection of biomolecules.[138] The distinguishing features of iridium complexes are high quantum yields, long luminescence lifetimes and large Stokes shifts, which meet the key requirements for probes for the visualization of DNA strands. A series of Ir^{III} 1,10-phenanthroimidazole complexes, capable of exhibiting luminescence when bound exclusively to G4s, were described by Castor *et al.*[139] The affinity (K_D) of the derivatives for the c-Myc and telG4 G-quadruplexes is in the submicromolar concentration range. The authors showed that ligand **73** (see Fig. 20) discriminates between duplex DNA and telG4 in the agarose gel electrophoresis staining assay by causing specific luminescence enhancement. Therefore, this class of compounds can be considered as highly promising for the development of selective probes for G4s, overcoming the drawbacks of fluorescent bioimaging agents.

Weynand *et al.*[140] synthesized ruthenium(II) complexes based on 1,10-phenanthroimidazole and 1,4,5,8-tetraazaphenanthroimidazole (see Fig. 20) targeting nucleic acid secondary structures and having unusual photooxidizing action. The evaluation by different methods [SPR, CD and biolayer interferometry (BLI)] demonstrated a good ability of the ligands to form complexes with telG4s but not with duplex DNA. Based on the results of molecular docking, the authors suggested that derivative **74** can bind to telG4 in two ways (Fig. 21): through π – π-stacking with the G-tetrad or the insertion of the complex into the TTA loop of G4. Ligand **74** is well accumulated in U2OS osteosarcoma cells and shows photocytotoxicity. Thus, the irradiation in the presence of 10 μM compound **74** caused 100% cell death, while the inhibition of the growth of non-irradiated tumour cells was < 5%. Apparently, the observed photocytotoxicity is associated with the selective degradation of telomeric fragments through a type II photoreaction (*i.e.*, the formation of singlet oxygen) or photoinduced electron transfer (PET). If these assumptions will be confirmed by the comprehensive biological evaluation announced by the authors, such metal complexes will be the first highly phototoxic compounds targeting telomeric DNA without influencing telomerase inhibition.

McQuaid *et al.*[141, 142] studied the interactions of chemically structurally similar Ru^{II} complexes **75** and **76** (see Fig. 20) with intermolecular G4 (Fig. 22) consisting of four strands of d(TAGGGTTA). Upon the crystallization of complex **75** (the so-called Λ enantiomer, see Fig. 22 *a*), the parallel d(TAGGGTTA) tetraplex is transformed into the antiparallel form (see Fig. 22 *b*), in which guanine of the G-tetrad is adjacent to complex **75** at the 5′ end of the quadruplex core; the same topological changes occur in solution. The Δ enantiomer of **75**, on the contrary, is

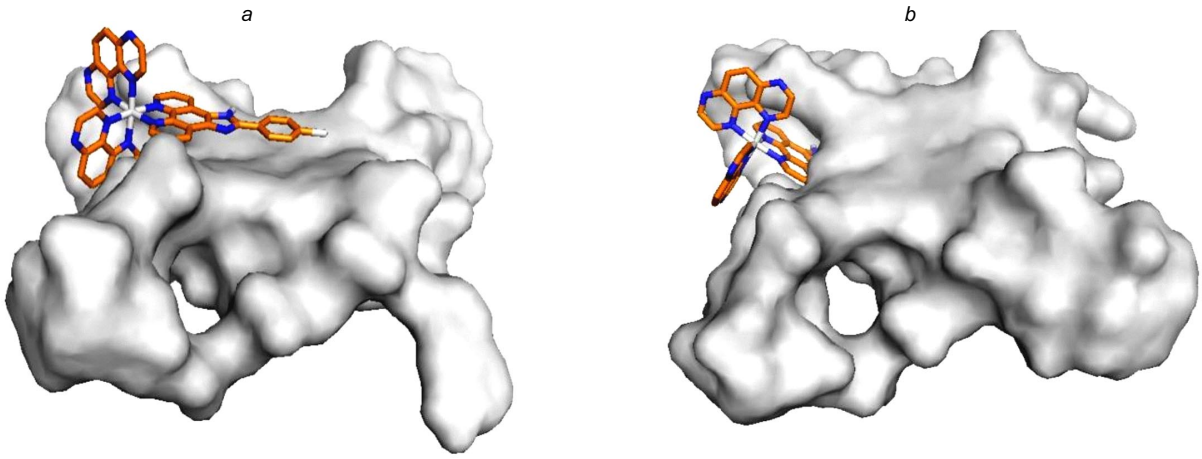


Figure 21. Molecular models (docking) of the interaction between complex **74** and telG4: π-stacking with the G-tetrad (*a*) and the interaction with the TTA loop (*b*).[140] Reproduced with the permission of Wiley.

stacked at the ends of the complex, which do not form G-quartets (see Fig. 22,*b*). These differences demonstrate the potential of the rational design of luminescent probes and G4-specific photochemical 'nucleases' based on metal complexes.

Relying on the empirical observation that ligands containing polyaromatic moieties (*e.g.*, anthracene, naphthalene, benzopyrene) have high selectivity towards G4s, Gama *et al.*[143] synthesized a series of Pt^{II} and Cu^{II} anthracene-containing tripyridine complexes. Complexes **77** and **78** (Fig. 23) stabilize c-Myc G4 and the telomeric quadruplex with good selectivity over duplex DNA. One can observe that the platinum(II) complexes have a much higher binding affinity for the c-Myc G-quadruplex. The metallation of free ligands by platinum ions leads to a 3 – 7-fold increase in ΔT_m, whereas the introduction of a Cu^{II} ion has almost no effect on the properties of anthracene-containing tripyridines. The binding constants of complexes **77** and **78**, which were determined by spectroscopic titration, have similar values, whereas the affinity of the non-metallated ligands is three orders of magnitude lower. The introduction of a longer (diethylene glycol) linker between the tripyridine and anthracene moieties leads to a slight enhancement of the interaction between the ligand and G4 compared to the monoethylene glycol-bridged analogue.

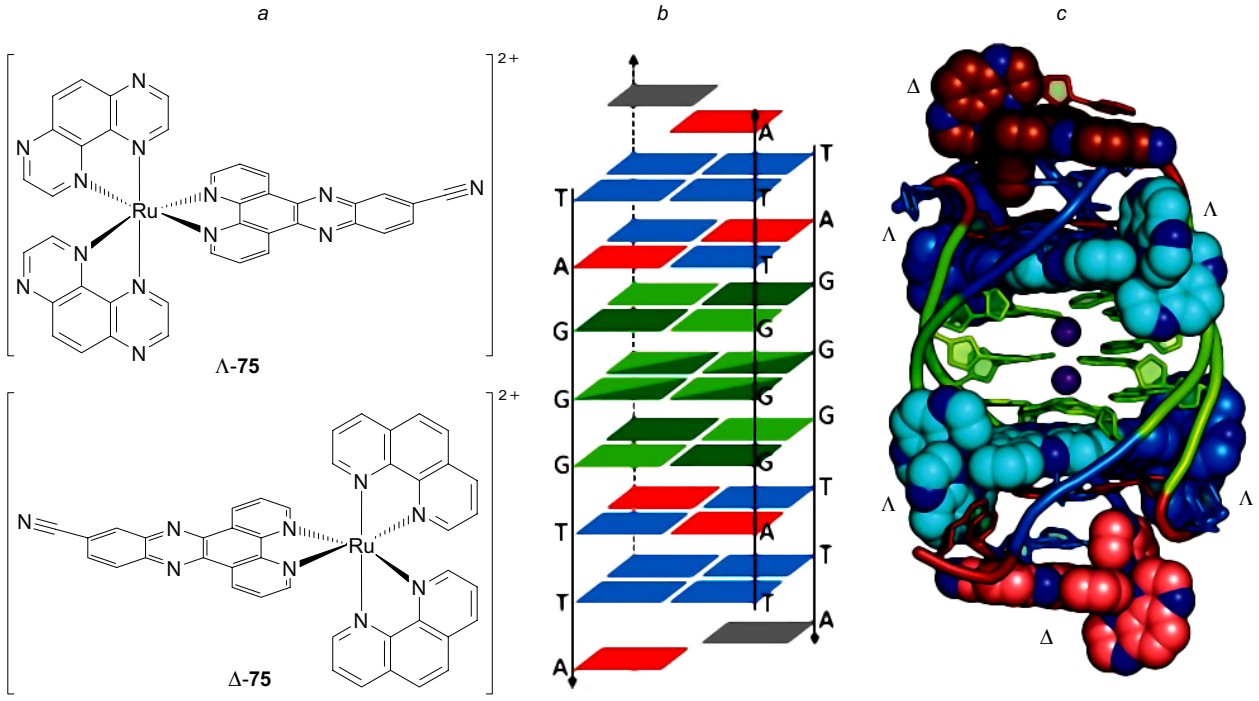


Figure 22. Structures of Λ and Δ enantiomers of complex **75** (*a*); schematic representation of the intermolecular antiparallel G-quadruplex d(TAGGGTTA) (*b*) and the structure of a co-crystal of Λ and Δ enantiomers of **75** with the intermolecular G-quadruplex (*c*).[141] Reproduced with the permission of Wiley.

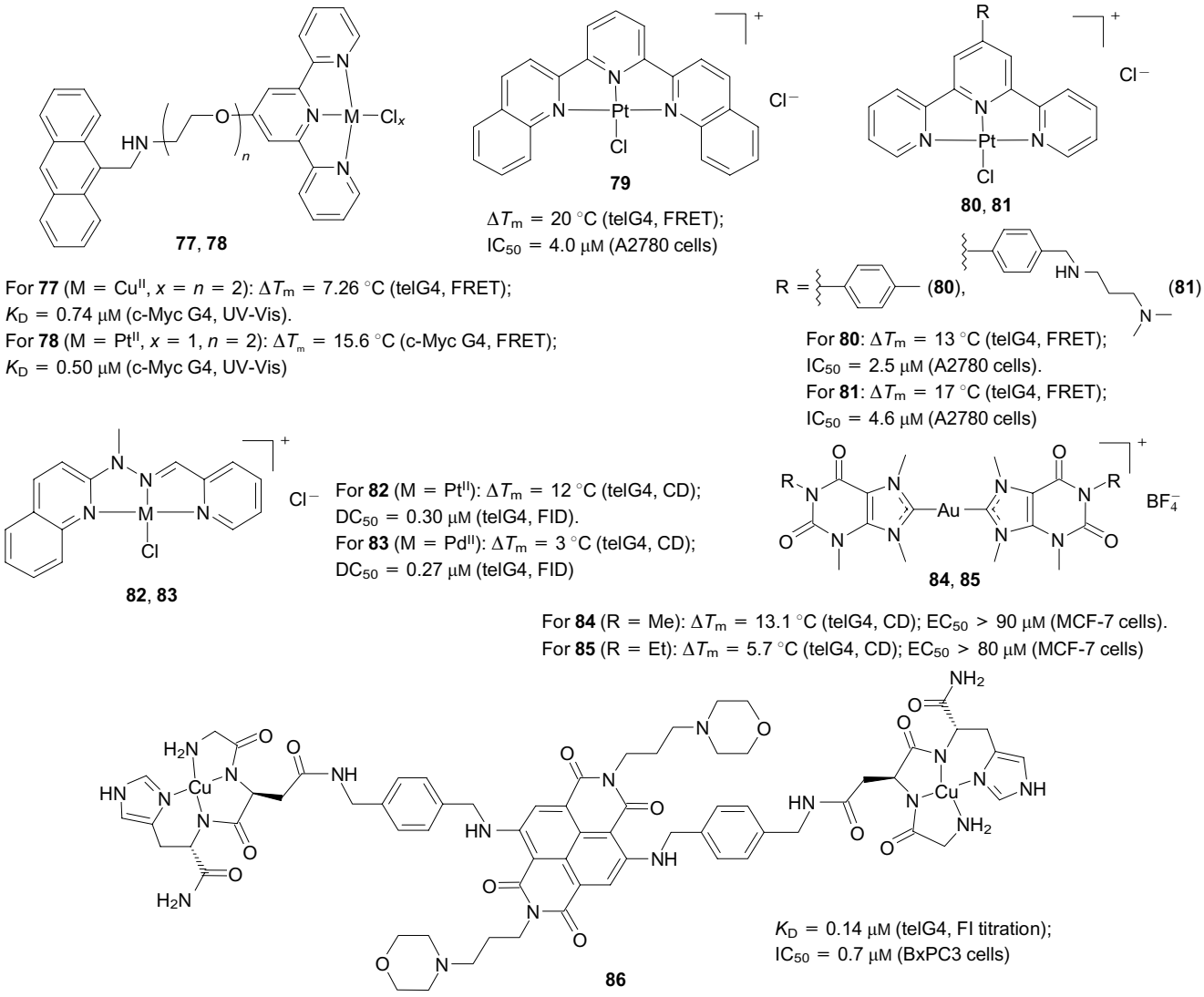


Figure 23. G4-Stabilizing compounds **77**–**86** based on metal complexes of platinum, palladium, copper and gold with different ligands.

Morel *et al.*[144] performed the following modifications of tripyridine-based Pt^{II} complexes: the expansion of the aromatic system by the introduction of quinoline or tolyl moieties (to increase the selectivity of ligands) and the addition of a side chain bearing the terminal amino group (to improve the solubility in water and increase the G4-binding affinity). Figure 23 presents ligands **79**–**81**, which show the highest stabilization of the telG4 and c-Myc G-quadruplexes with ΔT_m in the range from 8 to 20 °C, which are somewhat less efficient than the reference PhenDC3 ligand (see Fig. 2). Complexes **79**–**81** have a higher binding affinity towards telG4s. It is noteworthy that the selectivity of G4/duplex was surprisingly low. Thus, the addition of 10 equiv. of duplex DNA leads to a more than twofold decrease in ΔT_m. The introduction of the benzene ring actually led to a 4–6 -fold increase in the affinity of derivatives **80** and **81** compared to unsubstituted tripyridine Pt^{II} complex **79**. Metal complexes **79** and **80** are prone to platination of quadruplexes (up to 60%), whereas aminoalkyl-containing analogues, including compound **81**, are not subjected to this reaction. Ligands **79**–**81** showed high cytotoxic activity against A2780 ovarian cancer cells, none of these complexes having cross-resistance with cisplatin.

The replacement of the central pyridine ring of tripyridine-based ligands by the hydrazone moiety in Pt^{II} and Pd^{II} complexes affords new compounds capable of interacting with human G4-forming sequences.[145] Using the FID assay, Schmidt *et al.*[145] determined the concentration required to displace half of TO for the c-Myc and tel G-quadruplexes and the duplex DNA. Complexes **82** and **83** (see Fig. 23) were found to have much higher binding affinity for G4s than for double-stranded DNA. The G4-binding selectivity of the Pt^{II}-based complexes was generally higher than that of their palladium analogues. No general features were revealed using the structure–activity relationship analysis, except for the fact that the quinoline moiety provides better binding activity than derivatives containing two pyridine rings (they are not shown in the figure). It is of interest to evaluate the properties of metal complexes containing two hydrazone-bridged quinoline cores.

Bertrand *et al.*[146] synthesized unusual organometallic caffeine-based Au^{I} *N*-heterocyclic carbene complexes, which stabilize telG4s, causing DNA damage.[146] Advances of the use of *N*-heterocyclic carbenes as ligands in com-

plexes for the development of DNA-binding agents are considered in the review by Karaca *et al.*[147] As part of continuing research on G4-stabilizing gold complexes, the authors synthesized a series of new ligands.[148] However, as in the previous study,[146] the replacement of the methyl group in lead ligand **84** (see Fig. 23) by other groups, for example, by the ethyl (compound **85**), phenyl, 2-(cyclohexyl)ethyl, *etc.* groups, results in a significant decrease in the ligand-induced change in the melting temperature of telG4. Higher selectivity of ligand **84** for telG4s compared to duplex DNA was explained based on experimental data. Thus, the size of complex **84** does not allow it to intercalate between base pairs of double-stranded oligonucleotide, but allows one caffeine moiety to stack on its external G-tetrad.[149] The cytotoxic activity of the ligands does not correlate with their effect on G4s. The highest activity against cancer cells was observed for the 2-(cyclohexyl)ethyl derivative. Therefore, G4s are not the main target for anticancer activity of gold heterocyclic carbene complexes.

Copper(II) complexes were used to develop artificial hexameric nucleases that induce a reduction of the telomere length through the cleavage of G-quadruplex telomeric DNA. [150] The design of these ligands is based on the conjugation of two functional moieties: naphthalene diimide for the binding to G4 and the amino terminal Cu^{II}- and Ni^{II}-binding (ATCUN) motif for DNA cleavage under physiological conditions by the formation of ROS. All these compounds (including complex **86**) showed good binding affinity for telG4s and high selectivity comparable with the corresponding parameters of G4 ligands of the naphthalene diimide series lacking the ATCUN motif. The rapid telomere degradation in MCF-7 cancer cells was already observed after one-day incubation, and the absence of DNA fragmentation is indicative of a low level of non-selective DNA cleavage. As opposed to protein-based nucleases, a significant cellular uptake and nuclear localization were observed for chemical 'nucleases' based on Cu^{II} complexes. The telomere reduction occurs during the S-phase of the cell cycle (DNA synthesis), which is consistent with the fact that more G4 elements form in the cell during DNA replication compared to other phases of the cell cycle. This investigation is an example of a new strategy for anticancer therapies targeting the cleavage of G-quadruplex nucleic acids.

About two dozens of metals, including Pt, Pd, Cu, Fe, Ru, Ir, Zn, Au, Ni, Mn, Co, In, Mg, V, Ce, Tb, *etc.*, were described as ions for complexes serving as ligands for G-quadruplex nucleic acid structures. According to the literature data, Pt, Cu, Fe, Ni, Zn and Ru complexes are most often used to construct G4 ligands. Generally, the metal is selected empirically. Undoubtedly, there are some privileged ions for particular classes of G4 ligands. For example, Pt^{II}, Cu^{II} and Ni^{II} ions are most commonly used for planar complexes, whereas Ru^{II}, Fe^{III} and Ir^{III} are preferred for octahedral complexes with planar ligands. Evidently, Pt^{II} ions are very popular due to efficient anticancer activity of platinum-based agents, such as cisplatin and its analogues, which also act in the stage of DNA synthesis.

5. G4 ligands based on (het)arenes

In recent years, the chemical diversity of G4 ligands was considerably expanded due to molecular scaffolds containing no polyfused arenes and hetarenes. The expected advantages of these compounds are the change in the character of interactions, primarily due to the loss of rigid $\pi-\pi$-stacking with G-quartets, and a higher drug-likeness. Polyaromatic compounds are known to have multi-target action on human cells, causing numerous side effects typical of this class of drugs. Hence, G4 ligands constructed based on pharmaceutically relevant building blocks are more likely to successfully pass preclinical and clinical trials as drug candidates.

Pyridine and quinoline derivatives proved to be particularly valuable structural scaffolds for the design of highly specific G4 ligands. Pyridostatin (see Fig. 2) [151] is the most well-known pyridine- and quinoline-based G4 ligand. Derivatives of pyridinium salts are used for the preparation of fluorescent probes [152] specific for G4 elements.[153] For instance, a 50-fold fluorescence enhancement of 2,6-bis[2-(indol-3-yl)vinyl]-*N*-methylpyridine (**87**, Fig. 24) was observed upon the binding to telG4, whereas the presence of dsDNA, the i-motif or RNA hairpins has almost no effect on fluorescence. The introduction of the third 2-(indol-3-yl)vinyl moiety at the 4 position of pyridine **87**, or the removal of one 2,6-substituent, leads to a 2.5 – 5-fold decrease in the fluorescence intensity of the complex. The limit of detection of the telG4 oligonucleotide was 33.7 nm, which is approximately 10 times higher compared to the classical dye thiazole orange commonly used as a non-specific analyte for nucleic acids. Apart from the telomeric sequence, the fluorescence of ligand **87** is enhanced upon the binding to G4s in the c-Myc, c-Kit1 and VEGF promoters. Dye **87** can visualize PC3 cells (the human prostate cancer cell line) with the maximum fluorescence in the nuclei, allowing the *in vivo* analysis of the formation of G4 DNA during the cell cycle.

Das *et al.*[154] synthesized a series of 2,6-bis(quinolin-2-yl)pyridines containing side chains in quinoline moieties. Most of these derivatives, in particular ligand **88** (see Fig. 24), stabilize telG4s; however, the introduction of the *N*-methylpiperazine and particularly morpholine moieties at the terminal positions of the side chains impairs the binding ability. The addition of a 15 – 50-fold excess of competitive dsDNA has virtually no effect on ΔT_m. It was found that G4 ligands of this type are selective for parallel G4 topology over antiparallel topology. Ligand **88**, taken at a concentration of 1 μM, fully inhibits telomerase activity in K562 and MV-4-11 cell lysates and suppresses the growth of K562 human leukaemia cells when present at 3 μM concentration.

The hybridization of the dye TO by the vinylcarbazole moiety of the 3,6-bis(*N*-methyl-4-vinylpyridinio)carbazole ligand affords fluorescent probe **89** (see Fig. 24), which binds to G4s both *in vitro* and *in cellulo*.[155] The complexation of ligand **89** with G4s caused the dose-dependent increase in the light emission at $\lambda_{max} = 613$ nm, and the limit of detection of G4s was 2.4 nM. Hybrid **89** selectively interacts with G4-forming oligonucleotides (the telomeric region, c-Myc, H-Ras), without changing their topology; the binding to double-stranded (hairpin and duplex) and single-stranded DNAs (T21 and A21) was not observed. The authors attributed high specificity of this ligand to the optimal molecular size that fits for the G-tetrad and the electrostatic potential surface, resulting in the reduction of non-specific electrostatic interactions with phosphate residues of loops.

The research group headed by Professor Pozmogova [156] evaluated the ability of new derivatives of benzothiazole orange to stabilize nucleic acid secondary structures.

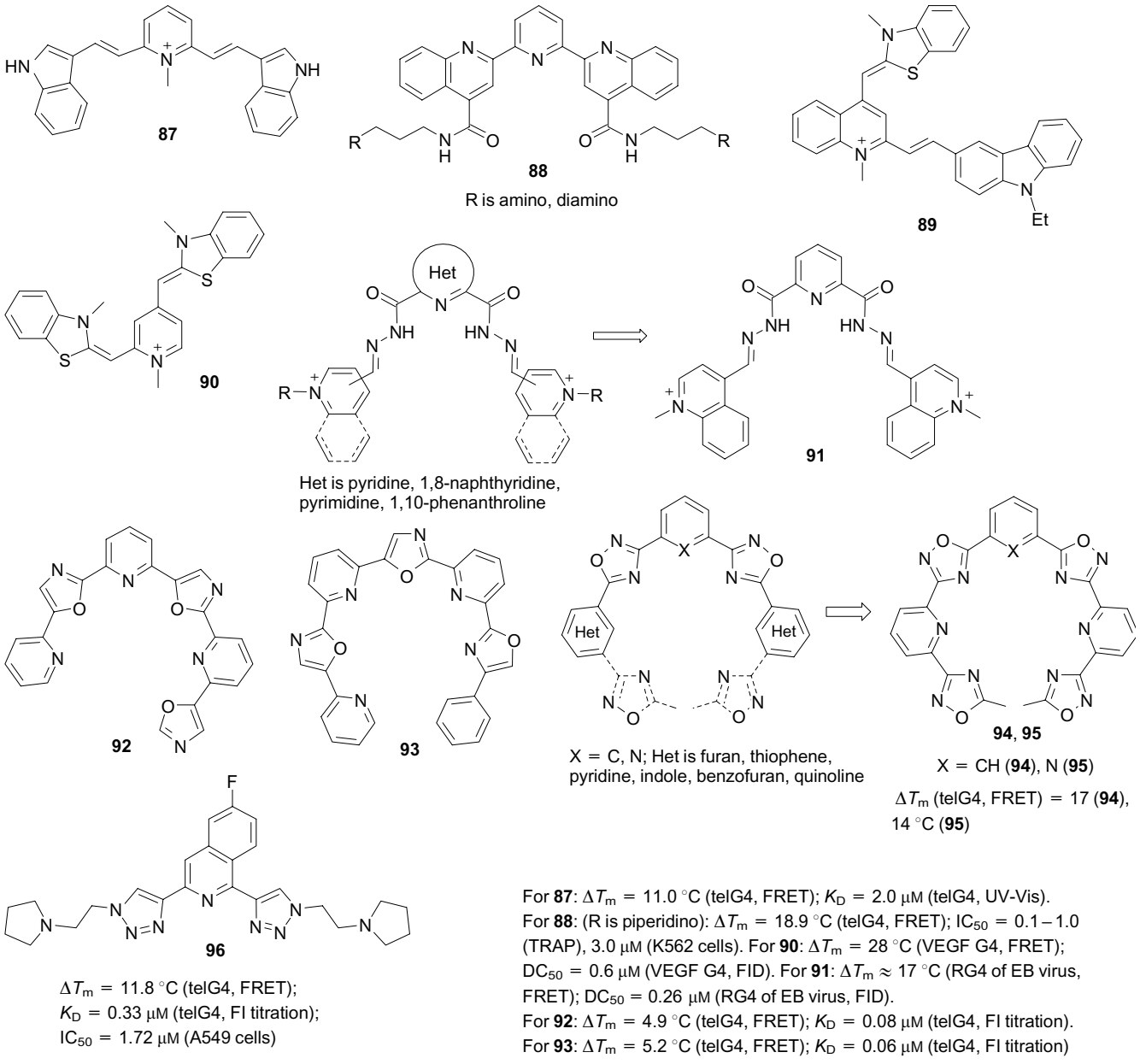


Figure 24. G4 Ligands **87** – **96** based on pyridine and quinoline derivatives.

2,4-Disubstituted pyridine **90** (see Fig. 24) proved to have the highest stabilizing effect towards c-Kit1 and VEGF G4. The introduction of the third substituent in the 6 position significantly impairs the affinity of the compound for all types of secondary structures, whereas derivatives containing one benzothiazole moiety are selective for parallel G4 topology. The fluorescence quantum yield of ligand **90** is comparable with that of thioflavin T, making it a promising candidate as a quadruplex probe (so-called light-up probe).

Reznichenko *et al.*[157] demonstrated an unusual treatment strategy of Epstein – Barr (EB) virus based on the interaction of G4 ligands with its mRNA. The EB virus is associated with human cancers. One mechanisms of its evasion of the immune system is based on the limitation of the EBNA1 protein expression. The regulatory region of EBNA1 mRNA has RG4 elements, the binding of which to the nucleolin (NCL) leads to the inhibition of EBNA1 translation and the formation of antigenic peptides. Using the PhenDC3 ligand (see Fig. 2) as the starting point, the authors[157] designed a series of its analogues based on heterocyclic bishydrazones, capable of interacting with G4 EBNA1 mRNA. Ligand **91** (see Fig. 24) and its analogue in which the central pyridine moiety is replaced by 2,9-disubstituted 1,10-phenanthroline showed the highest binding properties. The use of the pyridine moiety instead of quinoline in side chains and the quaternization of the nitrogen atoms of lateral heterocyclic residues by the ethyl or benzyl group lead to a decrease in ΔT_m. Ligand **91**, being bound to RG4, blocks the recognition of the regulatory EBNA1 mRNA region by NCL, which stimulates the EBNA1 expression and antigenic peptide synthesis, thereby interfering with immune evasion of EB virus virions. Unlike the PhenDC3 ligand, these compounds did not exhibit cytotoxicity at concentrations required for the enhancement of the production of antigenic peptides, which make them promising candidates for G4-mediated immunomodulation.

Apart from telomestatin (see Fig. 2) and its analogues (see Fig. 17), polyheterocyclic open-chain macrocyclic derivatives also stabilize G-quadruplex nucleic acids. Rizeq and Georgiades [158] synthesized a series of linear and branched heterocycles based on pyridine and oxazole. It was shown that molecules containing six or seven alternating rings (compounds **92** and **93**, see Fig. 24) display the higher stabilizing effect for telG4 and c-Myc G4 than the branched isomers or homologues consisting of a smaller number of units.[159] The addition of a 25-fold excess of competitive dsDNA has no effect on ΔT_m.

Later, Doria *et al.*[160] varied heterocyclic cores attached to the central pyridine or benzene moiety through a 1,2,4-oxadiazole ring. As in the previous studies,[158] polyheterocyclic derivatives **94** and **95** (see Fig. 24) containing seven units exhibited high affinity for G4s. In the presence of the benzene ring (derivative **94**), a somewhat higher ligand binding affinity was observed in the series of all the nucleotides under study. Telomeric G4 proved to be the most sensitive for compounds **94** and **95**, whereas these compounds do not stabilize dsDNA.

Maiti *et al.*[161] synthesized 1,3-bis(triazolyl)-6-fluoroizoquinoline derivatives stabilizing a number of G4s. Bispyrrolidine derivative **96** (see Fig. 24) specifically binds to telG4, without changing its topology, which was confirmed by a combination of methods (FRET melting, fluorescence titration, CD, ^{1}H and ^{19}F NMR spectroscopy). It should be noted that compound **96** stabilizes neither G4s (*e.g.*, c-Myc, c-Kit, K-Ras, Bcl-2) nor duplex DNA. The physicochemical characteristics of the effect of ligand **96** on G4s are consistent with the biological effects. This ligand accumulates in cell nuclei and inhibits telomerase activity (IC_{50} = 10 μM), but does not reduce the expression of the c-Myc oncogene or the apoptosis regulator Bcl-2. The cancer cell death associated with the effect on telomerase is additionally confirmed by the arrest of the cells in the S-phase of the cell cycle apparently due to stabilization of telomeric G4 DNA.

Compounds based on bisindoles are a rather new and poorly characterized class of G4 ligands. Chorell' research group [162] made the main contribution to the design of these compounds. They used the known agent PhenDC3 (see Fig. 2) as the basis and replaced the rigid phenanthroline core by more flexible di(indol-2-yl)methane, resulting in the synthesis of unique G4 ligands. The screening (FID assay) demonstrated that compound **97** (Fig. 25), like the starting PhenDC3, displaces the fluorescent dye thioflavin T (DC_{50} = 0.2 – 2.2 μM) from telG4, c-Myc G4 and the ribosomal quadruplex from the yeast *Schizosaccharomyces pombe*, which confirms its high affinity for G4s. However, attempts to determine ΔT_m failed because of thermal instability of these ligands.

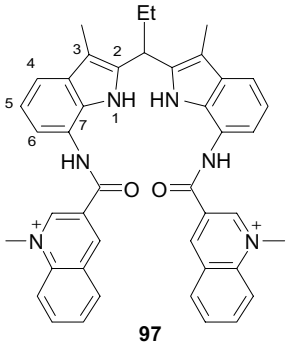
As part of continuing research on bisindole G4 ligands, Chorell and co-workers [163] replaced the 2,2′-methylene spacer between indoles by the carbonyl group bound to heterocyclic nitrogen atoms (see Fig. 25). No definite correlation between the structures of the substituents that quaternize the quinoline nitrogen atom was found. However, compound **98** (R = Me) showed the best binding properties evaluated by the FID and Taq polymerase stop assays. Derivatives bearing the rigid bisindole moiety, *i.e.*, containing the 2,2′ bond between the indole rings, showed higher activity compared to their analogues lacking this bridge. This fact confirms the key role of the stacking between the aromatic moiety of the ligand and guanines. The stabilizing effect of lead ligand **98** on telG4 and ribosomal G4 DNA from *S. pombe* is characterized by good values of the parameters ΔT_m and K_D (see Fig. 25). Apparently, the new derivatives are thermally more stable than bisindole **97**, although the authors do not focus on this fact.

In one of the recent studies,[164] the same research group synthesized derivatives isomeric with compound **97**. These di(indol-3-yl)methanes chemically bound at the 3 and 3′ positions of (see Fig. 25) can also interact with G4s. There are the following key features of the SAR for these derivatives:

— activity depends on the positions of the side chains in indole (5 > 6 ≫ 4 or 7);

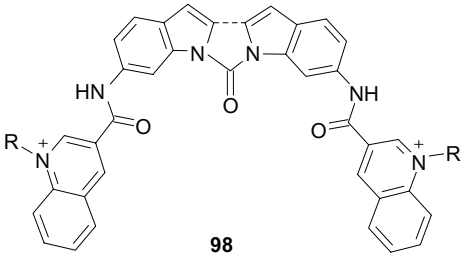
— activity is exhibited only by compounds bearing quaternized quinoline or piperazine moieties in side chains.

Ligands **99** and **100** (see Fig. 25) were found to have the highest binding affinity and selectivity towards duplex DNA. The complexation was confirmed by NMR spectroscopy by following the signals of guanine imino groups of G-tetrads, which are broadened up to complete disappearance upon ligand binding. Significant changes were observed in the spectra of compounds **99** and **100**. Ligand



97

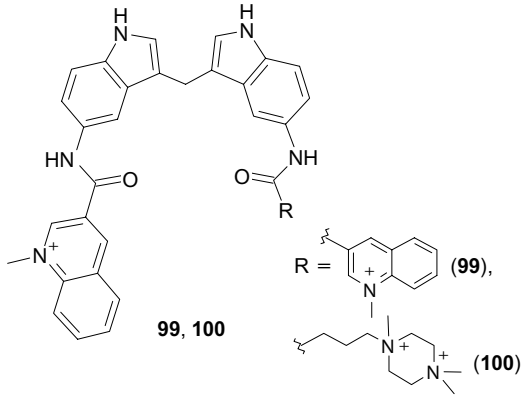
DC_{50} (FID) = 0.2 (c-Myc G4), 2.2 μM (telG4)



98

R is alkyl, allyl, benzyl

For **98** (R = Me): ΔT_m (CD) = 17 (ribosomal G4), 9 °C (telG4); K_D = 0.82 μM (ribosomal G4, FID)



99, **100**

For **99**: ΔT_m = 17.5 °C (c-Myc G4, FRET); K_D = 0.49 μM (c-Myc G4, MST).
For **100**: ΔT_m = 12.4 °C (c-Myc G4, FRET); K_D = 3.05 μM (c-Myc G4, MST)

Figure 25. G4 Ligands **97** – **100** based on bisindoles.

100 showed the largest effect, which was manifested even in the presence of a 10-fold excess of the oligonucleotide.

An important result of the studies performed by Chorell and co-workers [162 – 164] is that they demonstrated a good example of structurally flexible ligands exhibiting high affinity and selectivity for G4s. It would be expected that the effect of a larger series of terminal amines (in particular quaternized) on the binding properties and the *N*-alkylation of indoles will be examined in the ongoing research.

Recent studies§ demonstrated that the folding of individual polynucleotides into G4 occurs through rather stable G-triplex (G3) intermediates. Like G4s, triplexes consist of three guanines stabilized by Hoogsteen hydrogen bonds, but they are less stable than G4s because of a smaller number of hydrogen bonds, which interferes with their *in vitro* and *in vivo* studies.[165] The search for molecules capable of interacting with and stabilizing G3s is a promising area of research required for an understanding of the putative biological and therapeutic value of G3 structures. Amato *et al.*[166] developed dual G3/G4 ligands using a combination of the virtual screening and physicochemical methods. Fifteen compounds were selected for experimental studies by the docking of 60 000 molecules onto the surface of the 11-mer-TBA nucleotide (pdb: 2MKM). All these compounds do not alter the G3 topology; however, only one compound (ligand **101**, Fig. 26) induced thermal stabilization of the G-triplex (ΔT_m = 8.5 °C). Interestingly, apart from G3s, quinazoline **101** can stabilize only parallel G4s (particularly c-Myc G4), having no effect on other G4 topologies and duplex DNA. The visualization of U2OS human osteosarcoma cells by G4-specific antibodies BG4 demonstrated that the treatment with ligand **101** leads to the dose-dependent fluorescence enhancement, thereby confirming the formation and stabilization of a larger number of G4s in certain chromatin sites.

Chorell's group [167] performed the independent FID screening of 28 000 compounds and characterized the pyrimidinoquinazoline chemotype as a promising class for the further optimization of selective G4 ligands. Four years later, this research group [168] synthesized and characterized dual pyrimidinoquinazoline-based ligands acting on G4s and the STAT3 signaling protein. Ligands **102** and **103** (see Fig. 26) were selected out of 47 compounds. These ligands showed the highest binding affinity and specificity towards G4s. Studies by NMR spectroscopy and molecular dynamics simulations demonstrated that compound **102** can intercalate between the first and second G-tetrads of c-Myc G4, whereas several models of interaction with G4s are possible for derivative **103** (Fig. 27). Both ligands not only bind to the STAT3 protein but also suppress its activation (the phosphorylation level) in HeLa cells. It is worth noting that ligand **102** has nearly the same effect on the STAT3 protein and the formation of G4s in cells (the level of fluorescence of BG4 antibodies), whereas its analogue **103**

§ See P.Stadlbauer, P.Kührová, L.Vicherek, P.Banbáš, M.Otyepka, L.Trantírek, J.Sponer. *Nucleic Acids Res.*, **47**, 7276 (2019); https://doi.org/10.1093/nar/gkz610; V.Limongelli, S.De Tito, L.Cerofolini, M.Fragai, B.Pagano, R.Trotta, S.Cosconati, L.Marinelli, E.Novellino, I.Bertini, A.Randazzo, C.Luchinat, M.Parrinello. *Angew. Chem., Int. Ed.*, **52**, 2269 (2013); https://doi.org/10.1002/anie.201206522

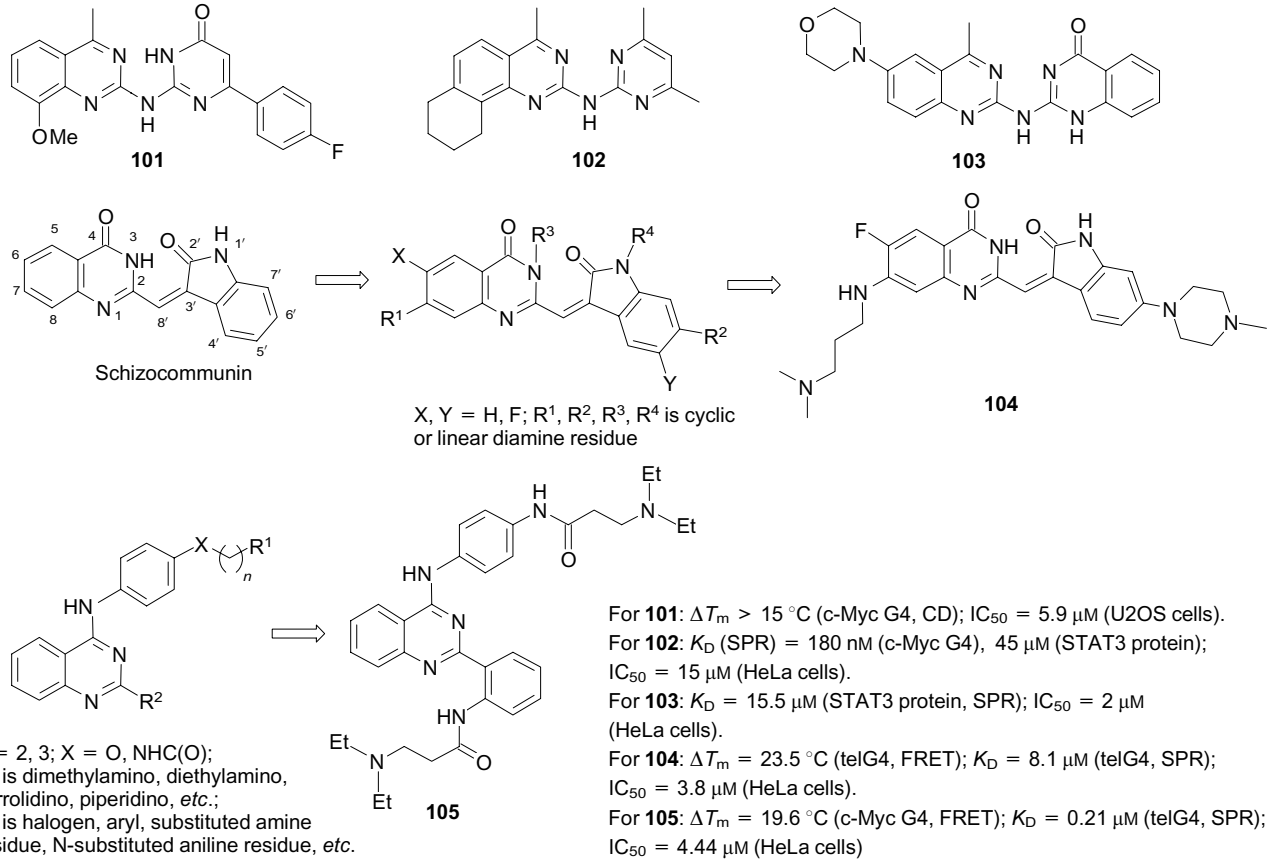


Figure 26. G4 Ligands **101** – **105** based on quinazoline derivatives.

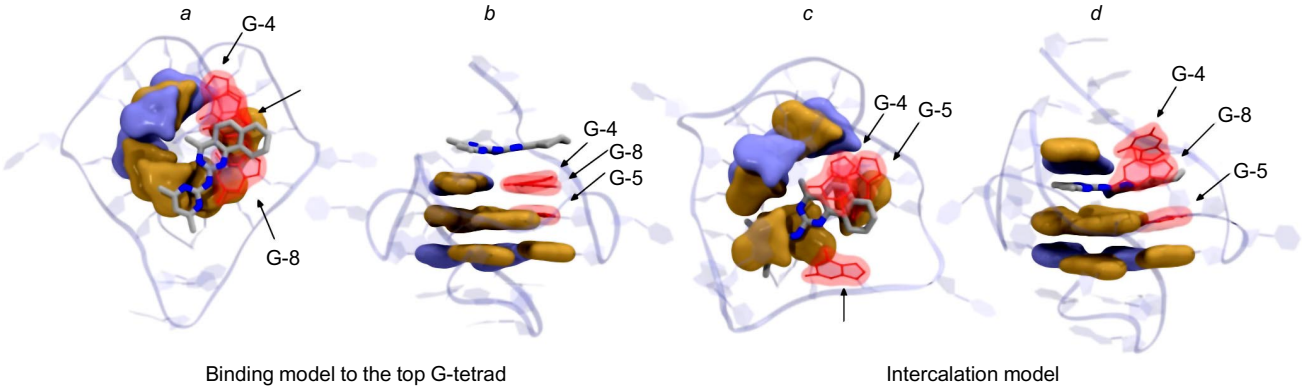


Figure 27. Binding model (docking + NMR analysis) of ligand **102** to the c-Myc G-quadruplex Pu24T through stacking with the top G-tetrad [top view (*a*) and side view (*b*)] and the model of intercalation between G-tetrads [top view (*c*) and side view (*d*)].[168] The observed chemical shift changes in the NMR spectrum are shown in red (large shifts), yellow (moderate shifts) and blue (small shifts). Reproduced with the permission of American Chemical Society.

initiates the tumour cell suppression primarily through the effect on the STAT3 protein.

The alkaloid schizocommunin (see Fig. 26) is a promising scaffold for the development of G4 ligands, because an intramolecular hydrogen bond maintains a large planar structure required for stacking interactions with G-tetrads. The modification of schizocommunin by the introduction of a fluorine atom (to improve lipophilicity and bioavailability) and side chains bearing amino groups afforded a series of new G4 ligands.[169] The presence of one substituent R^1 at the 7 position of schizocommunin leads to an increase in the degree of stabilization telG4 from 0 to 10 – 12 °C, and the addition of the second diamine moiety (R^2) increases ΔT_m to 20 – 25 °C. The transposition and(or) introduction of substituents at the nitrogen atoms of heterocycles (at the 3 and 1′ positions) reduces the stabilizing effect, whereas the replacement of each hydrogen atom by fluorine (groups X, Y) increases ΔT_m by 1 – 2 °C. The electron-withdrawing effect of a fluorine atom reduces the electron density in the ligands, which apparently facilitates stacking interaction with the electron-rich π-system of the G-tetrad. Figure 26 presents the structure of lead ligand **104**, which, taken at micromolar concentrations, inhibits telomerase and the growth of six cancer cell lines. Immunofluorescence assays showed that compound **104** induces the formation of G4s in cells, causes telomeric DNA damage in chromosome regions and leads to telomere dysfunction. At a dose of 20 mg kg^{-1}, ligand **104** exhibits significant antitumour activity (TGI = 65.2% 21 days after the tumour transplantation) in the SiHa xenograft model of human cervical cancer.

Jiang *et al.*[170] synthesized a series of 4-anilinoquinazolines and showed that these compounds stabilize G4s in the c-Myc promoter. The SAR analysis demonstrated that the introduction of an amino-containing side chain at the 2 position of quinazolines enhances the stabilizing effect compared to that of the derivatives with R^2 = Hal or Ar. Ligand **105** (see Fig. 26) containing terminal *N*,*N*-diethylamino groups proved to be the most active towards c-Myc G4. This series of compounds provide additional evidence that the basicity of terminal amino groups of side chains plays an important role in the interaction of ligands with G4s. Thus, morpholine derivatives have much lower binding affinity for the target than their piperidine analogues. Compound **105** causes the dose-dependent decrease in the c-Myc gene expression and inhibits the synthesis of the corresponding oncoprotein, suppressing the *in vitro* cancer cell growth at micromolar concentrations.

The development of aryl-substituted imidazoles as a chemotype of G4 ligands started about ten years ago after the successful computer-aided design.[171] Later, Chinese researchers synthesized ligands containing three[172] and even four aryl substituents.[173] The conjugation of diarylimidazoles with the dye (coumarin) afforded ligand **106** (Fig. 28), which can be used as the selective probe for parallel G4s. The introduction of carbazole or anisole moieties into the imidazole ring improves the binding affinity and selectivity of ligand **107** (see Fig. 28) for Myc G4 (K_D = 0.1 μM, SI ≈ 10). The high specificity was explained using a molecular model, which shows that the ligand perfectly fits the structure of the top G-tetrad. Thus, the optimal stacking is achieved due to the location of the central positively charged imidazole moiety in the ion channel of the quartet. It was established that tetraarylimidazole **107** binds to c-Myc G4 at the cellular level, inhibiting the c-Myc protein transcription and synthesis and inducing the cancer cell death with overexpression of c-Myc. The evaluation of anticancer activity of compound **107** in the SiHa xenograft model of human cervical cancer showed its high efficacy (TGI = 69% after 24 days) in the treatment at a dose 20 mg kg^{-1} every other day.

Hu *et al.*[174] performed the bioisosteric modification of the imidazole moiety of ligands **106** and **107** by quinoxaline, assuming that the structurally related heterocycles should have similar properties. There are the following important SAR features found for this chemotype:

— electron-withdrawing groups in the quinoxaline core increase the binding ability, whereas electron donating groups decrease it;

— introduction of piperazine into the quinoxaline core has almost no effect on the activity, whereas the replacement of the piperazine moiety at one of the benzene rings by a fluorine atom decreases K_D by a factor of 10;

— expansion of the polycyclic quinoxaline structure (fusion of the benzene ring) improves the binding to c-Myc G4.

The most promising derivative **108** (see Fig. 28) proved to be 3 – 4 times more selective for c-Myc G4 over other G4

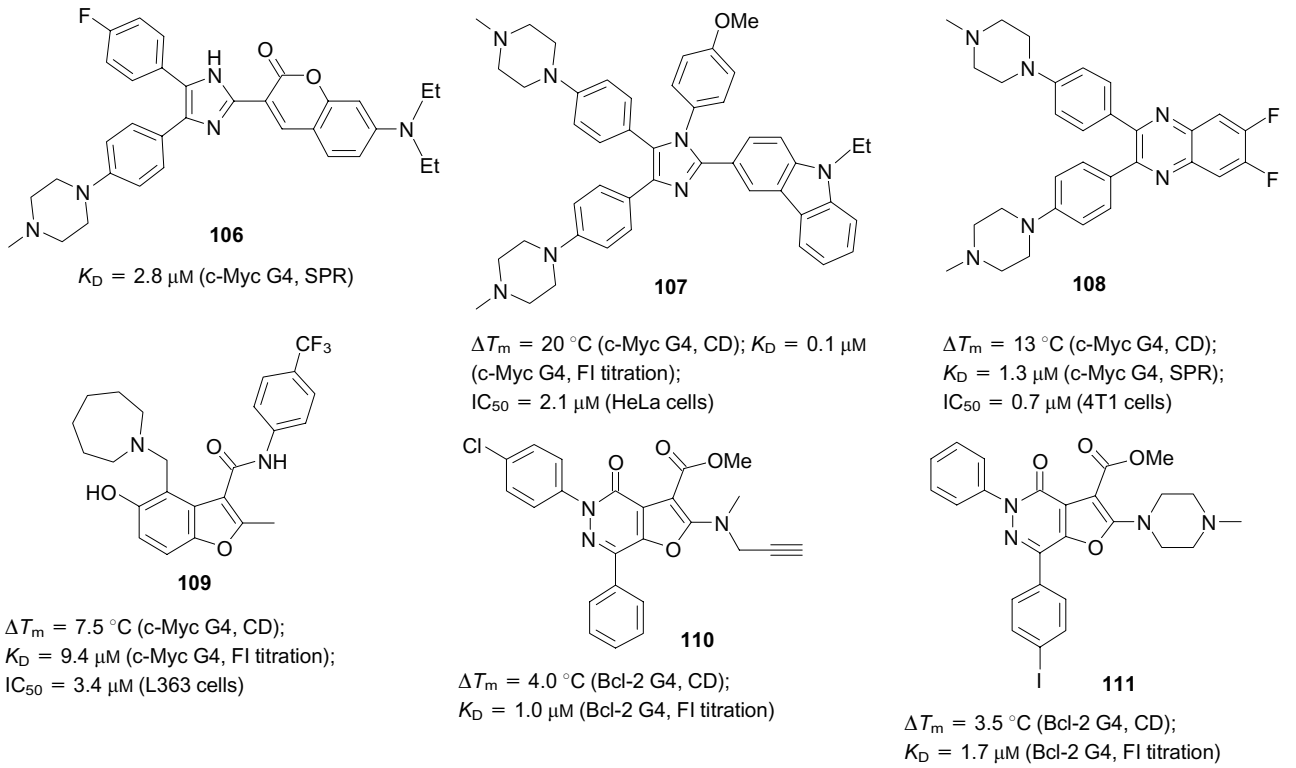


Figure 28. G4 Ligands **106**–**111** based on aryl-substituted imidazoles, quinoxalines and furopyridazinones.

elements and does not bind to single- and double-stranded oligonucleotides. Quinoxaline **108** was found to stack on the 5′-G-tetrad to form a stacking structure, and the nitrogen atoms of piperazine moieties interact with phosphate residues of lateral loops. The biological activity of ligand **108** is well consistent with stabilization of G4s. Compound **108** decreases the expression of c-Myc, without altering the transcriptional activity of the Bcl-2, c-Kit and H-Ras genes, which confirms the selectivity at the cellular level, and also exhibits *in vitro* and *in vivo* antitumour activity. At a dose of 10 mg kg^{-1}, ligand **108** leads to a significant tumour growth retardation (by 60%) in the 4T1 mouse breast cancer cell line, which is comparable with the effect of doxorubicin as the reference compound.

Benzofuran derivatives were shown to be promising for the development of anticancer agents based on G4 ligands. In a series of 25 compounds, which were synthesized by the sequential Nenitescu reaction and Mannich aminomethylation, ligand **109** (see Fig. 28) exhibited high selectivity for c-Myc G4, causing a significant reduction of the myc gene expression (up to 0.4% at a concentration of 10 μM).[175] The following SAR features were found: the introduction of electron-donating substituents at the benzene ring of the amide moiety, a change in the position of the CF_3 group, the methylation of the amide nitrogen atom or the replacement of the azepane ring by a hydroxy group lead to a decrease in the binding affinity for c-Myc G4. The specificity for c-Myc G4 was confirmed by the fact that benzofuran **109** has virtually no effect on the expression level of other G4-regulated Bcl-2, K-Ras, HIF-1α and VEGF oncogenes. The importance of the results obtained by Calabrese *et al.*[175] is supported by the experimental data (NMR) on the complex [**109**–G4]. Thus, ligand **109** is involved in efficient π–π stacking with terminal c-Myc G-tetrads, enhancing the binding by a network of electrostatic interactions.

Amato *et al.*[176] empirically designed G4 ligands from the promoter region of the gene encoding the anti-apoptotic Bcl-2 protein based on furopyridazinone derivatives. In a series of eleven compounds, only furopyridazinones **110** and **111** (see Fig. 28) proved to be capable of stabilizing Bcl-2 G4 (ΔT_m = 3.5–4.0 °C). Despite low values of ΔT_m, both ligands did not interact at all with other G4s and duplex DNA. According to the NMR data, furopyridazinones **110** and **111** bind to Bcl-2 G4 primarily *via* interactions in the long lateral loop and the groove between the fourth and first parallel G strands. The treatment of Jurkat cells with ligand **111** at a concentration of 25 μM reduces the Bcl-2 gene expression and decreases the total level of this protein. Compound **111** exhibited moderate cytotoxicity, and the highest effect (30% inhibition at a concentration of 10 μM) was achieved in the Jurkat T-cell leukaemia cell line, in which the Bcl-2 expression plays a crucial role in the regulation of cell viability. Therefore, furopyridazinones can be considered as a promising molecular basis for the further development of G4 ligands with a non-classical binding mode.

Propeller-like *N*,*N*,*N*-triphenylamine derivatives with D_3 symmetry, like many other scaffolds, can form efficient π–π-stacking interactions with G-tetrads. Hence, these compounds have attracted great attention as G4 ligands. Triphenylamine derivatives containing one, two or three polyaminomacrocyclic side chains were synthesized and characterized.[177] The affinity of the ligands correlates with the number of side groups. Thus, trisubstituted ligand **112** (Fig. 29) exhibited the highest binding affinity. The addition of even a 100-fold excess of competitive dsDNA does not cause changes in ΔT_m, which confirms its high binding selectivity for G4s. Moreover, the binding of triphenylamine **112** exclusively to G4 structures leads to a significant fluorescence enhancement, making this ligand a promising

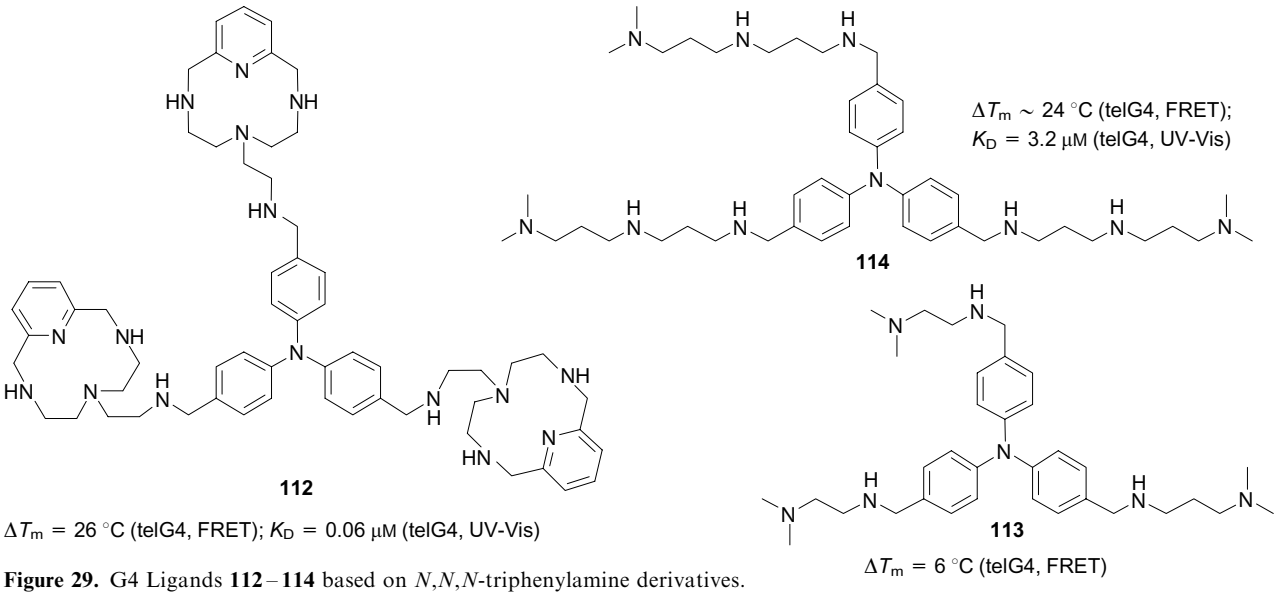


Figure 29. G4 Ligands **112** – **114** based on *N*,*N*,*N*-triphenylamine derivatives.

candidate for the development of biochemical probes for G-quadruplexes.

Pont *et al.*[178] synthesized the second generation of this class of G4 ligands based on triphenylamine and linear

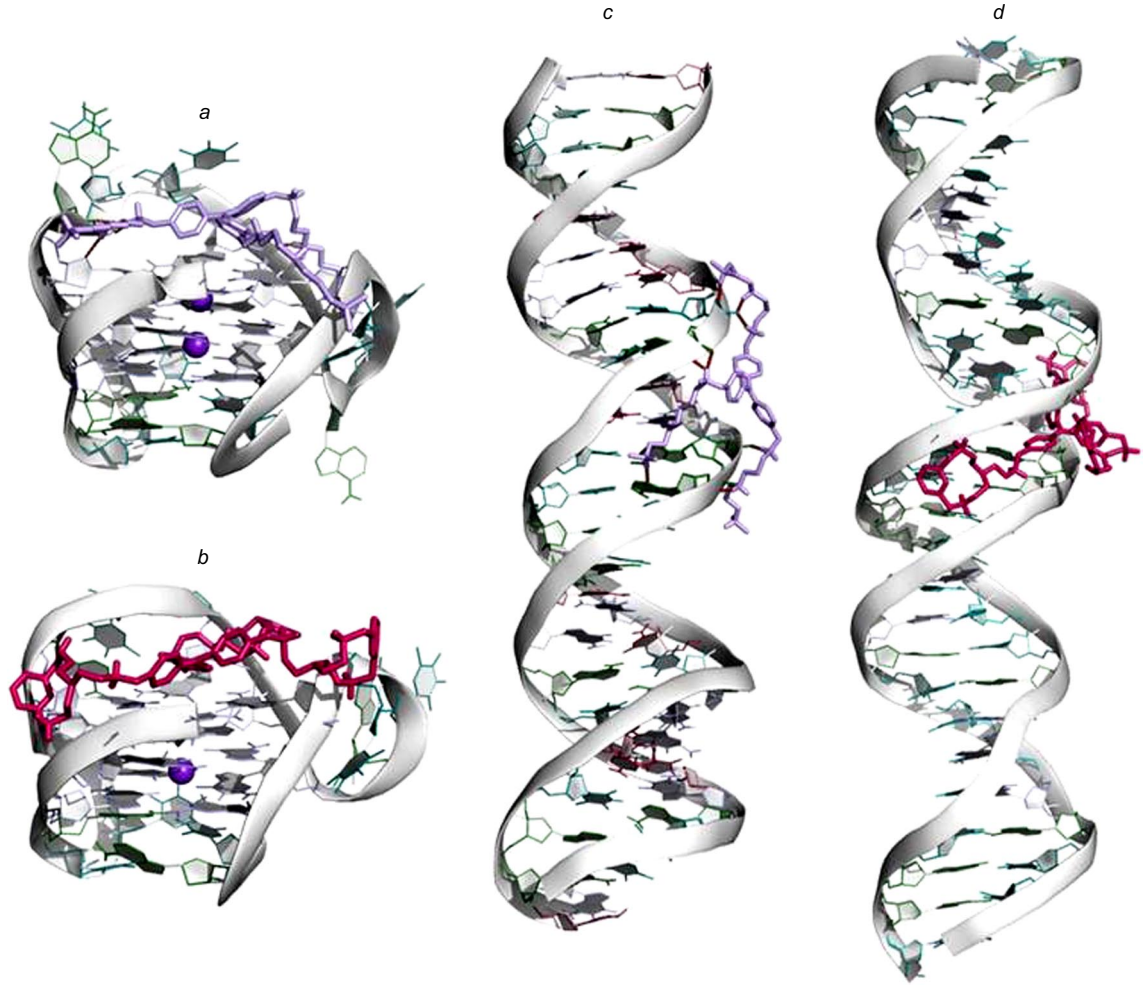
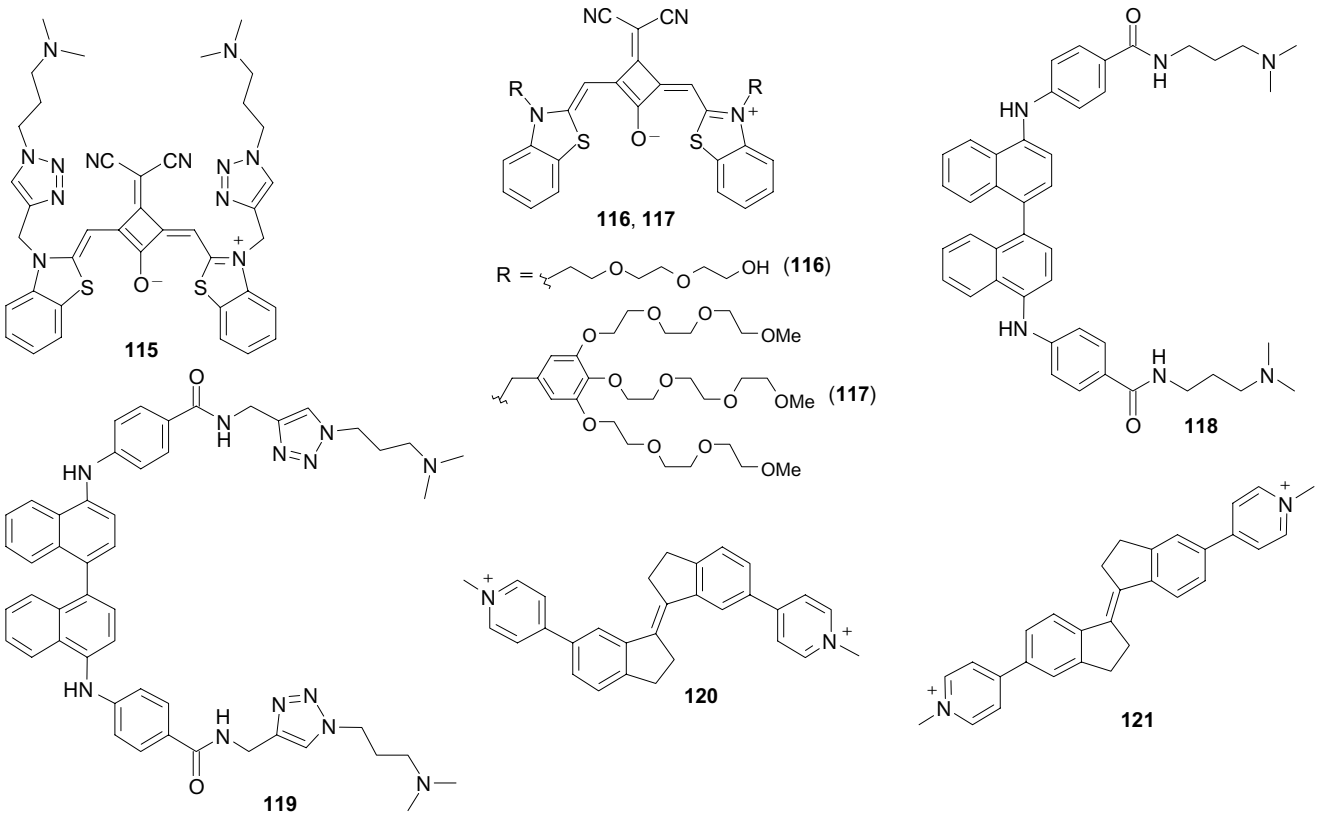


Figure 30. Molecular models of interactions of telomeric G4 with ligands **114** (*a*) and **112** (*b*) and of duplex DNA with ligands **114** (*c*) and **112** (*d*).[178] Reproduced with the permission of Wiley.



For **115**: ΔT_m = 9 °C (c-Kit G4, CD); K_D = 0.04 μM (c-Kit G4, UV-Vis). For **117**: K_D = 2.5 nM (c-Kit G4, UV-Vis).
For **118**: ΔT_m = 15 °C (c-Myc G4, FRET); K_D = 21.4 μM (c-Myc G4, UV-Vis); IC_{50} = 7.24 μM (HeLa cells).
For **119**: ΔT_m = 23 °C (c-Myc G4, FRET); K_D = 4.2 μM (c-Myc G4, UV-Vis); IC_{50} = 5.53 μM (HeLa cells).
For **120**: ΔT_m = 33 °C (telG4, FRET); K_D = 0.4 μM (telG4, UV-Vis); IC_{50} = 0.06 μM (HeLa cells).
For **121**: ΔT_m = 28 °C (telG4, FRET); K_D = 2.0 μM (telG4, UV-Vis); GI_{50} = 0.11 μM (HeLa cells)

Figure 31. G4 Ligands **115** – **121** based on dicyanovinylsquaraine, 1,1′-bisnaphthalene and stilbene derivatives.

polyamines in order to increase the index of selectivity for G4/dsDNA.[178] Due to an increase in the number of secondary amino groups in the molecule (compounds **113** and **114**, see Fig. 29), their protonated forms enhance electrostatic interactions between the ligands and G4s. It is worth noting that the authors achieved their goal by replacing cyclic polyamine groups with linear groups. For instance, the degree of thermal stabilization of double-stranded DNA by ligand **114** is equal to 0 °C, whereas ΔT_m = 4 °C for first-generation ligand **112**. An analysis of the CD spectra and the molecular modelling of interactions of compounds **112** and **114** with telG4 showed that the triphenylamine moiety stacks on the top G-tetrad through stacking interactions, and the side chains fold into G4 loops by forming a network of electrostatic and hydrogen bonding interactions (Fig. 30). Another binding mode was observed for double-stranded DNA. Triphenylamine **112** containing macrocyclic polyamino groups, when bound to the duplex in the minor groove, interacts with both DNA strands, causing the compaction of the groove. Ligand **114** interacts exclusively with one of the two strands demonstrating a smaller number of electrostatic interactions with double-stranded DNA. Apparently, this is responsible for higher specificity of the second-generation ligand for G4s.

Squaraine-based dyes are used as G4 ligands. Zhang *et al.*[179] synthesized a series of dicyanomethylene derivatives of bis(benzothiazol-2-ylidene)squaraine modified with different side chains by means of click chemistry. Hydroxy, carboxy and *N*,*N*-dimetylamino groups, phthalimide and a moiety of the antiviral drug azidothymidine were utilized as terminal groups. As expected, only compound **115** (Fig. 31) containing 3-(*N*,*N*-dimethylamino)propyl side chains stabilizes G-quadruplexes (ΔT_m = 9 °C for the c-Kit2 G-quadruplex). The absence of cytotoxic activity (IC_{50} > 30 μM), fluorescence enhancement upon the binding of ligand **115** to G4s and efficient accumulation in cells, with the predominant localization in lysosomes, suggest that this compound is a promising candidate for the design of probes for *in vivo* bioimaging.

In other works,¶ dicyanovinylsquaraine derivatives are considered as agents exceptionally selective for parallel quadruplex topology. It was proved that amphiphilic squaraine **116** (see Fig. 31) is rapidly self-organized in water to form a nonfluorescent aggregate.[180] However, due to high binding affinity, parallel G4s can displace monomeric dye molecules **116** from its aggregates to form the sandwich complex [G4 – ligand] in a ratio of 2 : 1, causing fluorescence enhancement of squaraine. Quadruplexes with another architecture cannot form efficient π – π stacking

¶ See V.Grande *et al.*[180] and the publication by B.Jin, X.Zhang, W.Zheng, X.Liu, J.Zhou, N.Zhang, F.Wang, D.Shangguan. *Anal. Chem.*, **86**, 7063 (2014); https://doi.org/10.1021/ac501619v.

with ligand **116**, resulting in the low affinity of the latter for G4s with other topologies. The introduction of several triethylene glycol chains afforded water-soluble analogue **117** (see Fig. 31) with an excitation maximum in the near-IR region, which has higher total affinity for G4s and retains high selectivity for parallel G-quadruplex topology.[181]

Chauhan *et al.*[182] synthesized bisnaphthalene derivatives **118** and **119** (see Fig. 31) and evaluated their affinity for G4s. The screening showed that both compounds stabilize G4s in the K-Ras, c-Kit1 and c-Kit2 oncogene promoter regions, and the highest effect was observed for c-Myc G4. Ligand **119** containing the triazole spacer between the aromatic core and the aminoalkyl chain induced a larger increase in thermal stabilization but was less soluble under experimental conditions. An analysis of the ^{1}H NMR spectra suggests that bisnaphthalene **119** interacts with the 3′-end of the G-tetrad apparently through the restructuring of the TAA-3′-capping. At the cellular level, bisnaphthalene **119** better suppresses the c-Myc gene expression compared to compound **118** and inhibits the synthesis of the corresponding oncoprotein, causing tumour cell apoptosis.

Stiff stilbenes show a great potential as the basis for the design of G4 ligands with unusual properties. O'Hagan *et al.*[183] synthesized (*E*)-stilbene ligand **120** (see Fig. 31) capable of causing the unfolding of quadruplexes. Ligand **120** induces the stabilization of (3 + 1)-hybrid telG4 topology in the presence of potassium ions, but causes the unfolding of this sequence with antiparallel topology that is formed in sodium buffer. If necessary, this effect can be eliminated by irradiation of the solution with light at $\lambda = 400$ nm, resulting in the degradation of the ligand through photooxidation. It should be emphasized that the conformation of G4 DNA can be switched five times by the addition (deactivation) of photolabile stilbene **120**. Later, this research group[184] modified the structure of ligand **120** and prepared G4-binding derivatives exhibiting antitumour and antiparasitic activity. The transition from the *E* to *Z* configuration of stilbene **120**, like the introduction of the pyridinium moiety at the adjacent position of the benzene ring (ligand **121**, see Fig. 31), has almost no effect on its excellent stabilizing ability for a series of G4s. Meanwhile, the replacement of the *N*-methylpyridinium group by the 3-(*N*-methylpiperazin-1-yl)propylamine moiety decreases the activity of both geometric isomers. It is important that ligands **120** and **121** stabilize the quadruplex identified in the *T. brucei* genome ($\Delta T_m = 17 - 22$ °C), only insignificantly stabilizing duplex DNA ($\Delta T_m = 3 - 5$ °C). Based on the analysis of NMR spectra, the authors suggested different binding modes of two stilbenes: compound **120** interacts predominantly through the groove binding, whereas stacking interactions play a key role for its isomer **121**. Both compounds display significant antiparasitic activity (predominantly against *T. brucei*); however, their cytotoxicity against normal cells is rather high [the concentration causing 50% inhibition of cell proliferation (GI_{50}) is 0.46 – 1.80 μM].

6. Conclusion

Quadruplex ligands have a great potential for practical application in pharmaceutics. Hence, the synthesis and characterization of new ligands have attracted attention of numerous research groups from academic institutions and pharmaceutical companies. However, despite great efforts and evident attractiveness of G4-targeting therapeutic agents, it should be stated that more than twenty-year research in this area did not lead to their introduction into medical practice. Moreover, there is a skeptical thought that G4 elements are undruggable targets in the development of new chemotherapeutic agents. Contrary to this opinion, the absence of examples of the practical application of G4 ligands in medicine is not an obstacle to continuing research in this area. In recent years, new functions and mechanisms of regulation of cellular processes involving G4 structures were found, resulting in the development of new promising strategies for the therapeutic use of G4 ligands.

New G4 ligands are searched for employing a wide range of medicinal chemistry methods. The application of an empirical approach, the target-oriented design of biologically active compounds and the high-throughput experimental and virtual screening of libraries of chemical compounds made it possible to identify tens of classes of organic compounds as candidates for the further development of novel drugs.

Derivatives bearing structural units classical for G4 ligands, such as acridines, carbazoles, anthraquinones, porphyrins and polyoxazole macrocycles, continue to attract attention even 20 years after they were first reported. On the one hand, this can be attributed to the interest of researchers in optimizing the structures of known G4 ligands in order to put them into practical application. On the other hand, the use of privileged structures in the design of ligands increases the chance of success because researchers select modifications, which cannot greatly impair the binding to G4s but can improve other pharmacological properties of the compounds.

In some cases, other cellular targets were found for polyfused ligands, which casts doubt on the key role of stabilization of G4 structures in the specific pharmacological activity of these compounds. Many lead ligands based on polyaromatic compounds have drawbacks in the absorption, distribution, metabolism, excretion and toxicity (ADME/T) profiles, which were found in later stages of preclinical and clinical trials. In recent years, polyfused systems have been often considered as building blocks giving false-positive results in biological assays (pan-assay interference compounds, PAINS).[185] Hence, it is expected that the use of compounds lacking these structural motifs would help in designing G4-targeting drugs.

The replacement of rigid polycyclic molecular scaffolds (see Figs 3, 8, 11, 13, 14, *etc.*) by pharmaceutically relevant mono- and bicyclic systems (see Figs 23 – 25, 26, 28, *etc.*) becomes increasingly successful strategy for the development of new G4 ligands. The affinity, selectivity and biological activity of such compounds (*e.g.*, ligands **82**, **87**, **96**, **99**, **101** – **111**, *etc.*) are comparable with and often higher than the corresponding properties of polyaromatic precursors. Moreover, conformationally flexible ligands ensure the interaction with grooves or loops, which increases their potential for the selective recognition of quadruplex topologies. The rational design of ligands employing the molecular modelling and virtual screening methods, which take into account the compliance of chemotypes with the requirements imposed on potential drugs (drug-likeness), are ever-increasingly used in this area of research. Computational methods are widely employed to explain the character of interactions between the ligands and G4s and to predict the promising directions of further modification.[112, 127, 171]

The comprehensive analysis of relationships between the binding ability to G4 and the structure of ligands, which covers several chemical classes, is a difficult problem. The general features are as follows:

— larger planar surface of the aromatic system promotes stabilization through stronger π – π-stacking with G-tetrads;

— introduction of a cationic centre into the central moiety of the ligand (a metal or ammonium ion) enhances the interaction through cation – π-stacking with the electron-excessive G-quartet;

— binding directly depends on the pK_a value of terminal basic groups; however, an excessive charge of side chains can exert a negative effect, in particular, can impair the intracellular uptake;

— introduction of a primary amino group decreases the selectivity of ligands for G4 over duplex DNA due to a too small steric environment and, consequently, compounds bearing such substituents are not considered in many studies.

Besides, each class of G4 ligands has its own SAR features. Hence, a comparison of the properties of compounds belonging to the same class shows their evolution.[31–33,147] It is difficult to quantitatively compare the efficiency of ligand chemotypes because different research groups employ different physicochemical methods for the screening of affinity and perform experiments using oligonucleotides with different sequences and lengths, including various dyes. Hence, the hybridization. *i.e.*, the transfer of structural units of lead ligands to other classes of G4 ligands, is not always efficient, as it might appear at first glance.

As mentioned above, the main practical application of G4 ligands is the design of new therapeutic agents and tools for investigation of the biological role of G4 structures in cellular processes. In many studies, the authors mentioned that these ligands hold promise, but reported only the physicochemical characterization and results of traditional evaluation of the antiproliferative activity. Among these studies, let us mention publications in which the authors reported relevant relationships between the affinity of ligands for G4 elements and mediated secondary effects, such as the inhibition of telomerase, blocking of transcription or translation of oncogenes and, which is particularly important, *in vivo* antitumour activity.

For example, the stabilization of G4s in promoter regions of c-Myc (ligands **26**, **27**, **40**, **105**, **108**, **109**), c-Kit (ligand **15**), K-Ras (ligands **38**, **49**), H-Ras (ligand **48**) or Bcl-2 oncogenes (ligands **36**, **111**) leads to the reduction of transcription of the corresponding genes, decreasing the viability and the level of proliferation of cancer cells. Dual inhibitors acting simultaneously on G-quadruplex/G-triplex (ligand **101**), c-Myc G4 and the STAT3 protein (ligand **102**) were prepared. The recently synthesized innovative ligands acting on RG4s in the 5′-untranslated region of mRNA can be applied to control the expression of the N-Ras (ligand **41**) and K-Ras (ligand **49**) oncogenes at the translation stage. The properties of new cationic porphyrins (ligand **51**), which combine RG4 stabilization and photosensitizing activity, demonstrate a considerable promise for the development of RG4-targeted photodynamic therapy. Metal complexes based on ruthenium (**74**) and copper (**86**), capable of binding to telG4 and causing degradation of telomeric regions of chromosomes by local ROS induction, have a good chance to serve as the basis for the development of a new way of action on telG4, without inhibiting telomerase.

It should be emphasized that the recently characterized ligands, stabilizing G4s in promoter sequences of oncogenes and RG4 in regulatory mRNA regions, efficiently suppress *in cellulo* expression of the c-Myc, H-Ras and K-Ras oncogenes and the HIF-1 transcription factor, thereby successfully blocking the cancer cell proliferation with overexpression of these targets, which are commonly recognized as undruggable cancer targets.[186] Due to specific features of the three-dimensional structures of these proteins, attempts to develop their direct inhibitors failed. Hence, the selective down-regulation of their expression by targeting G4 elements is the novel and still the only potentially efficient strategy for the suppression of these privileged anticancer therapeutic targets.[187,188]

Worthy of particular mention are G4 ligands exhibiting antiviral and antiparasitic activity, which demonstrate a new field of application of G4s as therapeutic targets. Naphthalene diimide **10** and stilbene **121** bind to *T. brucei*-specific quadruplex-forming oligonucleotides, causing the parasite death. Naphthalene diimide derivative **2** specifically binds to G4 HIV-1 and has high antiviral activity against human immunodeficiency virus. Ligand **91** deserves special mention since it provides unique opportunities for the modulation of the immune response to the EB virus through the binding to the quadruplex in the regulatory region of EBNA1 mRNA.

Apart from the above-mentioned applied functions, a series of new ligands, in particular compounds **73**, **87**, **89**, **90** and **112**, are of interest for the preparation of specific probes for different G4 topologies. The use of *in vivo* bioengineering for the analysis of homeostasis of G4 DNA at different stages of the cell cycle and the development of new specific dyes for high-throughput FID screening systems can be considered as the two main, but not the only, fields of application of these biological tools in the future.

Therefore, the review of the literature data published in the past five years demonstrates that ligands of G-quadruplex nucleic acids have been extensively studied and new strategies were developed for their potential use in medicine. The main driving force for this research is still the evident relationship between the validated functions of G4s, stabilization of G4s by low-molecular-weight compounds and their anticancer activity. The confirmed formation of the quadruplex secondary structure of nucleic acids in eukaryotic DNA and RNA, the virus genome and protozoans and the elucidation of their most important regulatory functions show the importance of both fundamental and applied aspects of the development of new G4 ligands. Taking into account the potential of the modern rational design methods, the accumulated knowledge and experience, there are good reasons to expect that first therapeutic agents based on G4-stabilizing ligands will be designed in the ongoing decade.

This work was prepared with the financial support of the D.Mendeleev University of Chemical Technology of Russia.

References

1. M.D.F.Kamenetskii. *Annu. Rev. Biochem.*, **64**, 65 (1995); https://doi.org/10.1146/annurev.biochem.64.1.65
2. H.Abou Assi, M.Garavís, C.González, M.J.Damha. *Nucleic Acids Res.*, **46**, 8038 (2018); https://doi.org/10.1093/nar/gky735

3. H.J.Lipps, D.Rhodes. *Trends Cell Biol.*, **19**, 414 (2009); https://doi.org/10.1016/j.tcb.2009.05.002
4. C.K.Kwok, C.J.Merrick. *Trends Biotechnol.*, **35**, 997 (2017); https://doi.org/10.1016/j.tibtech.2017.06.012
5. J.Spiegel, S.Adhikari, S.Balasubramanian. *Trends Chem.*, **2**, 123 (2020); https://doi.org/10.1016/j.trechm.2019.07.002
6. M.Krafcikova, H.Robert, L.Trantirek, S.Foldynova-Trantirkova. *G-Quadruplex Nucleic Acids*. (New York: Springer, 2019); https://doi.org/10.1007/978-1-4939-9666-7
7. J.W.Shay, W.E.Wright. *Semin. Cancer Biol.*, **21**, 349 (2011); https://doi.org/10.1016/j.semcancer.2011.10.001
8. A.Bernal, L.Tusell. *Int. J. Mol. Sci.*, **19**, 294 (2018); https://doi.org/10.3390/ijms19010294
9. V.S.Chambers, G.Marsico, J.M.Boutell, M.Di Antonio, G.P.Smith, S.Balasubramanian. *Nat. Biotechnol.*, **33**, 877 (2015); https://doi.org/10.1038/nbt.3295
10. G.Marsico, V.S.Chambers, A.B.Sahakyan, P.McCauley, J.M.Boutell, M.Di Antonio, S.Balasubramanian. *Nucleic Acids Res.*, **47**, 3862 (2019); https://doi.org/10.1093/nar/gkz179
11. J.Tan, L.Lan. *Cell Biosci.*, **10**, 47 (2020); https://doi.org/10.1186/s13578-020-00409-z
12. S.Cogoi, A.Ferino, G.Miglietta, E.B.Pedersen, L.E.Xodo. *Nucleic Acids Res.*, **46**, 661 (2018); https://doi.org/10.1093/nar/gkx1142
13. V.González, K.Guo, L.Hurley, D.Sun. *J. Biol. Chem.*, **284**, 23622 (2009); https://doi.org/10.1074/jbc.M109.018028
14. P.Sengupta, S.Chattopadhyay, S.Chatterjee. *Drug Discov. Today*, **22**, 1165 (2017); https://doi.org/10.1016/j.drudis. 2017.05.001
15. D.Sun, W.J.Liu, K.Guo, J.J.Rusche, S.Ebbinghaus, V.Gokhale, L.H.Hurley. *Mol. Cancer Ther.*, **7**, 880 (2008); https://doi.org/10.1158/1535-7163.MCT-07-2119
16. R.Rigo, W.L.Dean, R.D.Gray, J.B.Chaires, C.Sissi. *Nucleic Acids Res.*, **45**, 13056 (2017); https://doi.org/10.1093/nar/gkx983.
17. D.Varshney, J.Spiegel, K.Zyner, D.Tannahill, S.Balasubramanian. *Nat. Rev. Mol. Cell Biol.*, **21**, 459 (2020); https://doi.org/10.1038/s41580-020-0236-x.
18. E.Lavezzo, M.Berselli, I.Frasson, R.Perrone, G.Palù, A.R.Brazzale, S.N.Richter, S.Toppo. *PLOS Comput. Biol.*, **14** (12), e1006675 (2018); https://doi.org/10.1371/journal.pcbi. 1006675
19. F.Dumetz, C.Merrick. *Molecules*, **24**, 1339 (2019); https://doi.org/10.3390/molecules24071339
20. M.Anas, R.Sharma, V.Dhamodharan, P.I.Pradeepkumar, A.Manhas, K.Srivastava, S.Ahmed, N.Kumar. *Biochemistry*, **56**, 6691 (2017); https://doi.org/10.1021/acs.biochem.7b00964
21. P.Murat, J.Zhong, L.Lekieffre, N.P.Cowieson, J.L.Clancy, T.Preiss, S.Balasubramanian, R.Khanna, J.Tellam. *Nat. Chem. Biol.*, **10**, 358 (2014); https://doi.org/10.1038/nchembio.1479
22. E.Butovskaya, B.Heddi, B.Bakalar, S.N.Richter, A.T.Phan. *J. Am. Chem. Soc.*, **140**, 13654 (2018); https://doi.org/10.1021/jacs.8b05332
23. D.Ji, M.Juhas, C.M.Tsang, C.K.Kwok, Y.Li, Y.Zhang. *Brief. Bioinform.*, (2020) (in the press); https://doi.org/10.1093/bib/bbaa114
24. P.Majee, S.K.Mishra, N.Pandya, U.Shankar, S.Pasadi, K.Muniyappa, D.Nayak, A.Kumar. *Sci. Rep.*, **10**, 1477 (2020); https://doi.org/10.1038/s41598-020-58406-8
25. H.J.Sullivan, C.Readmond, C.Radicella, V.Persad, T.J.Fasano, C.Wu. *ACS Omega*, **3**, 14788 (2018); https://doi.org/10.1021/acsomega.8b01574
26. H.Yaku, T.Murashima, H.Tateishi-Karimata, S.i.Nakano, D.Miyoshi, N.Sugimoto. *Methods*, **64**, 19 (2013); https://doi.org/10.1016/j.ymeth.2013.03.028
27. S.Balasubramanian, L.H.Hurley, S.Neidle. *Nat. Rev. Drug Discov.*, **10**, 261 (2011); https://doi.org/10.1038/nrd3428
28. S.Asamitsu, T.Bando, H.Sugiyama. *Chem. – Eur. J.*, **25**, 417 (2019); https://doi.org/10.1002/chem.201802691
29. M.P.O Hagan, J.C.Morales, M.C.Galan. *Eur. J. Org. Chem.*, 4995 (2019); https://doi.org/10.1002/ejoc.201900692
30. P.Chilka, N.Desai, B.Datta. *Molecules*, **24**, 752 (2019); https://doi.org/10.3390/molecules24040752
31. V.Pirota, M.Nadai, F.Doria, S.Richter. *Molecules*, **24**, 426 (2019); https://doi.org/10.3390/molecules24030426
32. Y.-X.Xiong, Z.-S.Huang, J.-H.Tan. *Eur. J. Med. Chem.*, **97**, 538 (2015); https://doi.org/10.1016/j.ejmech.2014.11.021
33. T.Che, Y.Q.Wang, Z.L.Huang, J.H.Tan, Z.S.Huang, S.B.Chen. *Molecules*, **23**, 493 (2018); https://doi.org/10.3390/molecules 23020493
34. Q.Cao, Y.Li, E.Freisinger, P.Z.Qin, R.K.O.Sigel, Z.-W.Mao. *Inorg. Chem. Front.*, **4**, 10 (2017); https://doi.org/10.1039/C6QI00300A
35. A.Sengupta, A.Ganguly, S.Chowdhury. *Molecules*, **24**, 582 (2019); https://doi.org/10.3390/molecules24030582
36. E.Ruggiero, S.N.Richter. *Nucleic Acids Res.*, **46**, 3270 (2018); https://doi.org/10.1093/nar/gky187
37. C.Yang, R.Hu, Q.Li, S.Li, J.Xiang, X.Guo, S.Wang, Y.Zeng, Y.Li, G.Yang. *ACS Omega*, **3**, 10487 (2018); https://doi.org/10.1021/acsomega.8b01190
38. A.R.Duarte, E.Cadoni, A.S.Ressurreiåao, R.Moreira, A.Paulo. *ChemMedChem.*, **13**, 869 (2018); https://doi.org/10.1002/cmdc.201700747
39. N.S.Ilyinsky, A.M.Varizhuk, A.D.Beniaminov, M.A.Puzanov, A.K.Shchyolkina, D.N.Kaluzhny. *Mol. Biol.*, **48**, 778 (2014); https://doi.org/10.1134/S0026893314060077
40. J.Jaumot, R.Gargallo. *Curr. Pharm. Des.*, **18**, 1900 (2012); https://doi.org/10.2174/138161212799958486
41. A.Decian, L.Guittat, M.Kaiser, B.Sacca, S.Amrane, A.Bourdoncle, P.Alberti, M.Teuladefichou, L.Lacroix, J.Mergny. *Methods*, **42**, 183 (2007); https://doi.org/10.1016/j.ymeth.2006.10.004
42. E.Largy, F.Hamon, M.-P.Teulade-Fichou. *Anal. Bioanal. Chem.*, **400**, 3419 (2011); https://doi.org/10.1007/s00216-011-5018-z
43. J.E.Redman. *Methods*, **43**, 302 (2007); https://doi.org/10.1016/j.ymeth.2007.05.008
44. M.L.Zhang, Y.P.Xu, A.Kumar, Y.Zhang, W.Q.Wu. *Biochemistry*, **58**, 3955 (2019); https://doi.org/10.1021/acs.bio-chem.9b00447
45. V.I.Polshakov, E.A.Batuev, A.B.Mantsyzov. *Russ. Chem. Rev.*, **88**, 59 (2019); https://doi.org/10.1070/RCR4836
46. C.Lin, J.Dickerhoff, D.Yang. *Methods Mol. Biol.*, **2035**, 157 (2019); https://doi.org/10.1007/978-1-4939-9666-7_9
47. H.Li. *Methods Mol. Biol.*, **2035**, 105 (2019); https://doi.org/10.1007/978-1-4939-9666-7_6
48. A.Funke, K.Weisz. In *G-Quadruplex Nucleic Acids*. (Eds D.Yang, C.Lin). (New York: Springer, 2019). P. 45
49. P.Murat, Y.Singh, E.Defrancq. *Chem. Soc. Rev.*, **40**, 5293 (2011); https://doi.org/10.1039/C1CS15117G
50. J.Jamroskovic, I.Obi, A.Movahedi, K.Chand, E.Chorell, N.Sabouri. *DNA Repair (Amsterdam)*, **82**, 102678 (2019); https://doi.org/10.1016/j.dnarep.2019.102678
51. J.Reed, M.Gunaratnam, M.Beltran, A.P.Reszka, R.Vilar, S.Neidle. *Anal. Biochem.*, **380**, 99 (2008); https://doi.org/10.1016/j.ab.2008.05.013
52. C.Sissi, L.Lucatello, A.P.Krapcho, D.J.Maloney, M.B.Boxer, M.V.Camarasa, G.Pezzoni, E.Menta, M.Palumbo. *Bioorg. Med. Chem.*, **15**, 555 (2007); https://doi.org/10.1016/j.bmc.2006.09.029
53. F.Cuenca, O.Greciano, M.Gunaratnam, S.Haider, D.Munnur, R.Nanjunda, W.D.Wilson, S.Neidle. *Bioorg. Med. Chem. Lett.*, **18**, 1668 (2008); https://doi.org/10.1016/j.bmcl.2008.01.050
54. A.M.Zhirov, D.A.Kovalev, D.V.Ulshina, S.V.Pisarenko, O.P.Demidov, I.V.Borovlev. *Chem. Heterocycl. Compd.*, **56**, 674 (2020); https://doi.org/10.1007/s10593-020-02717-1

55. M.M.Islam, S.Fujii, S.Sato, T.Okauchi, S.Takenaka. *Molecules*, **20**, 10963 (2015); https://doi.org/10.3390/molecules200610963
56. R.Perrone, F.Doria, E.Butovskaya, I.Frasson, S.Botti, M.Scalabrin, S.Lago, V.Grande, M.Nadai, M.Freccero, S.N.Richter. *J. Med. Chem.*, **58**, 9639 (2015); https://doi.org/10.1021/acs.jmedchem.5b01283
57. S.Sur, V.Tiwari, D.Sinha, M.Z.Kamran, K.D.Dubey, G.Suresh Kumar, V.Tandon. *ACS Omega*, **2**, 966 (2017); https://doi.org/10.1021/acsomega.6b00523
58. M.Arévalo-Ruiz, F.Doria, E.Belmonte-Reche, A.De Rache, J.Campos-Salinas, R.Lucas, E.Falomir, M.Carda, J.M.Pérez-Victoria, J.-L.Mergny, M.Freccero, J.C.Morales. *Chem. – Eur. J.*, **23**, 2157 (2017); https://doi.org/10.1002/chem.201604886
59. M.Zuffo, A.Stucchi, J.Campos-Salinas, M.Cabello-Donayre, M.Martinez-Garcia, E.Belmonte-Reche, J.M.Pérez-Victoria, J.L.Mergny, M.Freccero, J.C.Morales, F.Doria. *Eur. J. Med. Chem.*, **163**, 54 (2019); https://doi.org/10.1016/j.ejmech.2018. 11.043
60. E.Belmonte-Reche, M.Martinez-Garcia, A.Guédin, M.Zuffo, M.Arévalo-Ruiz, F.Doria, J.Campos-Salinas, M.Maynadier, J.J.López-Rubio, M.Freccero, J.L.Mergny, J.M.Pérez-Victoria, J.C.Morales. *J. Med. Chem.*, **61**, 1231 (2018); https://doi.org/10.1021/acs.jmedchem.7b01672
61. E.H.Blackburn, P.B.Challoner. *Cell*, **36**, 447 (1984); https://doi.org/10.1016/0092-8674(84)90238-1
62. R.Shen, Y.Chen, Z.Li, H.Qi, Y.Wang. *Bioorg. Med. Chem.*, **24**, 619 (2016); https://doi.org/10.1016/j.bmc.2015.12.025
63. M.Franceschin, D.Nocioni, A.Biroccio, E.Micheli, S.Cacchione, C.Cingolani, A.Venditti, P.Zizza, A.Bianco, A.Altieri. *Org. Biomol. Chem.*, **12**, 9572 (2014); https://doi.org/10.1039/c4ob01658k
64. M.K.Si, S.K.Pramanik, B.Ganguly. *Int. J. Biol. Macromol.*, **124**, 1177 (2019); https://doi.org/10.1016/j.ijbiomac.2018.12.019
65. J.Carvalho, E.Pereira, J.Marquevielle, M.P.C.Campello, J.L.Mergny, A.Paulo, G.F.Salgado, J.A.Queiroz, C.Cruz. *Biochimie*, **144**, 144 (2018); https://doi.org/10.1016/j.biochi.2017.11.004
66. C.Gao, W.Zhang, S.He, S.Li, F.Liu, Y.Jiang. *Bioorg. Chem.*, **60**, 30 (2015); https://doi.org/10.1016/j.bioorg.2015.04.002
67. Q.L.Guo, H.F.Su, N.Wang, S.R.Liao, Y.T.Lu, T.M.Ou, J.H.Tan, D.Li, Z.S.Huang. *Eur. J. Med. Chem.*, **130**, 458 (2017); https://doi.org/10.1016/j.ejmech.2017.02.051
68. N.Sato, S.Takahashi, H.Tateishi-Karimata, M.E.Hazemi, T.Chikuni, K.Onizuka, N.Sugimoto, F.Nagatsugi. *Org. Biomol. Chem.*, **16**, 1436 (2018); https://doi.org/10.1039/C7OB03179C
69. M.E.Hazemi, K.Onizuka, T.Kobayashi, A.Usami, N.Sato, F.Nagatsugi. *Bioorg. Med. Chem.*, **26**, 3551 (2018); https://doi.org/10.1016/j.bmc.2018.05.030
70. C.-C.Chang, J.-Y.Wu, C.-W.Chien, W.-S.Wu, H.Liu, C.-C.Kang, L.-J.Yu, T.-C.Chang. *Anal. Chem.*, **75**, 6177 (2003); https://doi.org/10.1021/ac034789i
71. A.K.Jain, A.Paul, B.Maji, K.Muniyappa, S.Bhattacharya. *J. Med. Chem.*, **55**, 2981 (2012); https://doi.org/10.1021/jm200860b
72. B.Maji, K.Kumar, M.Kaulage, K.Muniyappa, S.Bhattacharya. *J. Med. Chem.*, **57**, 6973 (2014); https://doi.org/10.1021/jm500427n
73. M.H.Kaulage, B.Maji, S.Pasadi, A.Ali, S.Bhattacharya, K.Muniyappa. *Eur. J. Med. Chem.*, **148**, 178 (2018); https://doi.org/10.1016/j.ejmech.2018.01.091
74. G.Li, H.Tang, C.Liu, X.Liao, S.Li, Z.Shu, H.Yu, P.Yang. *Bioorg. Chem.*, **90**, 103074 (2019); https://doi.org/10.1016/j.bioorg.2019.103074
75. A.Ou, A.Guédin, B.W.Skelton, S.Amrane, C.W.Evans, M.Norret, K.S.Iyer, J.L.Mergny, N.M.Smith. *Chem. Commun.*, **54**, 9647 (2018); https://doi.org/10.1039/c8cc03945c
76. B.Maji, K.Kumar, K.Muniyappa, S.Bhattacharya. *Org. Biomol. Chem.*, **13**, 8335 (2015); https://doi.org/10.1039/c5ob00675a
77. A.F.Larsen, T.Ulven. *Org. Lett.*, **13**, 3546 (2011); https://doi.org/10.1021/ol201321z
78. A.F.Larsen, M.C.Nielsen, T.Ulven. *Chem. – Eur. J.*, **18**, 10892 (2012); https://doi.org/10.1002/chem.201200081
79. M.C.Nielsen, A.F.Larsen, F.H.Abdikadir, T.Ulven. *Eur. J. Med. Chem.*, **72**, 119 (2014); https://doi.org/10.1016/j.ejmech. 2013.11.027
80. H.Li, C.Wei. Bioorg. *Med. Chem. Lett.*, **25**, 3798 (2015); https://doi.org/10.1016/j.bmcl.2015.07.085
81. L.Wang, Y.Wu, T.Chen, C.Wei. *Int. J. Biol. Macromol.*, **52**, 1 (2013); https://doi.org/10.1016/j.ijbiomac.2012.08.015
82. C.Wei, Y.Wang, M.Zhang. *Org. Biomol. Chem.*, **11**, 2355 (2013); https://doi.org/10.1039/c3ob27426h
83. N.M.Gueddouda, M.R.Hurtado, S.Moreau, L.Ronga, R.N.Das, S.Savrimoutou, S.Rubio, A.Marchand, O.Mendoza, M.Marchivie, L.Elmi, A.Chansavang, V.Desplat, V.Gabelica, A.Bourdoncle, J.-L.Mergny, J.Guillon. *ChemMedChem.*, **12**, 146 (2017); https://doi.org/10.1002/cmdc.201600511
84. J.Medeiros-Silva, A.Guédin, G.F.Salgado, J.L.Mergny, J.A.Queiroz, E.J.Cabrita, C.Cruz. Biochim. *Biophys. Acta – Gen. Sub.*, **1861**, 1281 (2017); https://doi.org/10.1016/j.bbagen.2016.11.024
85. F.Papi, C.Bazzicalupi, M.Ferraroni, G.Ciolli, P.Lombardi, A.Y.Khan, G.S.Kumar, P.Gratteri. *ACS Med. Chem. Lett.*, **11**, 645 (2020); https://doi.org/10.1021/acsmedchemlett.9b00516
86. R.Malhotra, C.Rarhi, K.V.Diveshkumar, R.Barik, R.D.Cunha, P.Dhar, M.Kundu, S.Chattopadhyay, S.Roy, S.Basu, P.I.Pradeepkumar, S.Hajra. *Bioorg. Med. Chem.*, **24**, 2887 (2016); https://doi.org/10.1016/j.bmc.2016.04.059
87. M.Franceschin, L.Cianni, M.Pitorri, E.Micheli, S.Cacchione, C.Frezza, M.Serafini, M.H.Hu, H.Su, Z.Huang, L.Gu, A.Bianco. *Molecules*, **23**, 1 (2018); https://doi.org/10.3390/molecules23061423
88. G.Zagotto, C.Sissi, L.Lucatello, C.Pivetta, S.A.Cadamuro, K.R.Fox, S.Neidle, M.Palumbo. *J. Med. Chem.*, **51**, 5566 (2008); https://doi.org/10.1021/jm800160v
89. D.M.Rasadean, B.Sheng, J.Dash, G.D.Pantos. *Chem. – Eur. J.*, **23**, 8491 (2017); https://doi.org/10.1002/chem.201700957
90. J.Amato, R.Morigi, B.Pagano, A.Pagano, S.Ohnmacht, A.De Magis, Y.-P.Tiang, G.Capranico, A.Locatelli, A.Graziadio, A.Leoni, M.Rambaldi, E.Novellino, S.Neidle, A.Randazzo. *J. Med. Chem.*, **59**, 5706 (2016); https://doi.org/10.1021/acs.jmedchem.6b00129
91. J.Amato, G.Miglietta, R.Morigi, N.Iaccarino, A.Locatelli, A.Leoni, E.Novellino, B.Pagano, G.Capranico, A.Randazzo. *J. Med. Chem.*, **63**, 3090 (2020); https://doi.org/10.1021/acs.jmedchem.9b01866
92. S.Pelliccia, J.Amato, D.Capasso, S.Di Gaetano, A.Massarotti, M.Piccolo, C.Irace, G.C.Tron, B.Pagano, A.Randazzo, E.Novellino, M.Giustiniano. *J. Med. Chem.*, **63**, 2035 (2020); https://doi.org/10.1021/acs.jmedchem.9b00262
93. B.Guyen, C.M.Schultes, P.Hazel, J.Mann, S.Neidle. *Org. Biomol. Chem.*, **2**, 981 (2004); https://doi.org/10.1039/b316055f
94. J.-L.Zhou, Y.-J.Lu, T.-M.Ou, J.-M.Zhou, Z.-S.Huang, X.-F.Zhu, C.-J.Du, X.-Z.Bu, L.Ma, L.-Q.Gu, Y.-M.Li, A.S.-C.Chan. *J. Med. Chem.*, **48**, 7315 (2005); https://doi.org/10.1021/jm050041b
95. H.Brito, A.C.Martins, J.Lavrado, E.Mendes, A.P.Francisco, S.A.Santos, S.A.Ohnmacht, N.S.Kim, C.M.P.Rodrigues, R.Moreira, S.Neidle, P.M.Borralho, A. Paulo. *PLoS One*, **10**, 1 (2015); https://doi.org/10.1371/journal.pone.0126891
96. D.Y.Zeng, G.T.Kuang, S.K.Wang, W.Peng, S.L.Lin, Q.Zhang, X.X.Su, M.H.Hu, H.Wang, J.H.Tan, Z.S.Huang, L.Q.Gu, T.M.Ou. *J. Med. Chem.*, **60**, 5407 (2017); https://doi.org/10.1021/acs.jmedchem.7b00016

97. T.S.Dexheimer, S.S.Carey, S.Zuohe, V.M.Gokhale, X.Hu, L.B.Murata, E.M.Maes, A.Weichsel, D.Sun, E.J.Meuillet, W.R.Montfort, L.H.Hurley. *Mol. Cancer Ther.*, **8**, 1363 (2009); https://doi.org/10.1158/1535-7163.MCT-08-1093
98. Y.Li, Y.Tong, Y.H.Wong. *Naunyn Schmiedebergs. Arch. Pharmacol.*, **388**, 243 (2015); https://doi.org/10.1007/s00210-014-1066-1
99. H.Y.Liu, A.C.Chen, Q.K.Yin, Z.Li, S.M.Huang, G.Du, J.H.He, L.P.Zan, S.K.Wang, Y.H.Xu, J.H.Tan, T.M.Ou, D.Li, L.Q.Gu, Z.S.Huang. *J. Med. Chem.*, **60**, 5438 (2017); https://doi.org/10.1021/acs.jmedchem.7b00099
100. W.Peng, Z.Y.Sun, Q.Zhang, S.Q.Cheng, S.K.Wang, X.N.Wang, G.T.Kuang, X.X.Su, J.H.Tan, Z.S.Huang, T.M.Ou. *J. Med. Chem.*, **61**, 6629 (2018); https://doi.org/10.1021/acs.jmedchem.8b00257
101. J.Amato, C.Platella, S.Iachettini, P.Zizza, D.Musumeci, S.Cosconati, A.Pagano, E.Novellino, A.Biroccio, A.Randazzo, B.Pagano, D.Montesarchio. *Eur. J. Med. Chem.*, **163**, 295 (2019); https://doi.org/10.1016/j.ejmech.2018.11.058
102. B.Pagano, J.Amato, N.Iaccarino, C.Cingolani, P.Zizza, A.Biroccio, E.Novellino, A.Randazzo. *ChemMedChem.*, **10**, 640 (2015); https://doi.org/10.1002/cmdc.201402552
103. G.Zoidis, A.Sosic, S.Da Ros, B.Gatto, C.Sissi, F.Palluotto, A.Carotti, M.Catto. *Bioorg. Med. Chem.*, **25**, 2625 (2017); https://doi.org/10.1016/j.bmc.2017.03.019
104. D.Sun, B.Thompson, B.E.Cathers, M.Salazar, S.M.Kerwin, J.O.Trent, T.C.Jenkins, S.Neidle, L.H.Hurley. *J. Med. Chem.*, **40**, 2113 (1997); https://doi.org/10.1021/jm970199z
105. S.Roy, A.Ali, M.Kamra, K.Muniyappa, S.Bhattacharya. *Eur. J. Med. Chem.*, 112202 (2020); https://doi.org/10.1016/j.ejmech.2020.112202
106. A.S.Tikhomirov, A.A.Shtil, A.E.Shchekotikhin. *Recent Pat. Anti-Cancer Drug Discov.*, **13**, 159 (2018); https://doi.org/10.2174/1574892813666171206123114
107. A.E.Shchekotikhin, V.A.Glazunova, L.G.Dezhenkova, Y.N.Luzikov, Y.B.Sinkevich, L.V.Kovalenko, V.N.Buyanov, J.Balzarini., F.-C.Huang, J.-J.Lin, H.-S.Huang, A.A.Shtil, M.N.Preobrazhenskaya. *Bioorg. Med. Chem.*, **17**, 1861 (2009); https://doi.org/10.1016/j.bmc.2009.01.047
108. S.Cogoi, A.E.Shchekotikhin, A.Membrino, Y.B.Sinkevich, L.E.Xodo. *J. Med. Chem.*, **56**, 2764 (2013); https://doi.org/10.1021/jm3019063
109. S.Cogoi, A.E.Shchekotikhin, L.E.Xodo. *Nucleic Acids Res.*, **42**, 8379 (2014); https://doi.org/10.1093/nar/gku574
110. D.Kaluzhny, N.Ilyinsky, A.Shchekotikhin, Y.Sinkevich, P.O.Tsvetkov, V.Tsvetkov, A.Veselovsky, M.Livshits, O.Borisova, A.Shtil, A.Shchyolkina. *PLOS One*, **6**, e27151 (2011); https://doi.org/10.1371/journal.pone.0027151
111. N.S.Ilyinsky, A.K.Shchyolkina, O.F.Borisova, O.K.Mamaeva, M.I.Zvereva, D.M.Azhibek, M.A.Livshits, V.A.Mitkevich, J.Balzarini, Y.B.Sinkevich, Y.N.Luzikov, L.G.Dezhenkova, E.S.Kolotova, A.A.Shtil, A.E.Shchekotikhin, D.N.Kaluzhny. *Eur. J. Med. Chem.*, **85**, 605 (2014); https://doi.org/10.1016/j.ejmech.2014.08.030
112. A.S.Tikhomirov, V.B.Tsvetkov, D.N.Kaluzhny, Y.L.Volodina, G.V.Zatonsky, D.Schols, A.E.Shchekotikhin. *Eur. J. Med. Chem.*, **159**, 59 (2018); https://doi.org/10.1016/j.ejmech.2018.09.054
113. S.Cogoi, S.Zorzet, A.E.Shchekotikhin, L.E.Xodo. *J. Med. Chem.*, **58**, 5476 (2015); https://doi.org/10.1021/acs.jmedchem. 5b00409
114. A.S.Tikhomirov, A.E.Shchekotikhin, Y.-H.Lee, Y.-A.Chen, C.-A.Yeh, V.V.Tatarskiy, L.G.Dezhenkova, V.A.Glazunova, J.Balzarini, A.A.Shtil, M.N.Preobrazhenskaya, P.J.Chueh. *J. Med. Chem.*, **58**, 9522 (2015); https://doi.org/10.1021/acs.jmedchem.5b00859
115. G.Miglietta, S.Cogoi, J.Marinello, G.Capranico, A.S.Tikhomirov, A.Shchekotikhin, L.E.Xodo. *J. Med. Chem.*, **60**, 9448 (2017); https://doi.org/10.1021/acs.jmedchem.7b00622
116. Y.-H.Lin, S.-M.Chuang, P.-C.Wu, C.-L.Chen, S.Jeyachandran, S.-C.Lo, H.-S.Huang, M.-H.Hou. *Sci. Rep.*, **6**, 31019 (2016); https://doi.org/10.1038/srep31019
117. R.T.Wheelhouse, D.Sun, H.Han, F.X.Han, L.H.Hurley. *J. Am. Chem. Soc.*, **120**, 3261 (1998); https://doi.org/10.1021/ja973792e
118. K.Shin-ya, K.Wierzba, K.Matsuo, T.Ohtani, Y.Yamada, K.Furihata, Y.Hayakawa, H.Seto. *J. Am. Chem. Soc.*, **123**, 1262 (2001); https://doi.org/10.1021/ja005780q
119. F.X.Han, R.T.Wheelhouse, L.H.Hurley. *J. Am. Chem. Soc.*, **121**, 3561 (1999); https://doi.org/10.1021/ja984153m
120. A.Ferino, G.Nicoletto, F.D Este, S.Zorzet, S.Lago, S.N.Richter, A.Tikhomirov, A.Shchekotikhin, L.E.Xodo. *J. Med. Chem.*, **63**, 1245 (2020); https://doi.org/10.1021/acs.jmedchem.9b01577
121. S.F.Jin, P.Zhao, L.C.Xu, M.Zheng, J.Z.Lu, P.L.Zhao, Q.L.Su, H.X.Chen, D.T.Tang, J.Chen, J.Q.Lin. *Bioorg. Chem.*, **60**, 110 (2015); https://doi.org/10.1016/j.bioorg.2015.05.001
122. P.Zhao, S.F.Jin, J.Z.Lu, J.L.Lv, G.Q.Wu, P.P.Chen, C.L.Tan, D.W.Chen. *Spectrochim. Acta, Part A*, **137**, 227 (2015); https://doi.org/10.1016/j.saa.2014.08.123
123. P.Maleki, Y.Ma, K.Iida, K.Nagasawa, H.Balci. *Nucleic Acids Res.*, **45**, 288 (2017); https://doi.org/10.1093/nar/gkw1090
124. S.Jonchhe, C.Ghimire, Y.Cui, S.Sasaki, M.McCool, S.Park, K.Iida, K.Nagasawa, H.Sugiyama, H.Mao. *Angew. Chem., Int. Ed.*, **58**, 877 (2019); https://doi.org/10.1002/anie.201811046
125. M.Sakuma, Y.Ma, Y.Tsushima, K.Iida, T.Hirokawa, K.Nagasawa. *Org. Biomol. Chem.*, **14**, 5109 (2016); https://doi.org/10.1039/c6ob00437g
126. Y.Ma, Y.Tsushima, M.Sakuma, S.Sasaki, K.Iida, S.Okabe, H.Seimiya, T.Hirokawa, K.Nagasawa. *Org. Biomol. Chem.*, **16**, 7375 (2018); https://doi.org/10.1039/C8OB01702F
127. Y.Ma, K.Iida, S.Sasaki, T.Hirokawa, B.Heddi, A.Phan, K.Nagasawa. *Molecules*, **24**, 263 (2019); https://doi.org/10.3390/molecules24020263
128. L.Sabater, M.L.Nicolau-Travers, A.De Rache, E.Prado, J.Dejeu, O.Bombarde, J.Lacroix, P.Calsou, E.Defrancq, J.L.Mergny, D.Gomez, G.Pratviel. *J. Biol. Inorg. Chem.*, **20**, 729 (2015); https://doi.org/10.1007/s00775-015-1260-8
129. L.Sabater, P.J.Fang, C.F.Chang, A.De Rache, E.Prado, J.Dejeu, A.Garofalo, J.H.Lin, J.L.Mergny, E.Defrancq, G.Pratviel. *Dalton Trans.*, **44**, 3701 (2015); https://doi.org/10.1039/c4dt03631j
130. N.C.Sabharwal, O.Mendoza, J.M.Nicoludis, T.Ruan, J.L.Mergny, L.A.Yatsunyk. *J. Biol. Inorg. Chem.*, **21**, 227 (2016); https://doi.org/10.1007/s00775-015-1325-8
131. Z.F.Chen, Q.P.Qin, J.L.Qin, Y.C.Liu, K.B.Huang, Y.L.Li, T.Meng, G.H.Zhang, Y.Peng, X.J.Luo, H.Liang. *J. Med. Chem.*, **58**, 2159 (2015); https://doi.org/10.1021/jm5012484
132. B.Q.Zou, Q.P.Qin, Y.X.Bai, Q.Q.Cao, Y.Zhang, Y.C.Liu, Z.F.Chen, H.Liang. *MedChemComm.*, **8**, 633 (2017); https://doi.org/10.1039/c6md00644b
133. M.-Y.Hu, Q.He, S.-J.Fan, Z.-C.Wang, L.-Y.Liu, Y.-J.Mu, Q.Peng, S.-F.Zhu. *Nat. Commun.*, **9**, 221 (2018); https://doi.org/10.1038/s41467-017-02472-6
134. L.He, Z.Meng, Y.Q.Xie, X.Chen, T.Li, F.Shao. *J. Inorg. Biochem.*, **166**, 135 (2017); https://doi.org/10.1016/j.jinorgbio.2016.11.011
135. K.Duskova, S.Sierra, M.S.Arias-Pérez, L.Gude. *Bioorg. Med. Chem.*, **24**, 33 (2016); https://doi.org/10.1016/j.bmc.2015.11.037
136. S.Jäger, L.Gude, M.S.Arias-Pérez. *Bioorg. Chem.*, **81**, 405 (2018); https://doi.org/10.1016/j.bioorg.2018.08.019
137. W.X.Chen, X.D.Song, J.X.Chen, X.H.Zhao, J.H.Xing, J.R.Ren, T.Wu, J.Sun. *Polyhedron*, **110**, 274 (2016); https://doi.org/10.1016/j.poly.2016.02.038
138. J.R.Shakirova, A.Sadeghi, A.A.Koblova, P.S.Chelushkin, E.Toropainen, S.Tavakoli, L.-S.Kontturi, T.Lajunen, S.P.Tunik, A.Urtti. *RSC Adv.*, **10**, 14431 (2020); https://doi.org/10.1039/D0RA01114B

139. K.J.Castor, K.L.Metera, U.M.Tefashe, C.J.Serpell, J.Mauzeroll, H.F.Sleiman. *Inorg. Chem.*, **54**, 6958 (2015); https://doi.org/10.1021/acs.inorgchem.5b00921
140. J.Weynand, A.Diman, M.Abraham, L.Marcélis, H.Jamet, A.Decottignies, J.Dejeu, E.Defrancq, B.Elias. *Chem. – Eur. J.*, **24**, 19216 (2018); https://doi.org/10.1002/chem.201804771
141. K.McQuaid, H.Abell, S.P.Gurung, D.R.Allan, G.Winter, T.Sorensen, D.J.Cardin, J.A.Brazier, C.J.Cardin, J.P.Hall. *Angew. Chem., Int. Ed.*, **58**, 9881 (2019); https://doi.org/10.1002/anie.201814502
142. K.McQuaid, J.P.Hall, L.Baumgaertner, D.J.Cardin, C.J.Cardin. *Chem. Commun.*, **55**, 9116 (2019); https://doi.org/10.1039/c9cc04316k
143. S.Gama, I.Rodrigues, F.Mendes, I.C.Santos, E.Gabano, B.Klejevskaja, J.Gonzalez-Garcia, M.Ravera, R.Vilar, A.Paulo. *J. Inorg. Biochem.*, **160**, 275 (2016); https://doi.org/10.1016/j.jinorgbio.2016.04.002
144. E.Morel, C.Beauvineau, D.Naud-Martin, C.Landras-Guetta, D.Verga, D.Ghosh, S.Achelle, F.Mahuteau-Betzer, S.Bombard, M.-P.Teulade-Fichou. *Molecules*, **24**, 404 (2019); https://doi.org/10.3390/molecules24030404
145. A.Schmidt, R.Guha, A.Hepp, J.Müller. *J. Inorg. Biochem.*, **175**, 58 (2017); https://doi.org/10.1016/j.jinorgbio.2017.07.003
146. B.Bertrand, L.Stefan, M.Pirrotta, D.Monchaud, E.Bodio, P.Richard, P.Le Gendre, E.Warmerdam, M.H.de Jager, G.M.M.Groothuis, M.Picquet, A.Casini. *Inorg. Chem.*, **53**, 2296 (2014); https://doi.org/10.1021/ic403011h
147. Ö.Karaca, S.M.Meier-Menches, A.Casini, F.E.Kühn. *Chem. Commun.*, **53**, 8249 (2017); https://doi.org/10.1039/C7CC03074F
148. S.M.Meier-Menches, B.Aikman, D.Döllerer, W.T.Klooster, S.J.Coles, N.Santi, L.Luk, A.Casini, R.Bonsignore. *J. Inorg. Biochem.*, **202**, 110844 (2020); https://doi.org/10.1016/j.jinorgbio.2019.110844
149. C.Bazzicalupi, M.Ferraroni, F.Papi, L.Massai, B.Bertrand, L.Messori, P. Gratteri, A.Casini. *Angew. Chem., Int. Ed.*, **55**, 4256 (2016); https://doi.org/10.1002/anie.201511999
150. Z.Yu, K.D.Fenk, D.Huang, S.Sen, J.A.Cowan. *J. Med. Chem.*, **62**, 5040 (2019); https://doi.org/10.1021/acs.jmedchem.9b00215
151. R.Rodriguez, S.Müller, J.A.Yeoman, C.Trentesaux, J.F.Riou, S.Balasubramanian. *J. Am. Chem. Soc.*, **130**, 15758 (2008); https://doi.org/10.1021/ja805615w
152. V.F.Traven, D.A.Cheptsov. *Russ. Chem. Rev.*, **89**, 713 (2020); https://doi.org/10.1070/RCR4909
153. Y.J.Lu, D.P.Hu, K.Zhang, W.L.Wong, C.F.Chow. *Biosens. Bioelectron.*, **81**, 373 (2016); https://doi.org/10.1016/j.bios.2016.03.012
154. R.N.Das, E.Chevret, V.Desplat, S.Rubio, J.L.Mergny, J.Guillon. *Molecules*, **23**, 81 (2018); https://doi.org/10.3390/molecules23010081
155. M.H.Hu, R.J.Guo, S.B.Chen, Z.S.Huang, J.H.Tan. *Dyes Pigm.*, **137**, 191 (2017); https://doi.org/10.1016/j.dyepig.2016.10.022
156. A.V.Turaev, V.B.Tsvetkov, M.V.Tankevich, I.P.Smirnov, A.V.Aralov, G.E.Pozmogova, A.M.Varizhuk. *Biochimie*, **162**, 216 (2019); https://doi.org/10.1016/j.biochi.2019.04.018
157. O.Reznichenko, A.Quillévéré, R.P.Martins, N.Loaàc, H.Kang, M.J.Lista, C.Beauvineau, J.González-García, R.Guillot, C.Voisset, C.Daskalogianni, R.Fåhraeus, M.-P.Teulade-Fichou, M.Blondel, A.Granzhan. *Eur. J. Med. Chem.*, **178**, 13 (2019); https://doi.org/10.1016/j.ejmech.2019.05.042
158. N.Rizeq, S.N.Georgiades. *Eur. J. Org. Chem.*, **2016**, 122 (2016); https://doi.org/10.1002/ejoc.201501269
159. N.Rizeq, S.Georgiades. *Molecules*, **22**, 2160 (2017); https://doi. org/10.3390/molecules22122160
160. F.Doria, V.Pirota, M.Petenzi, M.-P.Teulade-Fichou, D.Verga, M.Freccero. *Molecules*, **23**, 2162 (2018); https://doi.org/10.3390/molecules23092162
161. S.Maiti, P.Saha, T.Das, I.Bessi, H.Schwalbe, J.Dash. *Bioconjug. Chem.*, **29**, 1141 (2018); https://doi.org/10.1021/acs.bioconj-chem.7b00781
162. M.Livendahl, J.Jamroskovic, S.Ivanova, P.Demirel, N.Sabouri, E.Chorell. *Chem. – Eur. J.*, **22**, 13004 (2016); https://doi.org/10.1002/chem.201602416
163. B.Prasad, J.Jamroskovic, S.Bhowmik, R.Kumar, T.Romell, N.Sabouri, E.Chorell. *Chem. – Eur. J.*, **24**, 7926 (2018); https://doi.org/10.1002/chem.201800078
164. B.Prasad, R.N.Das, J.Jamroskovic, R.Kumar, M.Hedenström, N.Sabouri, E.Chorell. *Chem. – Eur. J.*, **26**, 9561 (2020); https://doi.org/10.1002/chem.202000579
165. L.Cerofolini, J.Amato, A.Giachetti, V.Limongelli, E.Novellino, M.Parrinello, M.Fragai, A.Randazzo, C.Luchinat. *Nucleic Acids Res.*, **42**, 13393 (2014); https://doi.org/10.1093/nar/gku1084
166. J.Amato, A.Pagano, S.Cosconati, G.Amendola, I.Fotticchia, N.Iaccarino, J.Marinello, A.De Magis, G.Capranico, E.Novellino, B.Pagano, A.Randazzo. *Biochim. Biophys. Acta – Gen. Sub.*, **1861**, 1271 (2017); https://doi.org/10.1016/j.bbagen.2016.11.008
167. J.Jamroskovic, M.Livendahl, J.Eriksson, E.Chorell, N.Sabouri. *Chem. – Eur. J.*, **22**, 18932 (2016); https://doi.org/10.1002/chem.201603463
168. J.Jamroskovic, M.Doimo, K.Chand, I.Obi, R.Kumar, K.Brännström, M.Hedenström, R.Nath Das, A.Akhunzianov, M.Deiana, K.Kasho, S.Sulis Sato, P.L.Pourbozorgi, J.E.Mason, P.Medini, D.Öhlund, S.Wanrooij, E.Chorell, N.Sabouri. *J. Am. Chem. Soc.*, **142**, 2876 (2020); https://doi.org/10.1021/jacs.9b11232
169. T.Che, S.Bin Chen, J.L.Tu, B.Wang, Y.Q.Wang, Y.Zhang, J.Wang, Z.Q.Wang, Z.P.Zhang, T.M.Ou, Y.Zhao, J.H.Tan, Z.S.Huang. Springer, *J. Med. Chem.*, **61**, 3436 (2018); https://doi.org/10.1021/acs.jmedchem.7b01615
170. Y.Jiang, A.C.Chen, G.T.Kuang, S.K.Wang, T.M.Ou, J.H.Tan, D.Li, Z.S.Huang. *Eur. J. Med. Chem.*, **122**, 264 (2016); https://doi.org/10.1016/j.ejmech.2016.06.040
171. S.-B.Chen, J.-H.Tan, T.-M.Ou, S.-L.Huang, L.-K.An, H.-B.Luo, D.Li, L.-Q.Gu, Z.-S.Huang. *Bioorg. Med. Chem. Lett.*, **21**, 1004 (2011); https://doi.org/10.1016/j.bmcl.2010.12.019
172. S.-B.Chen, W.-B.Wu, M.-H.Hu, T.-M.Ou, L.-Q.Gu, J.-H.Tan, Z.-S.Huang. *Chem. Commun.*, **50**, 12173 (2014); https://doi.org/10.1039/C4CC05394J
173. M.-H.Hu, Y.-Q.Wang, Z.-Y.Yu, L.-N.Hu, T.-M.Ou, S.-B.Chen, Z.-S.Huang, J.-H.Tan. *J. Med. Chem.*, **61**, 2447 (2018); https://doi.org/10.1021/acs.jmedchem.7b01697
174. M.-H.Hu, T.-Y.Wu, Q.Huang, G.Jin. *Nucleic Acids Res.*, **47**, 10529 (2019); https://doi.org/10.1093/nar/gkz835
175. D.R.Calabrese, X.Chen, E.C.Leon, S.M.Gaikwad, Z.Phyo, W.M.Hewitt, S.Alden, T.A.Hilimire, F.He, A.M.Michalowski, J.K.Simmons, L.B.Saunders, S.Zhang, D.Connors, K.J.Walters, B.A.Mock, J.S.Schneekloth. *Nat. Commun.*, **9**, 4229 (2018); https://doi.org/10.1038/s41467-018-06315-w
176. J.Amato, A.Pagano, D.Capasso, S.Di Gaetano, M.Giustiniano, E.Novellino, A.Randazzo, B.Pagano. *ChemMedChem.*, **13**, 406 (2018); https://doi.org/10.1002/cmdc.201700749
177. I.Pont, J.González-García, M.Inclan, M.Reynolds, E.Delgado-Pinar, M.T.Albelda, R.Vilar, E.García-Espana. *Chem. – Eur. J.*, **24**, 10850 (2018); https://doi.org/10.1002/chem.201802077
178. I.Pont, A.Martinez-Camarena, C.Galiana-Roselló, R.Tejero, M.T.Albelda, J.González-García, R.Vilar, E.García-Espana. *ChemBioChem.*, **21**, 1167 (2020); https://doi.org/10.1002/cbic.201900678
179. X.Zhang, Y.Wei, T.Bing, X.Liu, N.Zhang, J.Wang, J.He, B.Jin, D.Shangguan. *Sci. Rep.*, **7**, 1 (2017); https://doi.org/10.1038/s41598-017-04344-x

180. V.Grande, F.Doria, M.Freccero, F.Würthner. *Angew. Chem., Int. Ed.*, **56**, 7520 (2017); https://doi.org/10.1002/anie.201702096
181. V.Grande, C.-A.Shen, M.Deiana, M.Dudek, J.Olesiak-Banska, K.Matczyszyn, F.Würthner. *Chem. Sci.*, **9**, 8375 (2018); https://doi.org/10.1039/C8SC02882F
182. A.Chauhan, R.Paul, M.Debnath, I.Bessi, S.Mandal, H.Schwalbe, J.Dash. *J. Med. Chem.*, **59**, 7275 (2016); https://doi.org/10.1021/acs.jmedchem.6b00328
183. M.P.O'Hagan, S.Haldar, M.Duchi, T.A.A.Oliver, A.J.Mulholland, J.C.Morales, M.C.Galan. *Angew. Chem., Int. Ed.*, **58**, 4334 (2019); https://doi.org/10.1002/anie.201900740
184. M.O'Hagan, P.Penalver, R.Fisher, J.C.Morales, M.C.Galan. *Chem. – Eur. J.*, **26**, 6224 (2020); https://doi.org/10.1002/chem.201905753
185. J.B.Baell, G.A.Holloway. *J. Med. Chem.*, **53**, 2719 (2010); https://doi.org/10.1021/jm901137j
186. C.V.Dang, E.P.Reddy, K.M.Shokat, L.Soucek. *Nat. Rev. Cancer*, **17**, 502 (2017); https://doi.org/10.1038/nrc.2017.36
187. S.Kendrick, A.Muranyi, V.Gokhale, L.H.Hurley, L.M.Rimsza. *J. Med. Chem.*, **60**, 6587 (2017); https://doi.org/10.1021/acs. jmedchem.7b00298
188. W.Wang, S.Hu, Y.Gu, Y.Yan, D.B.Stovall, D.Li, G.Sui. *Biochim. Biophys. Acta — Rev. Cancer*, **1874**, 188410 (2020); https://doi.org/10.1016/j.bbcan.2020.188410